INFORMATION TO USERS

This manuscript has been reproduced from the microfilm master. UMI films the text directly from the original or copy submitted. Thus, some thesis and dissertation copies are in typewriter face, while others may be from any type of computer printer.

The quality of this reproduction is dependent upon the quality of the copy submitted. Broken or indistinct print, colored or poor quality illustrations and photographs, print bleedthrough, substandard margins, and improper alignment can adversely affect reproduction.

In the unlikely event that the author did not send UMI a complete manuscript and there are missing pages, these will be noted. Also, if unauthorized copyright material had to be removed, a note will indicate the deletion.

Oversize materials (e.g., maps, drawings, charts) are reproduced by sectioning the original, beginning at the upper left-hand corner and continuing from left to right in equal sections with small overlaps.

Photographs included in the original manuscript have been reproduced xerographically in this copy. Higher quality 6" x 9" black and white photographic prints are available for any photographs or illustrations appearing in this copy for an additional charge. Contact UMI directly to order.

ProQuest Information and Learning
300 North Zeeb Road, Ann Arbor, MI 48106-1346 USA
800-521-0600

Université d'Ottawa • University of Ottawa

Université d'Ottawa · University of Ottawa

FACULTÉ DES ÉTUDES SUPÉRIEURES ET POSTDOCTORALES

FACULTY OF GRADUATE AND POSTDOCTORAL STUDIES

MAINVILLE-DALE, Rachel M. E.

AUTEUR DE LA THÈSE - AUTHOR OF THESIS

M.Sc. (Chemistry)

GRADE - DEGREE

Department of Chemistry

FACULTÉ, ÉCOLE, DÉPARTEMENT - FACULTY, SCHOOL, DEPARTMENT

TITRE DE LA THÈSE - TITLE OF THE THESIS

Theoretical Prediction and Spectroscopic Characterization of Novel Norbornene and Norbornadiene Polymer Structures

D. Fogg

DIRECTEUR DE LA THÈSE - THESIS SUPERVISOR

EXAMINATEURS DE LA THÈSE - THESIS EXAMINERS

A. St-Amant

P. Sundararajan

J.-M. De Koninck, Ph.D.

LE DOYEN DE LA FACULTÉ DES ÉTUDES SUPÉRIEURES ET POSTDOCTORALES

SIGNATURE

DEAN OF THE FACULTY OF GRADUATE AND POSTDOCTORAL STUDIES

THEORETICAL PREDICTION AND SPECTROSCOPIC CHARACTERIZATION OF NOVEL NORBORNENE AND NORBORNADIENE POLYMER STRUCTURES

by

Rachel M.E. Mainville-Dale

B.Sc. (Hons. Co-Op), University of Waterloo, 1999

A Thesis Submitted in Partial Fulfilment of

the Requirements for the Degree of

Master of Science

in

the Faculty of Graduate Studies

Ottawa Carleton Chemistry Institute

Department of Chemistry

The University of Ottawa

September 2001

pour papa

ABSTRACT

This thesis describes efforts in theoretical prediction of the macrostructures of poly(norbornadienes) and poly(norbornenes). In contrast to existing synthetic helical polymers such as poly(isocyanides) and poly(methacrylates), the helical parameters of norbornene and norbornadiene polymers may be tunable by judicious choice of substituents. Computer modelling surveys were carried out to qualitatively compare effects from tacticity, steric bulk, π-stacking and hydrogen-bonding on polymer topology. Models capable of π-stacking and hydrogen-bonding displayed interactions between substituents on neighbouring repeat units. These modelling studies suggest that helical turns will collapse to form and enforce a tube-like structure.

Polymers of functionalized norbornenes and norbornadienes were produced using different achiral and racemic catalysts. Microstructural characterization was conducted by ^{1}H, ^{1}H-^{1}H COSY and $^{13}C\{^{1}H\}$ NMR spectroscopy. The tacticities of poly(norbornadienes) agreed well with literature reported values of the catalyst used. However, all three poly(norbornenes) had the same tacticity. Macrostructural characterization was accomplished by GPC, LS, polarimetry and CD spectroscopy. All polymers had a spherical conformation in solution. Polymers made of optically active monomers were optically active whereas polymers made of non-optically active monomers were not.

ACKNOWLEDGEMENTS

I would like to acknowledge all those who made this thesis possible. Thanks to Dr. Deryn Fogg for a challenging project and for corrections to this work. I am indebted to my colleagues, Dino Amoroso, Samantha Drouin, Jennifer Snelgrove, Nick Gambarotta and Dr. Yuwen Liu for their ideas, camaraderie and support. Thank you to Dr. P. "Sundar" Sundararajan, Dr. Paul Mayer and Dr. Alain St-Amant for answering my never-ending computer modeling questions and Dr. Glen Facey for rescuing my lost NMR spectra.

Many thanks to Dr. Jack Langstaff, Mr. Paul St-Louis, and Dr. Bill Power for introducing me to the wonderful world of chemistry and all its delicate intricacies. Thank you for making my career choice clear.

Je ne serais rien sans l'amour et l'encouragement de mon époux, de ma mère, ma soeur, mon frère, ma belle famille, ma parenté et mes amis. A mon cher mari, James, je te dois double et triple la tendresse et l'amour que tu m'as donné pendant les deux dernières années. Sache que ce travail aurait été trop dure sans ton amour. Je t'aime.

Merci Mom pour m'avoir toujours encouragé de faire de mon mieux et de viser au plus haut. Ton courage et ta determination m'ont bien servie pendant ma maîtrise. Merci Dad de m'avoir donné ta tête de mule et ton sens d'humour. A Monique pour nos jasettes et ton amitié et à Pierre de m'avoir prêté son ordinateur pour rédiger cette thèse.

Thank you to Maxine, Stewart, Roney, Munroe and Rob for all your love and support. You believed in me, encouraged me and gave me unconditional love for which I am grateful. I am truly blessed to have married into such a superb family.

And last but not least thank you to Jodie, Lisa, Matt, Luke, Adrien and the rest of my friends too numerous to mention. Thank you for keeping tabs on me and my progress. Thank you for reminding me there is a light at the end of this very long and dark tunnel. I am finally free!

TABLE OF CONTENTS

ABSTRACT III

ACKNOWLEDGEMENTS IV

TABLE OF CONTENTS V

LIST OF FIGURES VII

LIST OF TABLES X

LIST OF ABBREVIATIONS XII

CHAPTER 1 1

INTRODUCTION 1

1.1 BACKGROUND 1
1.2 STEREOCHEMICAL CONTROL 2
1.2.1 Ring Opening Metathesis Polymerization (ROMP) 4
1.2.2 Double Bond Stereochemistry 8
1.2.3 Tacticity Control 10
1.2.4 Tacticity Analysis 12
1.3 HELICAL POLYMERS 17
1.3.1 Poly(isocyanides) 18
1.3.2 Poly(isocyanates) 20
1.3.3 Poly(guanidines) 20
1.3.4 Poly(methacrylates) 21
1.4 MOLECULAR MODELLING 22
1.4.1 Theory of UFF (Universal Force Field)[45-49] 23
1.5 SCOPE OF THIS WORK 26
1.6 REFERENCES 28

CHAPTER 2 31

EXPERIMENTAL PROCEDURES AND TECHNIQUES 31

2.1 GENERAL PROTOCOL FOR MSI CERIUS[2] 31
2.1.1 Creation of Models 31
2.1.2 Polymer Builder 32
2.1.3 Force Field Minimization 33
2.1.4 Dynamics Simulation 34
2.1.5 First Method of Polymer Survey 34
2.1.6 Second Method of Polymer Survey 36
2.2 MATERIALS 38
2.3 INSTRUMENTATION 38

2.4 NUCLEAR MAGNETIC RESONANCE SPECTROSCOPY (NMR) 39
2.5 GEL PERMEATION CHROMATOGRAPHY/LIGHT SCATTERING (GPC/LS)[6-8] 42
2.6 OPTICAL ROTATORY DISPERSION (ORD)[10] 45
2.7 ULTRA-VIOLET-VISIBLE (UV-VIS) SPECTROSCOPY[11] 46
2.8 CIRCULAR DICHROISM (CD) SPECTROSCOPY[12] 49

CHAPTER 3 ..... **54**

RESULTS **54**

3.1 COMPUTER MODELLING 54
3.2 FIRST POLYMER MODELLING SURVEY 56
3.2.1 Unsubstituted Monomers *56*
3.2.2 Tactic Combinations *57*
3.2.3 Three-Dimensional Bulk *60*
3.2.4 Tether Type *61*
3.2.5 Tether Length *63*
3.2.6 Hydrocarbon vs. Oxygen-Containing Rings *64*
3.2.7 Summary of First Survey Results *66*
3.3 SECOND POLYMER COMPUTER MODELLING SURVEY 67
3.3.1 Tactic Combinations *68*
3.3.2 Three-Dimensional Bulk and π - Stacking *70*
3.3.3 Hydrogen Bonding *72*
3.3.4 Tether Type *74*
3.3.5 Hydrocarbon vs. Oxygen-Containing Rings *75*
3.3.6 Dynamics Simulation of a Model Helix *75*
3.3.7 Summary and Conclusions *78*
3.4 SPECTROSCOPIC CHARACTERIZATION OF POLYMERS 79
3.4.1 Cis/Trans and Tacticity Analysis *80*
3.4.2 Molecular Weight and Conformational Analysis *83*
3.4.3 Polarimetry and Circular Dichroism (CD) Spectroscopy *85*
3.4.4 Summary and Conclusions *87*
3.5 REFERENCES 89

CHAPTER 4 ..... **90**

CONCLUSIONS AND FUTURE DIRECTIONS **90**

APPENDICES **93**

APPENDIX A: NMR EXPERIMENTS 94
APPENDIX B: CONFORMATION PLOTS 121
APPENDIX C: CD SPECTRA 130
APPENDIX D: RESULTS FOR COMPUTER MODELLING 137

LIST OF FIGURES

Figure 1. 1. Stereoregular Polymers Derived from Monomer CH_2=CHR 3
Figure 1. 2. Chirality of Allylic Carbons in Norbornadiene 3
Figure 1. 3. Symmetry Elements of Stereoregular Norbornene/Norbornadiene Polymers 4
Figure 1. 4. Acyclic Olefin Metathesis 5
Figure 1. 5. Ring-Opening Metathesis Polymerization 5
Figure 1. 6. Structure of Stable M(IV) Catalysts 6
Figure 1. 7. Anti and Syn Rotamers of Molybdenum Alkylidenes 8
Figure 1. 8. Possible Stereochemistries Upon Monomer Addition to Syn and Anti Rotamers (adapted from [30]) 9
Figure 1. 9. First ROMP Insertion for Norbornadiene 11
Figure 1. 10. Second ROMP Insertion for Norbornadiene 12
Figure 1. 11. Poly(norbornene) Repeat Unit - Numbering of Carbon Atoms 13
Figure 1. 12. Possible Dyad Stereotacticities for Norbornene/Norbornadiene Systems (X* is chiral) 15
Figure 1. 13. Olefinic Region of the COSY Spectra for an Unsymmetrical Norbornadiene Monomer (a) high trans syndiotactic, (b) high cis isotactic)[31] 16
Figure 1. 14. Carbon NMR Signal for C_7 16
Figure 1. 15. Asymmetric Synthesis Polymerization of Poly(Methyl Methacrylate) Using a Chiral Template 18
Figure 1. 16. Poly(isocyanide) 18
Figure 1. 17. Living Ni(II) Catalyst for Polymerization of Isocyanides (A) non-helix-sense selective polymerization, (B) and (C) helix-sense selective polymerization). 19
Figure 1. 18. Poly(isocyanate) 20
Figure 1. 19. Poly(guanidine) 20
Figure 1. 20. Poly(methyl methacrylate) 21
Figure 1. 21. Anionic Initiator and Optically Active Diamines 22
Figure 1. 22. Monomers and Catalysts Studied 27

Figure 2. 1. Sketcher Card in Cerius[2] 31
Figure 2. 2. Head and Tail Definitions for a Diol Polymer 32
Figure 2. 3. Ring-Opened Norbornene/Norbornadiene Monomer in Cerius[2] 33
Figure 2. 4. Repeat Unit (Dyad) for Non Cis-Isotactic Polymers of Norbornene/Norbornadiene 35
Figure 2. 5. Definition of Helical Parameters for a General Helix 35
Figure 2. 6. Torsion Angle Definitions on Poly(isocyanide) 36
Figure 2. 7. Definition of Torsion Angles for Norbornene/Norbornadiene Polymers 37
Figure 2. 8. ^{1}H Labelling Scheme for Table 2. 1. 40
Figure 2. 9. $^{13}C\{^1H\}$ Labelling Scheme for Table 2. 2. 41
Figure 2. 10. Electromagnetic Radiation 45
Figure 2. 11. Linearly Polarized Light 45
Figure 2. 12. Rotation of Linearly Polarized Light by an Angle ϕ 46
Figure 2. 13. Electronic Energy Levels and Transitions 47
Figure 2. 14. Repeat Units for Norbornene and Norbornadiene Systems 48

Figure 2. 15. Right-Handed Circularly Polarized Light 49
Figure 2. 16 Comparison of UV-vis Absorbance and CD Spectra for a Single Chromophore (dashed line) and dimer (solid line) [(a) UV-vis Absorbance, (b) CD Spectra][12] 50
Figure 2. 17. Comparison of CD (dashed line) and ORD (solid line) Spectra [(a) UV-vis Absorbance, (b) Positive ORD (c) Negative ORD][12] 51
Figure 2. 18. Right-Handed (A) and Left-Handed (B) Poly(isocyanide) Helices and their Corresponding Circular Dichroism Spectra (C and D respectively)[14] 52

Figure 3. 1. Colour Scheme of Monomer Repeat Units in Cerius[2] 55
Figure 3. 2. Computer Models of Unsubstituted cis/iso (a) Poly(NBD) and (b) Poly(NBE) 57
Figure 3. 3. Computer Models of Poly(Exo,Endo NBE($CO_2{}^tBu)_2$) (50 units) (a) cis/isotactic, (b) trans/isotactic, (c) cis/syndiotactic, (d) trans/syndiotactic 59
Figure 3. 4. Steric Hindrance Between Bulky Substituents on a Cis/Isotactic Dyad 60
Figure 3. 5. Adamantyl 60
Figure 3. 6. Computer Models of Cis/Isotactic Poly(Exo,Endo NBE($CO_2R)_2$) (a) R = ^{t}Bu, (b) R = Ad 61
Figure 3. 7. Computer Model for Cis/Isotactic Poly(Exo, Endo NBE($CO_2CH_2{}^tBu)_2$) 63
Figure 3. 8. Computer Models of Cis/Isotactic Poly(NBD) {(a) and (b)} and Poly(NBE) {(c) and (d)}, CO_2Me substitution 65
Figure 3. 9. Computer Models of Poly(NBD(CO_2tBu)$_2$) (50 units except (c) 200 units) (a) cis/isotactic, (b) trans/isotactic, (c) cis/syndiotactic, (d) trans/syndiotactic 69
Figure 3. 10. Computer Model of Trans/Syndiotactic Poly(Exo, Endo NBE($CO_2{}^tBu)_2$) 50 units 70
Figure 3. 11 Menthyl 70
Figure 3. 12. Computer Models of Cis/Isotactic Poly(Exo, Endo NBE(CO_2Ph_2) 71
Figure 3. 13. Guanine 72
Figure 3. 14. Computer Model for Cis/Isotactic Poly(NBD(COGuanine)$_2$) 73
Figure 3. 15. Computer Model for c/s Poly(NBE(CO_2Menthyl)$_2$) 50 units 76
Figure 3. 16. Computer Models for Dynamics Simulation of Poly(NBE(CO_2Menthyl)$_2$) 50 units (a) 50 ps, (b) 100 ps, (c) 150 ps, (d) 200 ps, (e) 250 ps 77
Figure 3. 17. Target Momomers for Synthesis 78
Figure 3. 18. Polymerization Catalysts Used 80
Figure 3. 19. Expansion of Olefinic Region of $^{13}C\{^1H\}$ NMR Spectrum of 1B (75 MHz, $CDCl_3$) 81
Figure 3. 20. Expansion of Aliphatic Region $^{13}C\{^1H\}$ NMR Spectrum of 1B (75 MHz, $CDCl_3$) 82
Figure 3. 21. Expansion of Olefinic Region of ^1H-^1H COSY of 3A (300 MHz, $CDCl_3$). 83
Figure 3. 22. GPC Trace for 3B 84
Figure 3. 23. CD Spectrum of 4C (CH_2Cl_2) 86

Figure A. 1. ^1H NMR Spectrum (300 MHz, $CDCl_3$) of 1A 94
Figure A. 2. $^{13}C\{^1H\}$ NMR Spectrum (75 MHz, $CDCl_3$) of 1A 95
Figure A. 3. Expansion of Olefinic and Aliphatic Regions of $^{13}C\{^1H\}$ NMR Spectrum of 1A 96

Figure A. 4. ^{1}H NMR Spectrum (300 MHz, $CDCl_3$) of 1B 97
Figure A. 5. $^{13}C\{^{1}H\}$ NMR Spectrum (75 MHz, $CDCl_3$) of 1B 98
Figure A. 6. Expansion of Olefinic and Aliphatic Regions of $^{13}C\{^{1}H\}$ NMR Spectrum of 1B 99
Figure A. 7. ^{1}H NMR Spectrum (300 MHz, $CDCl_3$) of 2A 100
Figure A. 8. $^{13}C\{^{1}H\}$ NMR Spectrum (75 MHz, $CDCl_3$) of 2A 101
Figure A. 9. Expansion of Olefinic and Aliphatic Region of $^{13}C\{^{1}H\}$ NMR Spectrum of 2A 102
Figure A. 10. ^{1}H Spectrum (300 MHz, $CDCl_3$) of 3A 103
Figure A. 11. ^{1}H-^{1}H COSY NMR Spectrum (300 MHz, $CDCl_3$) of 3A 104
Figure A. 12. Expansion of Olefinic Region of ^{1}H-^{1}H COSY NMR Spectrum of 3A 105
Figure A. 13. $^{13}C\{^{1}H\}$ NMR Spectrum (75 MHz, $CDCl_3$) of 3A 106
Figure A. 14. Expansion of Olefinic Region of $^{13}C\{^{1}H\}$ NMR Spectrum of 3A 107
Figure A. 15. Expansion of Aliphatic Region of $^{13}C\{^{1}H\}$ NMR Spectrum of 3A 108
Figure A. 16. ^{1}H NMR Spectrum (300 MHz, $CDCl_3$) of 3B 109
Figure A. 17. ^{1}H-^{1}H COSY NMR Spectrum (300 MHz, $CDCl_3$) of 3B 110
Figure A. 18. Expansion of olefinic region of ^{1}H-^{1}H COSY NMR Spectrum of 3B 111
Figure A. 19. $^{13}C\{^{1}H\}$ NMR Spectrum (75 MHz, $CDCl_3$) of 3B 112
Figure A. 20. Expansion of Aliphatic Region of $^{13}C\{^{1}H\}$ NMR Spectrum of 3B 113
Figure A. 21. ^{1}H NMR Spectrum (300 MHz, $CDCl_3$) of 4B (same for 4Aand 4C) 114
Figure A. 22. ^{1}H-^{1}H COSY NMR Spectrum (300 MHz, $CDCl_3$) of 4A (same for 4B and 4C) 115
Figure A. 23. Expansion of Olefinic Region of ^{1}H-^{1}H COSY NMR Spectrum of 4A (same for 4B and 4C) 116
Figure A. 24. $^{13}C\{^{1}H\}$ NMR Spectrum (75 MHz, $CDCl_3$) of 4C (same for 4A and 4B) 117
Figure A. 25. Expansion of Olefinic and Aliphatic Region of $^{13}C\{^{1}H\}$ NMR Spectrum of 4C (same for 4A and 4B) 118
Figure A. 26. ^{1}H-^{13}C HMQC NMR Spectrum (300 MHz, $CDCl_3$) of 4B (same for 4A and 4C) 119
Figure A. 27. DEPT-135 NMR Spectrum (75 MHz, $CDCl_3$) of 4A (same for 4B and 4C) 120

Figure B. 1. Conformation Plot for 1A 121
Figure B. 2. Conformation Plot for 2A 122
Figure B. 3. Conformation Plot for 3A (Peak#2) 123
Figure B. 4. Conformation Plot for 3A (Peak#3) 124
Figure B. 5. Conformation Plot for 3B 125
Figure B. 6. Conformation Plot for 4A 126
Figure B. 7. Conformation Plot for 4B (Peak#2) 127
Figure B. 8. Conformation Plot for 4B (Peak#3) 128
Figure B. 9. Conformation Plot for 4C 129

Figure D. 1. Polymer Type Descriptions 137

LIST OF TABLES

Table 1. 1. Select Norbornadiene Polymers Produced with Stereochemical Control 7
Table 1. 2. Polymers Studied 27

Table 2. 1 ^{1}H NMR Peak Assignments for Norbornadiene (A) and Norbornene (B) Polymers 40
Table 2. 2. $^{13}C\{^{1}H\}$ NMR Peak Assignments for Norbornadiene (A) and Norbornene (B) Polymers 41
Table 2. 3. Tacticity Assignments Found by ^{1}H-^{1}H COSY NMR 42

Table 3. 1. Comparison of Unsubstituted Cis/Isotactic Poly(NBD) and Poly(NBE) (First Survey Results) 57
Table 3. 2. Effect of Tacticity on Poly(NBD) and Poly(NBE) (First Survey Results) 58
Table 3. 3. Effect of Increase in Three-Dimensional Bulk on Cis/Isotactic Poly(NBE) and Poly(NBD) (First Survey Results) 60
Table 3. 4. Effect of Tether Type on Cis/Isotactic Poly(NBD) (First Survey Results) 62
Table 3. 5. Effect of Tether Type on Cis/Isotactic Poly(NBE) (First Survey Results) 62
Table 3. 6. Effect of Proximity of Steric Bulk to Cis/Isotactic Poly(NBE) Backbone (First Survey Results) 63
Table 3. 7. Effect of Oxygen Bridge on Cis/Isotactic Poly(NBD) and Poly(NBE) (First Survey Results) 64
Table 3. 8. General Torsion Angle Rules for Tactic Dyads 68
Table 3. 9. Effect of Tacticity on Poly(NBD) and Poly(NBE) (Second Survey Results) 68
Table 3. 10. Effect of Increase in Three-Dimensional Bulk on Cis/Isotactic Poly(NBE) and Poly(NBD) (Second Survey Results) 72
Table 3. 11. Second Survey Results for Comparison of Amide and Amine Linked Poly(NBD) and Poly(NBE) (R = Guanine) 73
Table 3. 12. Effect of Tether Type on Cis/Isotactic Poly(NBD) (Second Survey Results) 74
Table 3. 13. Effect of Tether Type on Cis/Isotactic Poly(NBE) (Second Survey Results) 74
Table 3. 14. Effect of Oxygen Bridge on Cis/Isotactic Poly(NBD) and Poly(NBE) (First Survey Results) 75
Table 3. 15. Polymer Properties 79
Table 3. 16. Results of NMR Tacticity Analyses 83
Table 3. 17. Results of GPC/LS Analyses 85
Table 3. 18. Results of Polarimetry and CD Analyses 87

Table D. 1. First Survey Models of Poly(norbornadiene) With Ester (CO_2)Tether 137
Table D. 2. First Survey Models of Poly(norbornadiene) With Ether (CH_2O)Tether 138
Table D. 3. First Survey Models of Poly(norbornene) With Ester (CO_2)Tether 138
Table D. 4. First Survey Models of Poly(norbornene) With Ether (CH_2O)Tether 139
Table D. 5. Second Survey Models of Poly(norbornadiene) With Ester (CO_2)Tether ... 139
Table D. 6. Second Survey Models of Poly(norbornadiene) With Ether (CH_2O)Tether 140

Table D. 7. Second Survey Models of Poly(norbornene) With Ester (CO_2)Tether..... 140
Table D. 8. Second Survey Models of Poly(norbornene) With Ether (CH_2O)Tether 141

LIST OF ABBREVIATIONS

3D	Three Dimensional
ADMET	Acyclic Diene METathesis
CD	Circular Dichroism
COSY	Correlated Spectroscopy (NMR)
DEPT	Distortionless Enhancement by Polarization Transfer (NMR)
DNA	DeoxyRibonucleic Acid
GPC	Gel Permeation Chromatography
HMQC	Heteronuclear Multiple Quantum Coherence (NMR)
HPLC	High Pressure Liquid Chromatography
IR	Infra-Red Spectroscopy
iso	isotactic
LS	Light Scattering
m	meso
MW	Molecular Weight
NBE	Norbornene
NBD	Norbornadiene
NMR	Nuclear Magnetic Resonance Spectroscopy
OFF	Open Force Field
ORD	Optical Rotatory Dispersion
r	racemic
$\langle r_g \rangle$	Root Mean Square Radius
RCM	Ring Closing Metathesis
ROMP	Ring Opening Metathesis Polymerization
syndio	syndiotactic
tr	trans
UFF	Universal Force Field
UV-vis	Ultra-visible Spectroscopy

CHAPTER 1

INTRODUCTION

1.1 Background

The first synthetic plastics were rather crude materials with varying characteristics for every batch. Innovations such as co-polymerization, living polymerization, and metallocene catalysts have vastly improved the quality and the types of plastics made.[1] Natural polymers such as wool, silk, rubber and spider silk have consistent and predictable properties because of their well-defined micro and macrostructures.[2] Emulating such precise polymerizations may produce materials with desired characteristics such as hardness, opacity, elasticity, compressibility, strength, etc. without the need for plasticizers.

Ziegler was the first to produce unimodal molecular weight polymers of styrene and butadiene using living polymerization.[3] The first polymer produced under stereochemical control was polypropylene.[4, 5] Microstructure is defined as the manner in which repeat units are joined, whereas macrostructure is the macromolecular shape of the polymer chain. Rigorous control of microstructure may extend to precise definition of the macrostructure or three-dimensional shape of the polymer. There are examples of synthetic polymers with stable helices [poly(isocyanides)[6], poly(guanidines)[7] and

poly(methyl methacrylates)[8]]. The ability to tune a polymer helix through a change in monomer substituent would be an innovation upon current helical polymers. Such tunable helices may produce tube-like structures with an internal void capable of carrying, or masking another compound within it. Potential applications lie in the biomedical or microelectronics fields.

1.2 Stereochemical Control

The word tactic comes from the Greek for 'put in order'. There are two forms of tactic polymers, which have a regularly repeating order. The labelling convention developed by Ziegler and Natta in the 1950's was used to describe the poly(propylene) structures they were producing.[4] Since the primary mode of most polymerizations is head to tail, the possible stereochemistries are (Figure 1. 1):[9]

isotactic	each chiral centre has the same configuration
syndiotactic	alternate chiral centres have the same configuration
atactic	chiral centre configurations are randomly ordered

The polymers may also be described in terms of two consecutive repeat units known as dyads. Those dyads containing symmetry are meso (m), whereas racemic (r) dyads contain no symmetry (Figure 1. 1).

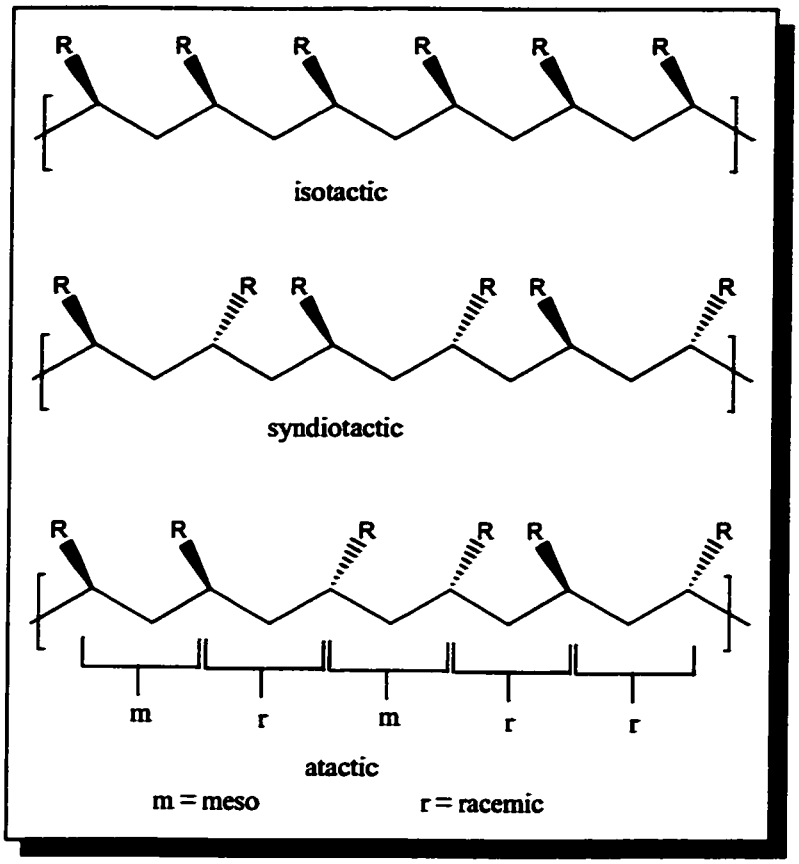

Figure 1. 1. Stereoregular Polymers Derived from Monomer CH_2=CHR

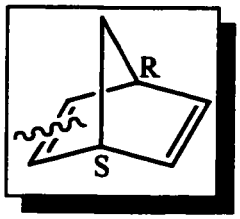

Figure 1. 2. Chirality of Allylic Carbons in Norbornadiene

Polymers of norbornene and norbornadiene are also capable of stereoregularity arising from the arrangement of neighbouring repeat units. The allylic carbons (Figure 1. 2) on the monomer have opposite chirality that does not change upon ring-opening as no bonds are made or broken at these carbons. Meso dyads are characterized by a symmetry element that bisects the double bond between the two C_5 rings. For cis-meso dyads, a mirror plane bisects the dyad; for trans-meso dyads an inversion centre relates the two halves. If the polymer chain contains only meso junctions then it must be isotactic as indicated by the configurations labelled in the accompanying figure (Figure 1. 3). Racemic dyads, in contrast, have no symmetry

elements. A polymer that includes only racemic dyads is syndiotactic. A polymer that contains a mixture of meso and racemic dyads is defined as atactic.

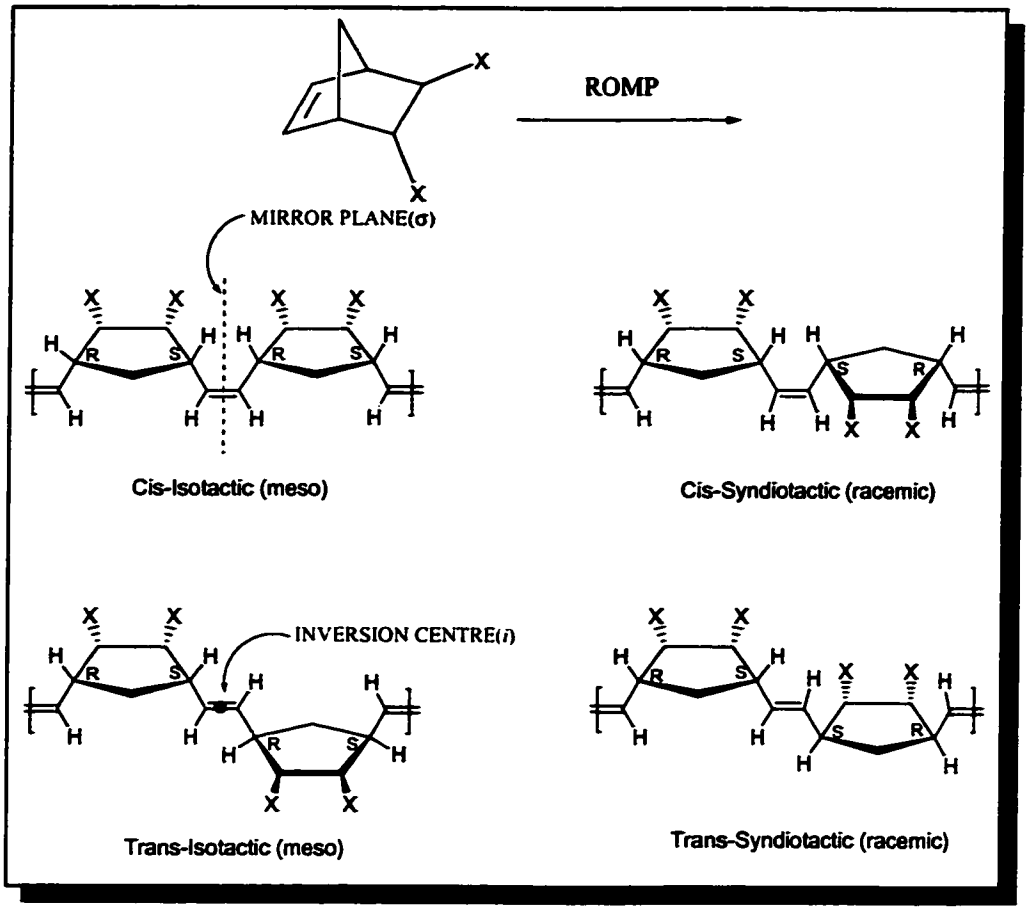

Figure 1. 3. Symmetry Elements of Stereoregular Norbornene/Norbornadiene Polymers

1.2.1 Ring Opening Metathesis Polymerization (ROMP)

Ring opening metathesis polymerization (ROMP), is a technique for polymerizing cyclic olefins that was first accomplished in the early 1960's.[10] Initially the polymerization was carried out on simple substrates such as cyclooctene using Ziegler-Natta type catalysts ($MoCl_5/Et_3Al$). At first, the mechanism in which these polymers were produced was poorly understood. Disproportionation experiments in the late 1960's established the

mechanism of olefin metathesis.[10] This affords powerful insight into the ROMP reaction, as well as acyclic diene metathesis (ADMET) and ring closing metathesis (RCM) reactions. The first step of the metathesis reaction is an electrophilic attack of the metal carbene on the olefinic double bond to form a metallocyclobutane complex.[11] Subsequent ring opening yields a second metal carbene and an olefin where the substituents have been exchanged as demonstrated in Figure 1. 4.

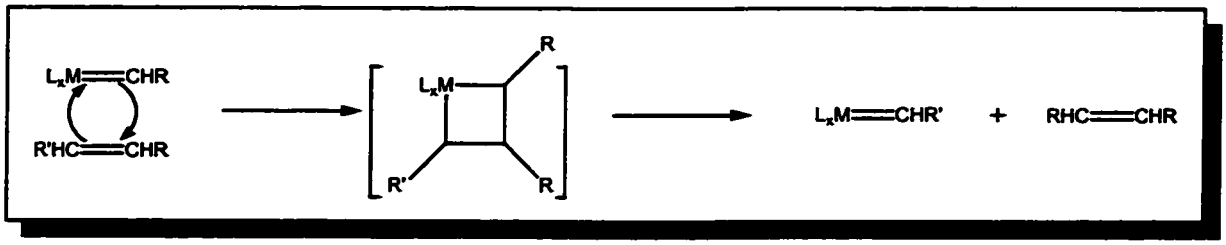

Figure 1. 4. Acyclic Olefin Metathesis

The olefin metathesis reaction is also the key reaction in ROMP, as shown in Figure 1. 5. The driving force for the polymerization is the release of ring strain in the polycyclic olefin upon ring-opening of the monomer. Living polymerizations can be achieved in ROMP if the rate of secondary metathesis (metathesis involving the polymer chain) is slow, the primary metathesis irreversible, and the rate of initiation (k_i) is approximately equal to the rate of propagation (k_p).[12] In other words, if each chain is initiated at the same time and propagates at the same rate without termination, a near-monodisperse polymer can be obtained.

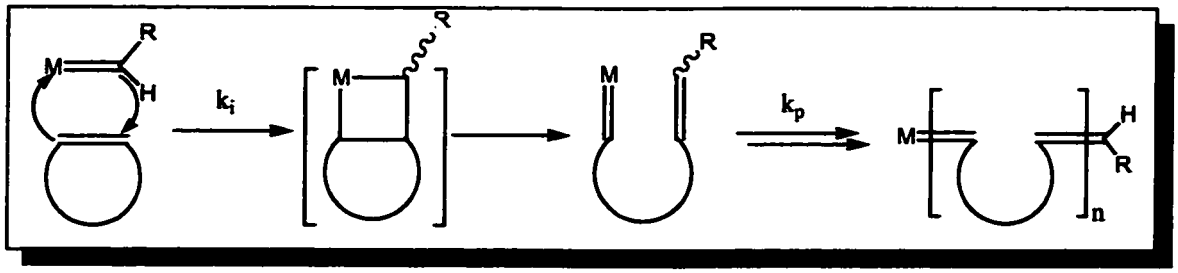

Figure 1. 5. Ring-Opening Metathesis Polymerization

Up until 1980, highly tactic polymers were made only by poorly defined catalysts such as $RuCl_3$[13], $OsCl_3$/PhC≡CH[14], (mesitylene)$W(CO)_3$/$EtAlCl_2$[15], $ReCl_5$[16], WCl_6/Bu_4Sn[17], and others.[10] However, evidence was growing that the metathesis active catalyst in solution was a transition metal '$M{=}CH_2$' species generated *in situ*.[18, 19] The first living polymerization of norbornene was effected by a titanium carbene generated *in situ*.[20] In the late 1980's, Schrock and co-workers reported various W(VI) and Mo(IV) complexes with the M=CHR'(NAr)$(OR)_2$ tetrahedral structure (Figure 1. 6).[12, 21] The bulky alkoxide (OR) and imido (NAr) groups stabilized the structure by preventing oligomerization reactions of these electron-deficient species. Tailoring of the alkoxides, imido ligand and carbene substituent changed the double bond stereochemistry and tacticity of the resulting polymer. Increasing the electron-withdrawing power of alkoxides (from –O^{t}Bu to –OCF_3), changed the polymer tacticity from high-trans syndiotactic[22] to high-cis isotactic.[23] Chiral and bulky alkoxides, such as binaphtholates, also produced high-cis isotactic polymers.[24-26] Both cis-isotactic and trans-isotactic polymers of 2,3-bis((menthyloxy)-carbonyl)norbornadiene can be made depending on which catalyst is used (Table 1. 1).[25] Increasing the steric bulk of the norbornadiene substituents from a methyl to a tert-butyl group, also increases tacticity of the resulting polymer.[27]

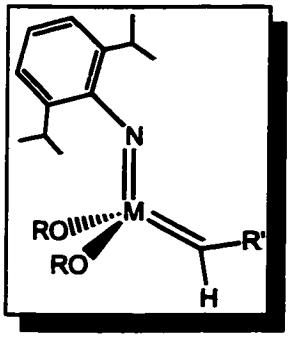

Figure 1. 6. Structure of Stable M(IV) Catalysts

Table 1. 1. Select Norbornadiene Polymers Produced with Stereochemical Control

Monomers 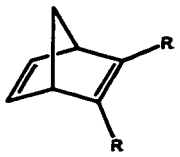	***Catalysts*** 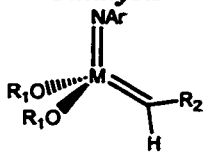		***% Cis***	***Tacticity***	***Reference***
R	***R_1***	***R_2***			
CO_2Me	$CMe(CF_3)_2$	CMe_2Ph	98	60 (iso)	24, 27
	$C(CF_3)_3$	CMe_2Ph	97	61 (iso)	27
	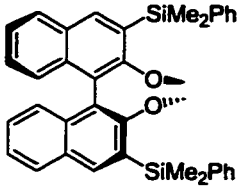	^tBu	93	97 (?)	24
	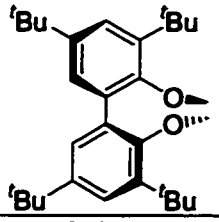	CMe_2Ph	>99	96 (?)	24
CO_2Et	$C(CF_3)_3$	CMe_2Ph	97	71 (iso)	27
$CO_2{}^iPr$	$CMe(CF_3)_2$	CMe_2Ph	97	65 (iso)	27
$CO_2{}^tBu$	$CMe(CF_3)_2$	CMe_2Ph	99	88 (iso)	27
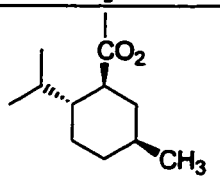	^tBu	CMe_2Ph	6	100 (syndio)	25
	$C(CF_3)_3$	CMe_2Ph	99	100 (iso)	25
	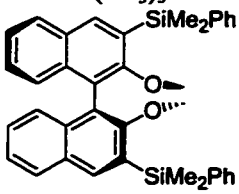	CMe_2Ph	99	100 (iso)	25
	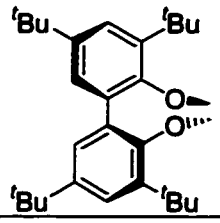	CMe_2Ph	99	100 (iso)	25

1.2.2 Double Bond Stereochemistry

The molybdenum alkylidenes can exist in either one of two rotational isomers (rotamers). These two rotameric forms are the syn and anti forms shown in Figure 1. 7. Interconversion between the two rotamers does occur, but typically the syn rotamer is predominant at room temperature with a barrier to conversion of 15-18 kcal/mol. The equilibrium ($K_{eq} \approx 1000$) can be manipulated by varying the bulk of the imido group or using electron-withdrawing alkoxides.[28, 29]

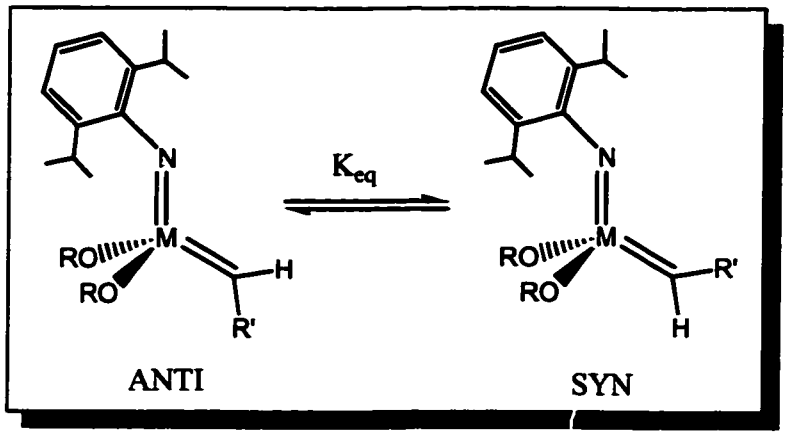

Figure 1. 7. Anti and Syn Rotamers of Molybdenum Alkylidenes

At lower temperatures (-30°C), monomers will react exclusively with the anti rotamer while the syn rotamer remains unreactive until the temperature is raised.[29] The anti rotamer is more reactive as a result of less steric hindrance between the imido group and the alkylidene, making it easier for the monomer to insert. As the temperature increases, the increasing internal motion of the complex raises the reactivity of the syn rotamer to a level comparable with the anti rotamer.

Schrock and co-workers have proposed that norbornene-based monomers may only approach the catalyst in the **7-syn** orientation (top portion of Figure 1. 8), where C_7 points towards the imido functionality due to the steric bulk of the equatorial alkoxide ligands.[29] Approach of the monomer in a **7-syn** orientation to syn rotamers results in cis polymers, whereas addition to anti rotamers yields trans polymers.

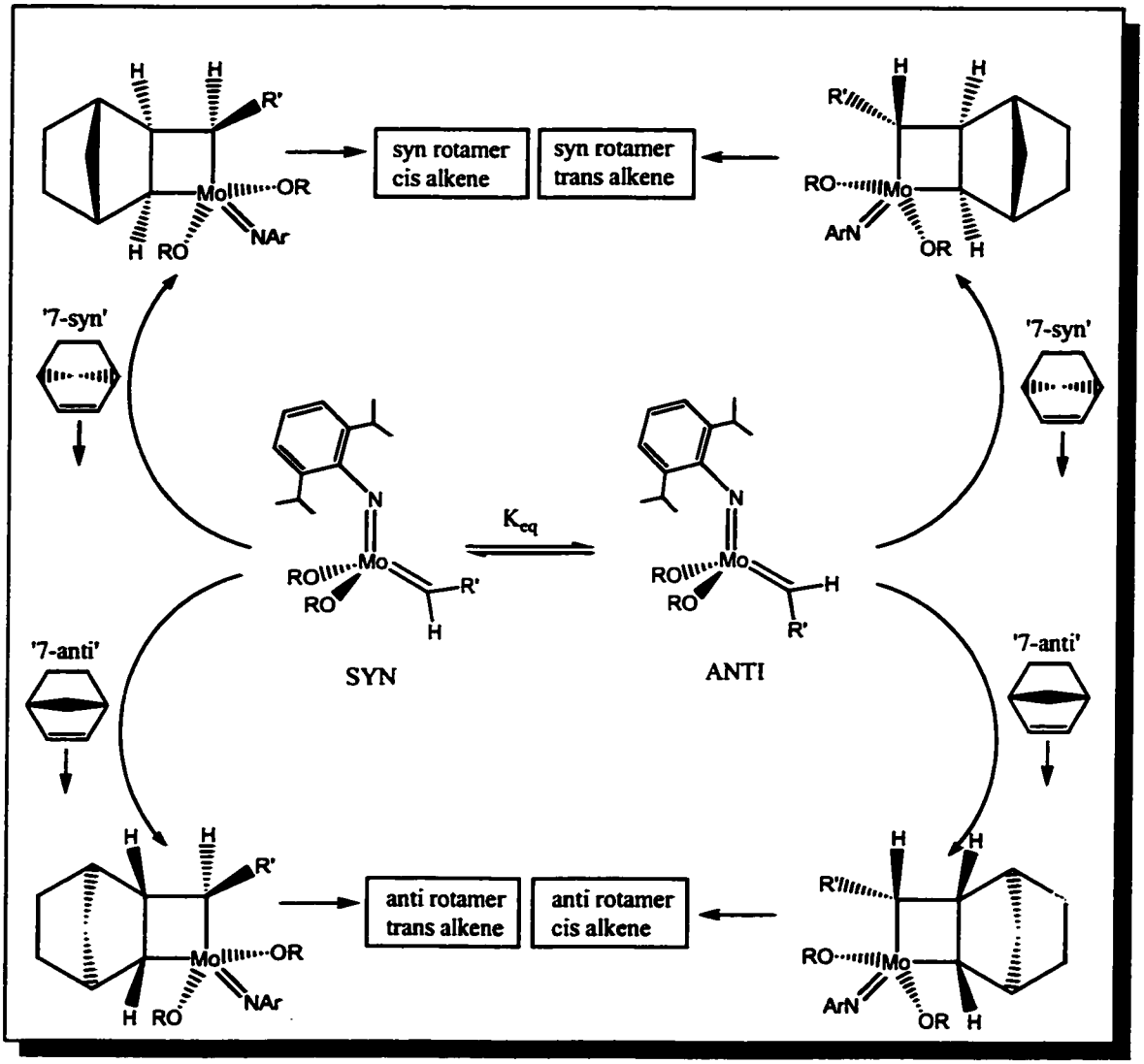

Figure 1. 8. Possible Stereochemistries Upon Monomer Addition to Syn and Anti Rotamers (adapted from [30])

Even though both first insertion products result in syn rotamers (top portion of Figure 1. 8), there is some conversion from syn to anti for some complexes with bulky alkoxides at higher temperatures. "Errors" in addition could occur if the monomer entered the coordination sphere in a **7-anti** fashion (see bottom half of Figure 1. 8). This is most likely to occur when alkoxides provide less electron-withdrawing power and steric bulk. Such errors lead to mixtures and atactic polymers.

An all-cis or all-trans polymer requires consistent addition of monomer in one direction (either **7-syn** or **7-anti**) to the same rotamer. Formation of an all-trans polymer requires that the anti rotamer be five orders of magnitude more reactive than the syn rotamer.[29] If the reactivity of the anti rotamer is comparable to that of the syn rotamer, a mixture of cis and trans double bonds will result. As the reactivity of the anti rotamer decreases, the anti rotamer becomes kinetically inaccessible in solution, ensuring exclusive polymerization through syn rotamers to yield cis double bonds.

1.2.3 Tacticity Control

Polymer tacticity is determined by the manner in which the monomer enters the coordination sphere of the catalyst relative to the previously added unit. In the molybdenum systems, monomer addition to the catalyst occurs at one of two CNO faces; that is, to one of the two sides of the Mo=C bond. If successive monomer additions occur at the same face of the Mo=C bond, then the relative orientation of neighbouring repeat units will be meso and an isotactic polymer produced. If the monomer adds to the two

CNO faces in an alternating fashion, there will be racemic dyads (syndiotactic polymer) (Figure 1. 9 and Figure 1. 10).[25]

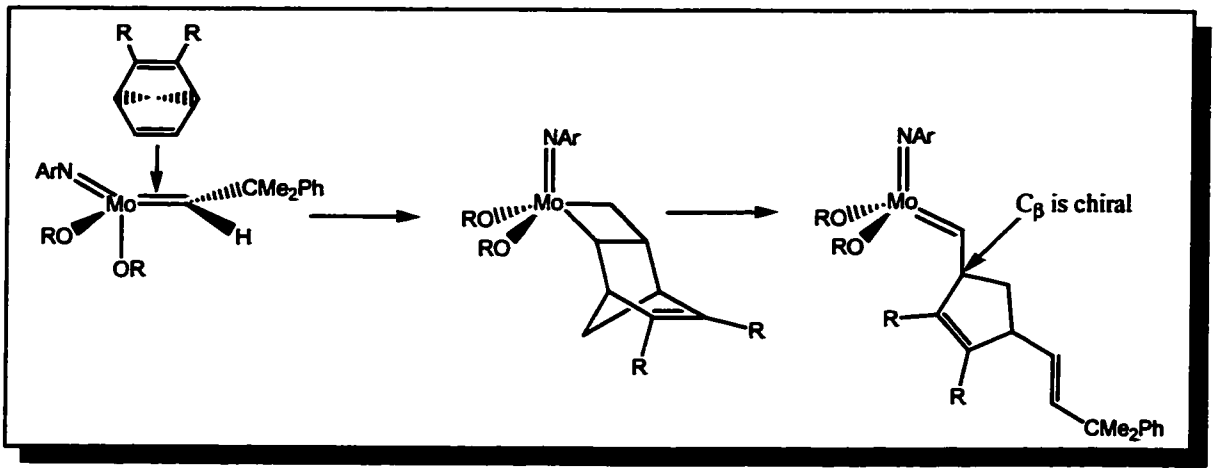

Figure 1. 9. First ROMP Insertion for Norbornadiene

Enantioselectivity can arise via either chain end control or enantiomorphic metal site control. Chain end control is exerted by the growing polymer chain, and in particular by the β carbon (C_β in Figure 1. 9). Following the first monomer insertion step, the β carbon of the growing polymer chain is chiral, rendering the two CNO faces inequivalent. "Errors" caused by the misdirection of monomers during polymerization will be propagated along the chain. In cases where the alkoxide ligands are chiral, the metal site itself is chiral and has two inequivalent CNO faces. The catalyst will tend to direct the monomer to the same face to yield an isotactic polymer. Enantiomorphic metal site control tends to correct "errors" made, rather than propagate them.[25]

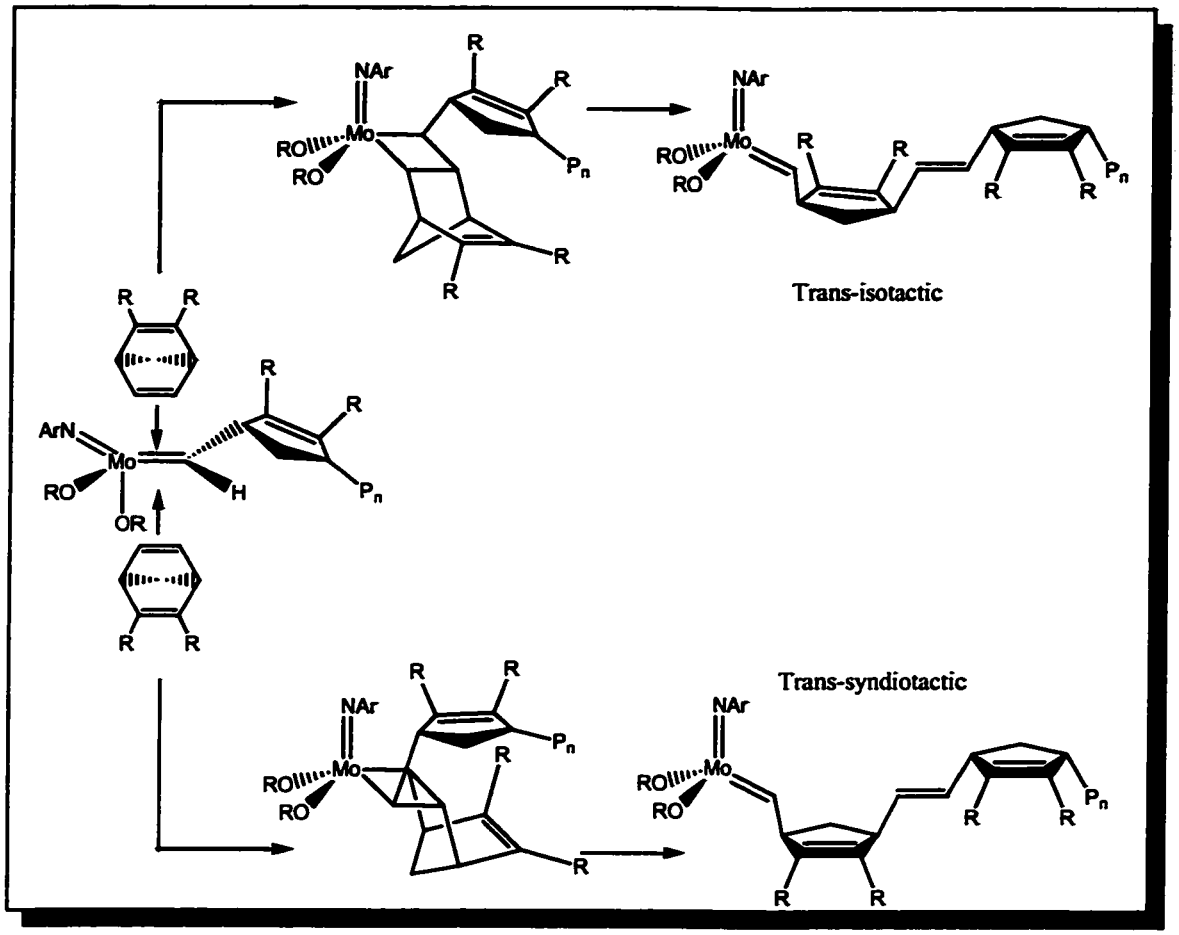

Figure 1. 10. Second ROMP Insertion for Norbornadiene

1.2.4 Tacticity Analysis

Determining the extent of polymer stereoregularity is of fundamental importance. Natta originally inferred the structure and hence the tacticity of poly(propylene) and poly(styrene) through IR and X-Ray diffraction experiments.[4, 5] Development of NMR methods for tacticity determination represented a breakthrough in this field.

The NMR spectra of tactic polymers exhibit fine structure owing to the sensitivity of any given repeat unit to its neighbouring repeat units. Such splitting in spectra of simple polymers such as poly(propylene) (Figure 1. 1), is sensitive to neighbours up to five repeat units away.[31] For poly(norbornenes) and poly(norbornadienes) (Figure 1. 3), such sensitivity is limited to immediate neighbours (dyads or triads depending on the signal) because of larger distances between repeat units.[31] The $^{13}C\{^{1}H\}$ NMR signals (carbons 1 to 4 in Figure 1. 11) can show fine structure due to variation of the double bond stereochemistry (cis or trans), as well as the tactic arrangement of adjacent repeat units (meso or racemic). The signal due to C_7 (Figure 1. 11) is unique in its sensitivity to triads. Any given triad (A.A′.A″) can be described by the tactic relationship between A and A′, and A′ and A″. This results in either a mm (meso-meso), rm/mr (racemic-meso/meso-racemic) or rr (racemic-racemic) arrangement. Carbons 5 and 6 (Figure 1. 11) are much less likely to exhibit fine structure because of their distance from the double bonds and chiral centres.

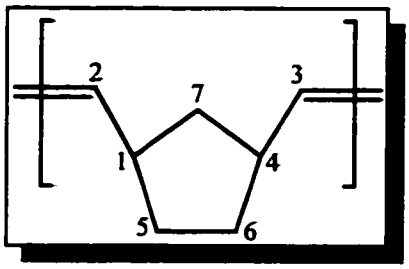

Figure 1. 11. Poly(norbornene) Repeat Unit - Numbering of Carbon Atoms

Two schools of thought have emerged in NMR analysis of ROMP polymers. One of these, as put forward by Ivin and Rooney is based on the assumption that a given double bond stereochemistry is associated with a certain type of tacticity.[14, 31] That is, cis stereochemistry is more likely to lead to syndiotactic structures, and trans stereochemistry to isotactic structures. Given that this method of tacticity assignment relies on assumptions, it is quite possibly flawed in its original and subsequent assignments and is

mentioned in order to give a complete background. The second method as put forth by Schrock allows for unambiguous determination of tacticity through ^{1}H-^{1}H COSY NMR for polymers of unsymmetrical monomers.[25] Polymers generated from symmetrical monomers cannot be analyzed by this second method, and must therefore rely on the analysis of the C_7 signals as discussed in Section 1.2.4.2 below.

1.2.4.1 Polymers Made From Unsymmetrical Monomers

Tacticity analysis of norbornene polymers by NMR was first explored in the early 1980's.[31] Tactic polymers were initially made by transition metal halides such as $ReCl_5$[16], $RuCl_3$[13], and $OsCl_3$[14], which exhibit stereochemical control over polymerizations of norbornenes and norbornadienes. Although norbornene was easily polymerized in high-cis or high-trans forms, its NMR spectrum did not exhibit fine structure due to tacticity, whereas the corresponding spectra of *substituted* poly(norbornenes) and poly(norbornadienes) did.

An unambiguous method of tacticity determination was reported by Schrock and co-workers in 1994.[25] For any polymer constructed of symmetrical repeat units, the *olefinic protons* are equivalent by virtue of a symmetry element. Thus, in the cis-isotactic dyad, a mirror plane bisects the olefinic double bond, while the cis-syndiotactic dyad has a C_2 axis in the C_2H_2 plane. The trans-isotactic dyad has an inversion centre in the middle of the olefinic double bond, and the trans-syndiotactic dyad has a C_2 axis in the plane of the paper.

Where the monomer is symmetrical, all olefinic protons are equivalent ($H_a = H_b$), and only one olefinic signal is expected in the ^1H NMR. If the monomer is unsymmetrical (if, for example, the substituent X^* is chiral (Figure 1. 12) or if the ring is exo, endo-substituted), the olefinic protons are no longer equivalent ($H_a \neq H_b$) and two olefinic signals should be observed in the ^1H NMR.

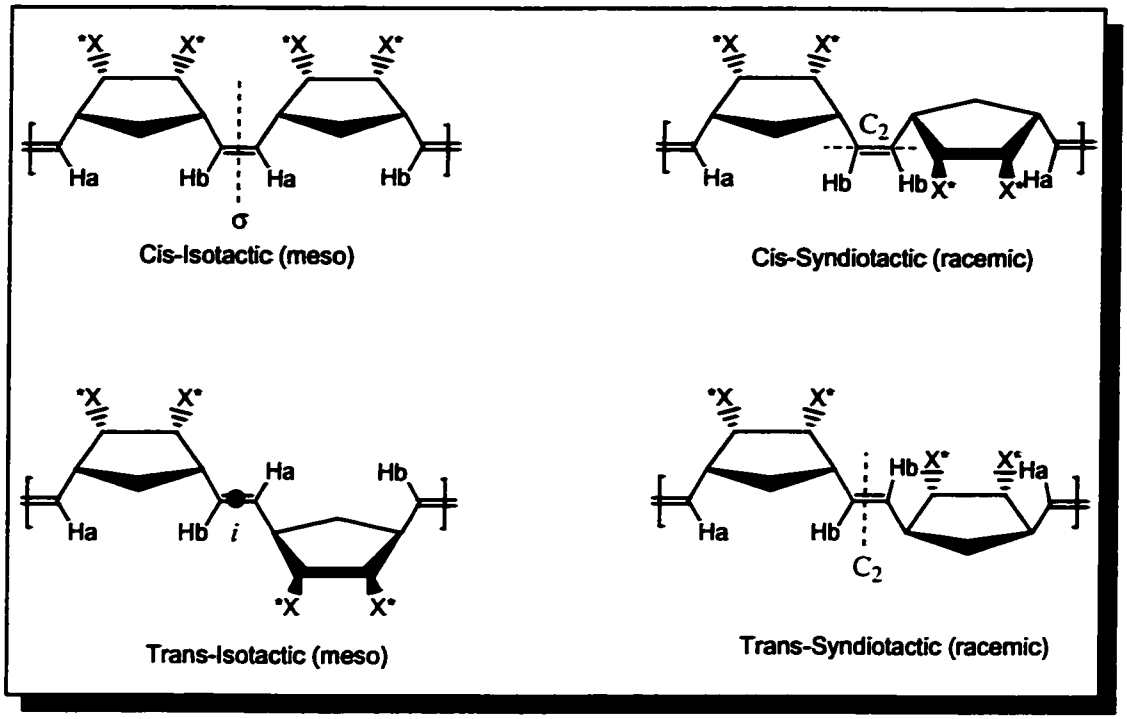

Figure 1. 12. Possible Dyad Stereotacticities for Norbornene/Norbornadiene Systems (X* is chiral)

The olefinic protons (H_a and H_b) in an isotactic polymer reside on the same double bond, and are therefore coupled, resulting in a cross-peak in the ^1H-^1H COSY NMR spectrum. For syndiotactic polymers, the olefinic protons (H_a and H_b) do not reside on the same double bond, and thus do not couple (Figure 1. 12). In consequence, syndiotactic polymers do not have a cross-peak between olefinic protons in the ^1H-^1H COSY NMR spectrum. Cross-peaks would also be observed for an atactic polymer which would

contain a mixture of meso and racemic dyads. The tacticity (or atacticity) of the polymer sample is thus readily evaluated by inspection of the $^{13}C\{^{1}H\}$ NMR spectrum. Spectra containing multiple signal splittings per carbon indicate atactic polymers. Consequently, spectra of tactic polymers contain relatively few signals per carbon.

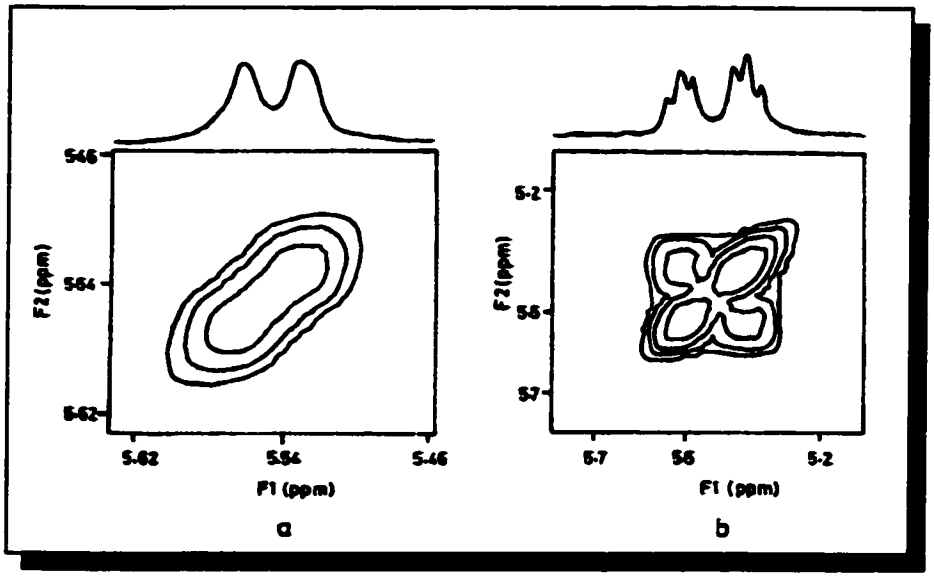

Figure 1. 13. Olefinic Region of the COSY Spectra for an Unsymmetrical Norbornadiene Monomer (a) high trans syndiotactic, (b) high cis isotactic)[31]

1.2.4.2 Polymers Made From Symmetrical Monomers

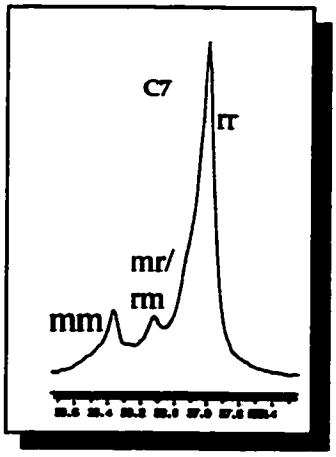

Figure 1. 14. Carbon NMR Signal for C_7

^{1}H-^{1}H COSY NMR analysis cannot be used to evaluate the tacticity of polymers derived from symmetrical monomers in which no chirality is present. In this case, tacticity estimation can be made only from integration of the C_7 signals (Figure 1. 11). As previously stated, C_7 exhibits fine structure arising from the presence of different triads, resulting in three signals centered at approximately 40 ppm: $\delta_{mm} > \delta_{mr/rm} > \delta_{rr}$ (where m = meso, r = racemic). Though this method is only an

estimation rather than an absolute measurement, the results agree well with those obtained for polymers made using the same catalyst and subjected to an absolute determination.

1.3 Helical Polymers

Polymers with precisely defined microstructure are of interest for their potential to exhibit well-defined macrostructures. This phenomenon is common in nature: biopolymers such as DNA, for example, exhibit a double helix, while various proteins and peptides exist as folded sheets and single helices.[2] Natural biopolymers such as DNA, maintain their helical shape in solution as a result of hydrogen bonding between base pairs.[32] Many synthetic chiral polymers have a helical structure in the solid state, but exist as random coils in solution.[33] Addition of bulky side groups can prevent "unwinding" or helix-coil transitions by steric repulsion between the bulky groups, such as that seen for poly(isocyanides)[6], poly(guanidines)[7] and poly(methyl methacrylates)[34]. Helices are described using many parameters, but the most useful is the number of repeat units per turn of the helix. For example, poly(isocyanides) have a 4/1 structure (4 repeat units for one turn of the helix) whereas poly(isocyanates) have an 8/3 structure.

Techniques for producing chiral polymers fall into three classes. In *asymmetric synthesis polymerization*, chiral templates attached to prochiral monomers enforce chiral synthesis of the main chain. Once the polymerization is complete, the chiral template is removed to yield a polymer with main-chain chirality (Figure 1. 15).[35] *Helix-sense selective*

polymerization is carried out using either a chiral initiator, or a chiral monomer to produce a single-screw sense. The single-screw sense is maintained in solution by steric repulsion of the side groups.[35] Both asymmetric synthesis and helix-sense selective polymerizations generate chiral centres along the main chain, and hence a chiral polymer. *Enantiomer-selective polymerization* relies on selective polymerization of one enantiomer in solution to produce a chiral polymer.[35] There are a few examples of stable synthetic helical polymers, of which four are described in the following sections. Only small changes in helical structure are possible through changes in substituents for these synthetic helical polymers given the small number of bonds per helical turn.

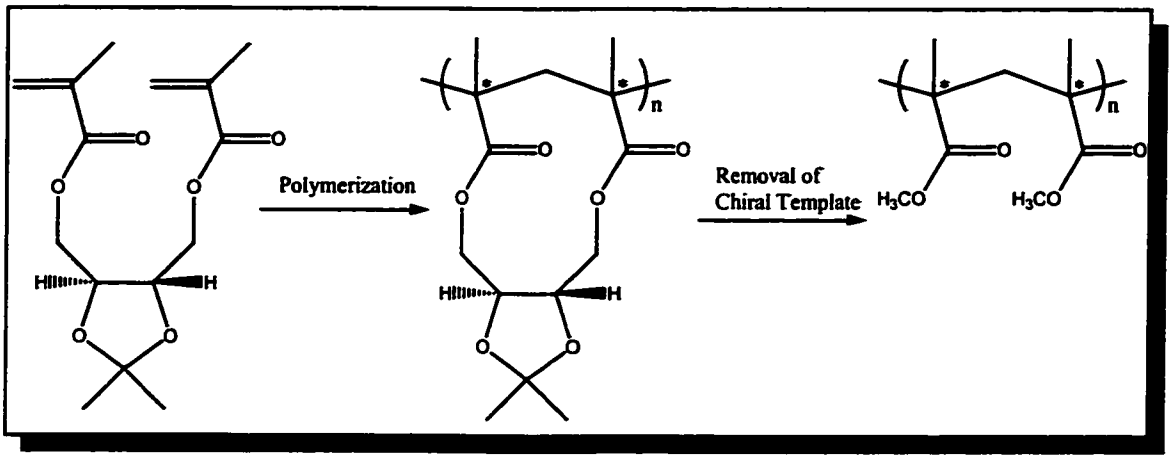

Figure 1. 15. Asymmetric Synthesis Polymerization of Poly(Methyl Methacrylate) Using a Chiral Template

1.3.1 Poly(isocyanides)

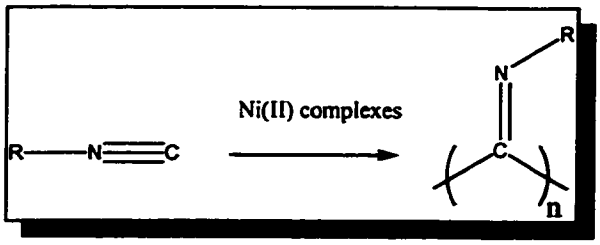

Helix-sense selective polymerization has been employed to general helical poly(isocyanides) with a 4/1 structure

Figure 1. 16. Poly(isocyanide)

(Figure 1. 16). The helicity is stable, or retained in solution, where the side group is sufficiently bulky to restrict rotation around the single bonds of the backbone. There are two ways of accomplishing helix-sense selective polymerization of isocyanides. If a chiral group is substituted on the monomer (R), polymerization with catalyst A (Figure 1. 17) will yield an excess of one hand of the helix. It is also possible to favour one hand of the helix for achiral isocyanides, by substituting the trifluoro-methyl group of complex A for groups B or C in Figure 1. 17.

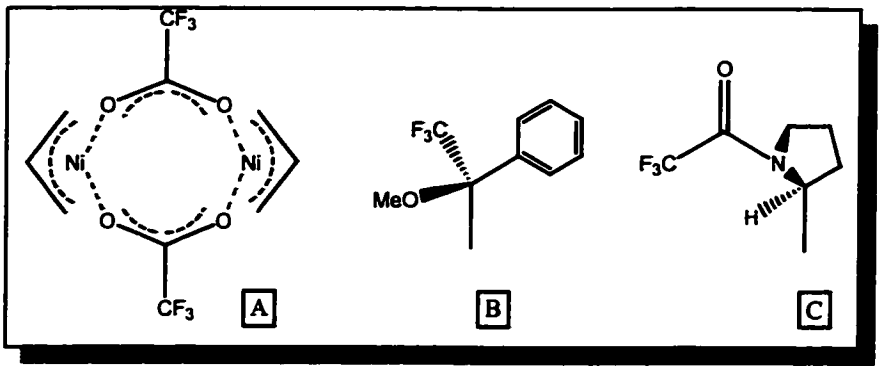

Figure 1. 17. Living Ni(II) Catalyst for Polymerization of Isocyanides (A) non-helix-sense selective polymerization, (B) and (C) helix-sense selective polymerization)

Nolte and co-workers were the first to demonstrate that tert-butyl isocyanide polymerized with nickel(II) salts existed as a mixture of stable right and left-handed helices.[36, 37] The mixture was chromatographically resolved on a chiral support medium composed of poly((+)-sec-butyl isocyanide), itself obtained via polymerization of enantiomerically pure S-C≡N-CH(CH_3)CH_2CH_3.[6, 37] The lowest energy conformation of the chiral support (poly((+)-sec-butyl isocyanide)) is of the left-handed screw (M-helix), as a result of better steric fitting of the substituents along the polymer chain. Screws of opposing senses adhere in a more compact fashion. Based on this rationale, Nolte proposed that the

column should retain the right-handed helix (P-helix), with the left-handed or M-helix eluting first.

1.3.2 Poly(isocyanates)

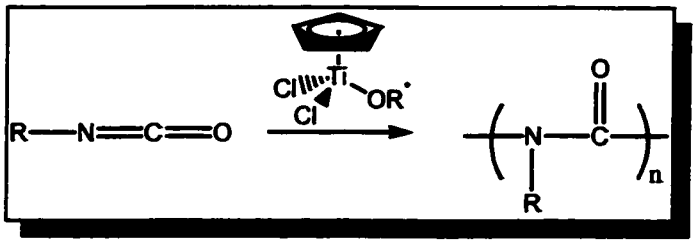

Figure 1. 18. Poly(isocyanate)

Isocyanates can also be polymerized to yield helices that exhibit an 8/3 structure in both the solid and solution states.[38] They are polymerized by titanium(IV) alkoxides of the form shown in Figure 1. 18. Although the poly(isocyanates) are similar to poly(isocyanides), the helical inversion barrier is very low (3-5 kcal/mol). Even where one "hand" of the helical polymer is synthesized, it will quickly racemize to yield equal amounts of both hands of helices in solution. The chain likely consists of rigid helical segments separated by helical reversals or bends in the chain.[39]

1.3.3 Poly(guanidines)

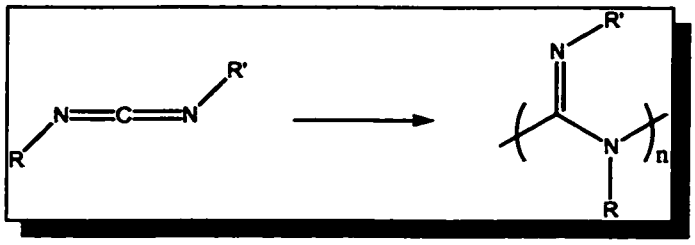

Figure 1. 19. Poly(guanidine)

Polymerization of carbodiimides to yield poly(guanidines) (6/1 helix) is effected using the Ti(IV) alkoxides described above.[7] The intent of substituting the carbonyl in the isocyanates with a bulky imine, was to combine the rigidity of helical

poly(isocyanates) with the high inversion barrier of the poly(isocyanides). The conformation of the helix in solution depends on the substituent side chains (R and R′ in Figure 1. 19.).[40] The polymer exists as an extended or stretched random coil when R is a long alkyl chain, and as a true rigid rod when R is a bulky chiral group.

1.3.4 Poly(methacrylates)

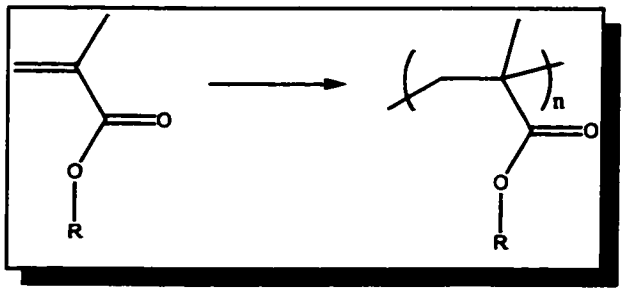

Figure 1. 20. Poly(methyl methacrylate)

Methacrylates and methyl methacrylates can be polymerized either by anionic or radical methods to produce highly isotactic polymers that display optical activity when the ester substituents are of significant bulk (R=CPh_3).[35] The polymer chain had a 7/2 helical structure, as determined by X-Ray crystal analysis.[41] Helical chains of poly(methacrylates) have a high inversion barrier, so that they are 'locked' in their original conformations.[34] Chiral anionic polymerization of methyl methacrylates is carried out with an anionic initiator (DPEDA-Li), in combination with an optically active chiral diamine (Figure 1. 21) to generate the chiral environment. The result is an excess of one helical sense over the other. [42]

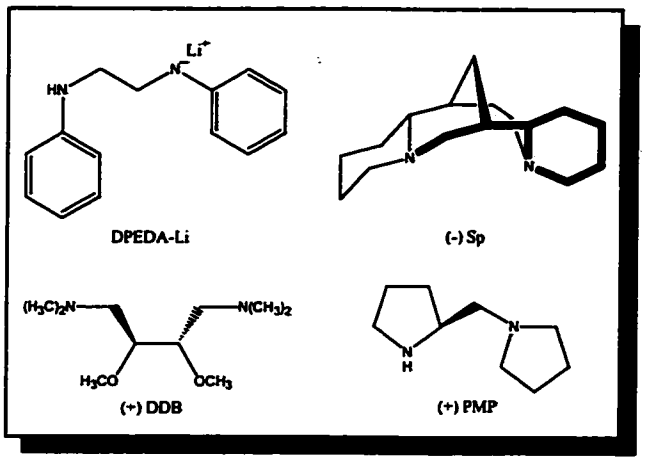

Figure 1. 21. Anionic Initiator and Optically Active Diamines

Radical polymerization, on the other hand, generates an equimolar mixture of right- and left- handed helices, which can be resolved by HPLC, as done for poly(tert-butyl isocyanide).[35] However, use of a chiral ester substituent permits formation of a single hand of the helix.[43] Formation of a single helix-sense is preferred, to avoid the need for resolution of the two senses.

1.4 Molecular Modelling

The exponential growth of computing power over the last half of the 20th century, has paved the way for better theoretical prediction of chemical reactions. In this thesis, a simple form of empirical calculations, molecular mechanics, is used to predict polymer macrostructure. Empirical calculations, such as molecular mechanics, ignore the motion of electrons and calculate the energy as a function of nuclear positions. Molecular mechanics calculations are much faster, and often just as precise as more sophisticated methods of calculation, given that they are based upon real molecules.[44]

1.4.1 Theory of UFF (Universal Force Field)[45-49]

Molecular mechanics functions by comparing a computer generated molecule to a force field (which is a set of bond lengths and angles for various atoms), and changing these values to their lowest potential energy conformation. Computer programs encompassing existing work on force fields for molecular mechanics were first written by Allinger and his co-workers in the 1970's (MME, MMP2, MM3).[50] These force fields were limited to particular combinations of atoms such as those used in organic chemistry. Though they were continually improved upon, they could not consistently predict molecular structure for all different types of molecules.

Rappé and his colleagues developed the Universal Force Field (UFF) in an effort to create a more broadly applicable force field, usable for organics, inorganics, organometallics, etc. The UFF is made up of 126 atom types whose parameters (bond radii and angle, various non-bonding terms and effective charge) are based on the element, its hybridization and connectivity. All of the parameters for each atom type were determined by comparison with various organic, inorganic and organometallic complexes.[45] For any given molecule, the potential energy of the molecule can be described as a sum of valence interactions (E_R), angular distortions (E_θ, E_ϕ, E_ω) and non-bonded interactions (E_{vdw}, E_{el}):

$$E = E_R + E_\theta + E_\phi + E_\omega + E_{vdw} + E_{el}$$

Equation 1

E_R = Bond Stretching
E_θ = Bond Angle Bending
E_ϕ = Dihedral Angle Torsion
E_ω = Inversion Term
E_{vdw} = van der Waals Energy
E_{el} = Electrostatic Energy

Valence interactions are responsible for the bond stretching (E_R) term in Equation 1. For any bond, the natural bond length is a sum of the single atom radii, the bond correction and an electronegativity correction. Still, a true bond will stretch and this must be taken into account. This stretch can be described either by a harmonic oscillator (Equation 2) or the Morse function (Equation 3), the latter of which gives a more accurate description since it includes a bond dissociation energy (D_{ij}) as well an anharmonic terms near the equilibrium bond length (r_{ij}).

$$E_R = \frac{1}{2} k_{ij}(r - r_{ij})^2$$

Equation 2 Harmonic Oscillator

$$E_R = D_{ij}[e^{-\alpha(r-r_{ij})} - 1]^2$$

Equation 3 Morse Function

k_{ij} = bond force constant
r_{ij} = equilibrium bond length
D_{ij} = bond dissociation energy
$\alpha = [k_{ij}/2D_{ij}]^{1/2}$

Angular distortions are the second part of the potential energy expression (Equation 1). Bond angle bending (E_θ), dihedral angle torsion (E_ϕ) and the inversion terms (E_ω) all describe different portions of bends and twists exhibited by the molecule. All three terms are expressed as Fourier expansions since they can be constructed to have the appropriate distortions found in molecular dynamics.[45]

A natural bond angle of θ_o was determined from a standard set of reference structures. A cosine Fourier expansion described in Equation 4 relates the potential energy of bond angle bending to the angle (θ). The coefficients, C_n are chosen to reflect the geometry of the molecule and satisfy appropriate boundary conditions.

$$E_\theta = K_{ijk} \sum_{n=0}^{m} C_n \cos n\theta$$

Equation 4 Bond Angle Bending

$$E_\phi = K_{ijkl} \sum_{n=0}^{m} C_n \cos n\phi_{ijkl}$$

Equation 5 Dihedral Angle Torsion

$$E_\phi = \tfrac{1}{2} V_\phi [1 - \cos n\phi_o \cos n\phi]$$

Equation 6 Dihedral Angle Torsion

K_{ijk} = bond angle bend constant
K_{ijkl} = dihedral angle torsion constant
n = periodicity
C_n = coefficients
$V_\phi = 2K_{ijkl}$ = torsional barrier
ϕ_o = equilibrium torsion angle

Equation 5 describes dihedral angle torsion energy (E_ϕ) in a similar fashion to bond angle bending. Torsion or the twisting of two bonds (IJ and KL) connected by a third (JK) has a rotational barrier (V_ϕ), which determines K_{ijkl} and C_n. The coefficients were chosen so that $E_\theta = 0$ at $\theta = \theta_o$ and similarly for E_ϕ.

$$E_\omega = K_{ijkl}(C_0 + C_1 \cos\omega_{ijkl} + C_2 \cos 2\omega_{ijkl})$$

Equation 7 Inversion Terms where ω_{ijkl} = angle between IL axis and the IJK plane

Inversion terms (Equation 7) describe the inversion associated with atom I bonded to atoms J, K and L. The reference inversion terms are again obtained from the standard set of structures. Again, the coefficients Cn were chosen so that $E_\omega = 0$ at $\omega = \omega_o$.

The van der Waals energy (E_{vdw}) and electrostatic energy (E_{el}) make up the non-bonded interactions for the potential energy expression. The van der Waals expression is based on a 6-12 Lennard-Jones form where ζ is a shape parameter constant for each atom type (Equation 8). The electrostatic attraction and repulsion are described by the standard Coulombic expression in Equation 9.

$$E_{vdw} = \left[G_{ij} \left(\frac{6}{\zeta - 6} \right) e^{\zeta} \right] e^{-\zeta \left(a / a_{ij} \right)} - \frac{\left[G_{ij} \left(\frac{\zeta}{\zeta - 6} \right) a_{ij}^{6} \right]}{a^{6}}$$

Equation 8 van der Waals Terms

G_{ij} = well depth
a_{ij} = van der Waals bond length
a=distance between atoms i and j
ζ = shape parameter
ε = dielectric constant (1)
Q_i = charge on atom i
Q_j = charge on atom j

$$E_{el} = 332.0637 \left(\frac{Q_i Q_j}{\varepsilon a_{ij}} \right)$$

Equation 9 Electrostatic Terms

In order to test the Universal Force Field (UFF), several organic, inorganic and organometallic complexes with known X-ray crystal structures were compared to computer models minimized by UFF.[46, 47, 49] In most cases the UFF structure was accurate within 0.02Å for bond lengths and 3° for bond angles. Errors increased for molecules with charge and congested structures. However, the largest errors are on the order of 0.1-0.2Å for bond lengths and 10-15° for bond angles for odd main group compounds.

1.5 Scope of this Work

The goal of this project was to undertake a computer modelling survey of norbornene and norbornadiene polymers in order to identify structural features associated with a helical structure, and to assess the effect of these features on helical pitch and radius. Variables studied include: substituent, tacticity, tether type (ester vs. ether), tether length, C_5 atom type (carbon vs. oxygen). Some representative monomers (Table 1. 2. and Figure 1. 22.)

were polymerized and their micro- and macro-structures were characterized spectroscopically by NMR, GPC/LS, polarimetry and CD.

Table 1. 2. Polymers Studied

Monomer	*Catalyst*	*Polymer Reference #*
1	A	1A
1	B	1B
2	A	2A
3	A	3A
3	B	3B
4	A	4A
4	B	4B
4	C	4C

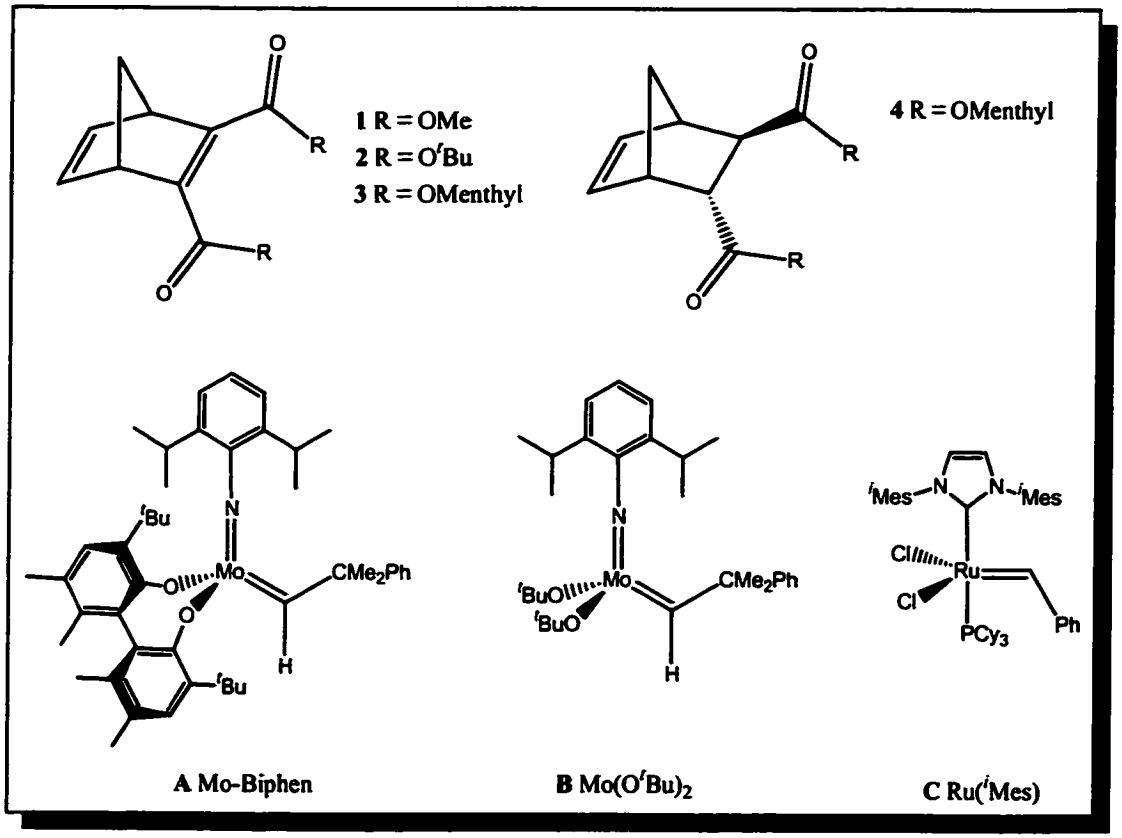

Figure 1. 22. Monomers and Catalysts Studied

1.6 References

1. Webster, O.W. *Science*, **1991**, *251*, 887

2. Ege, S.N. *Organic Chemistry: Structure and Reactivity*, D.C. Heath and Company, Toronto, **1994**,p.1229

3. Ziegler, K. *Angew. Chem.*, **1936**, *49*, 499

4. Natta, G. *J. Polymer Sci.*, **1955**, *16*, 143

5. Natta, G. *Sci. Amer.*, **1961**, *205*, 33

6. Nolte, R.J.M. *Chem. Soc. Rev.*, **1994**, 11

7. Goodwin, A.,Novak, B.M. *Macromolecules*, **1994**, *27*, 5520

8. Okamoto, Y., Suzuki, K., Ohta, K., Hatada, K.,Yuki, H. *J. Am. Chem. Soc.*, **1979**, *101*, 4763

9. Carraher, C.E. *Polymer Chemistry: 5th Edition, Revised and Expanded*, Marcel Dekker Inc., New York, **2000**, p.22

10. Ivin, K.J.,Mol, J.C. *Olefin Metathesis and Metathesis Polymerization*, Academic Press, Toronto, **1997**,p.5

11. Ivin, K.J.,Mol, J.C. *op. cit*, **1997**, p.7

12. Schrock, R.R. *Acc. Chem. Res.*, **1990**, *23*, 158

13. Michelotti, F.W.,Keaveney, W.P. *J. Polymer Sci.*, **1965**, *A3*, 895

14. Hamilton, J.G., Ivin, K.J.,Rooney, J.J. *J. Mol. Catal.*, **1985**, *28*, 255

15. Devine, G.I., Ivin, K.J., Mohamed, M.A.,Rooney, J.J. *J. Chem. Soc., Chem. Commun.*, **1982**, 1229

16. Ivin, K.J., Laverty, D.T.,Rooney, J.J. *Makromol. Chem.*, **1977**, *178*, 1545

17. Ivin, K.J., Reddy, B.S.R.,Rooney, J.J. *J. Chem. Soc., Chem. Commun.*, **1981**, 1062

18. Howard, T.R., Lee, J.B.,Grubbs, R.H. *J. Am. Chem. Soc.*, **1980**, *104*, 7491

19. Schrock, R.R., Rocklage, S.M., Wengrovius, J.H., Rupprecht, G.,Fellmann, J. *J. Mol. Catal.*, **1980**, *8*, 73

20. Gilliom, L.R.,Grubbs, R.H. *J. Am. Chem. Soc.*, **1986**, *108*, 733

21. Schaverien, C.J., Dewan, J.C.,Schrock, R.R. *J. Am. Chem. Soc.*, **1986**, *108*, 2771

22. Bazan, G.C., Khosravi, E., Schrock, R.R., Feast, W.J., Gibson, V.C., O'Regan, M.B., Thomas, J.K.,Davis, W.M. *J. Am. Chem. Soc.*, **1990**, *112*, 8378

23. Feast, W.J., Gibson, V.C.,Marshall, E.L. *J. Chem. Soc., Chem. Commun.*, **1992**, 1157

24. McConville, D.H., Wolf, J.R.,Schrock, R.R. *J. Am. Chem. Soc.*, **1993**, *115*, 4413

25. O'Dell, R., McConville, D.H., Hofmeister, G.E.,Schrock, R.R. *J. Am. Chem. Soc.*, **1994**, *116*, 3414

26. Totland, K.M., Boyd, T.J., Lavoie, G.G., Davis, W.M.,Schrock, R.R. *Macromolecules*, **1996**, *29*, 6114

27. Schrock, R.R., Lee, J.-K., O'Dell, R.,Oksam, J.H. *Macromolecules*, **1995**, *28*, 5933

28. Oskam, J.H.,Schrock, R.R. *J. Am. Chem. Soc.*, **1992**, *114*, 7588

29. Oskam, J.H.,Schrock, R.R. *J. Am. Chem. Soc.*, **1993**, *115*, 11831

30. Moore, J.S. *Transition Metals in Polymer Synthesis: Ring-opening Metathesis Polymerization and Other Transition Metal Polymerization Techniques*, in Comprehensive Organometallic Chemistry II, vol.**12**, p.1222, Abel, E.W., Stone, F.G.A.,Wilkinson, G. ed., Elsevier Science Inc., New York, **1995**

31. Hamilton, J.G. *Polymer*, **1998**, *39*, 1669

32. Ege, S.N. *op. cit.*, **1994**, p.1251

33. Heintz, A.M.,Novak, B.M. *Polymer Preprints*, **1998**, *39*, 429

34. Nakano, T., Okamoto, Y.,Hatada, K. *J. Am. Chem. Soc.*, **1992**, *114*, 1318

35. Okamoto, Y.,Nakano, T. *Chem. Rev.*, **1994**, *94*, 349

36. Nolte, R.J.M., Van Beijnen, A.J.M.,Drenth, W. *J. Am. Chem. Soc.*, **1974**, *96*, 5932

37. Van Beijnen, A.J.M., Nolte, R.J.M., Drenth, W.,Hezemans, A.M.F. *Tetrahedron*, **1976**, *32*, 2017

38. Goodman, M.,Chen, S. *Macromolecules*, **1970**, *3*, 398

39. Novak, B.M., Goodwin, A.A., Schlitzer, D., Patten, T.E.,Deming, T.J. *Polymer Preprints*, **1996**, *37*, 446

40. Nieh, M.-P., Goodwin, A.A., Stewart, J.R., Novak, B.M.,Hoagland, P.A. *Macromolecules*, **1998**, *31*, 3151

41. Nakano, T., Ute, K., Okamoto, Y., Matsuura, Y.,Hatada, K. *Polym. J.*, **1989**, 935

42. Okamoto, Y., Nakano, T., Habaue, S., Shiohara, K.,Maeda, K. *J.M.S. Pure Appl. Chem.*, **1997**, *A34*, 1771

43. Nakano, T., Mori, M.,Okamoto, Y. *Macromolecules*, **1993**, *26*, 867

44. Leach, A.R. *Molecular Modelling: Principles and Applications*, Addison Wesley Longman Ltd., London, **1996**, p.131

45. Rappe, A.K., Casewit, C.J., Colwell, K.S., Goddard, W.A.,Skiff, W.M. *J. Am. Chem. Soc.*, **1992**, *114*, 10024

46. Casewit, C.J., Colwell, K.S.,Rappe, A.K. *J. Am. Chem. Soc.*, **1992**, *114*, 10035

47. Casewit, C.J., Colwell, K.S.,Rappe, A.K. *J. Am. Chem. Soc.*, **1992**, *114*, 10046

48. Castonguay, L.A.,Rappe, A.K. *J. Am. Chem. Soc.*, **1992**, *114*, 5832

49. Rappe, A.K., Colwell, K.S.,Casewit, C.J. *Inorg. Chem.*, **1993**, *32*, 3438

50. Allinger, N.L. *J. Am. Chem. Soc.*, **1977**, *99*, 8127

CHAPTER 2

EXPERIMENTAL PROCEDURES AND TECHNIQUES

2.1 General Protocol for MSI Cerius²

2.1.1 Creation of Models

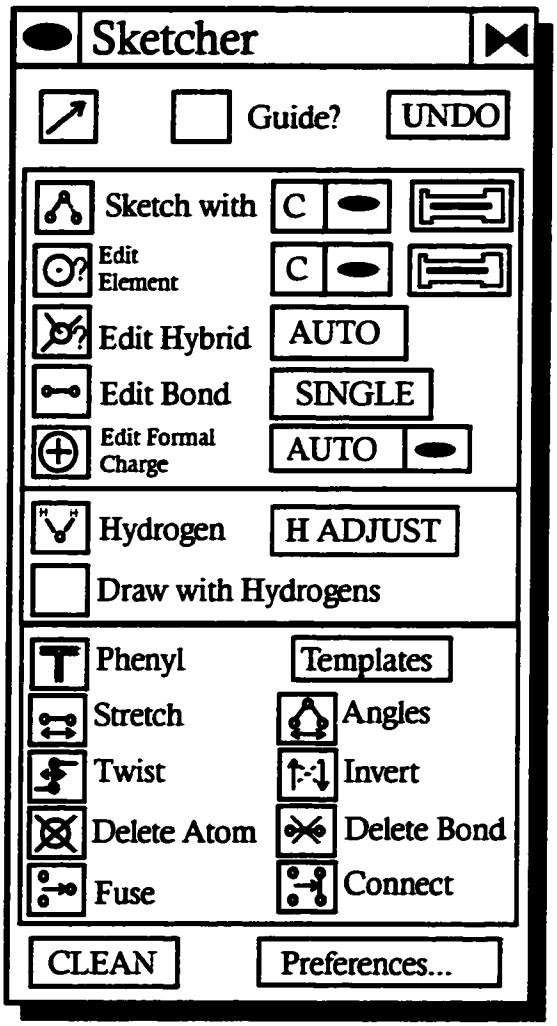

Figure 2. 1. Sketcher Card in Cerius²

Molecules used for any manipulation or calculations are drawn into the visualizer window by using the sketcher card shown on the left. The molecule sketcher tools (Figure 2. 1) are accessed by clicking on 'Build' in the toolbar, and choosing '3D-Sketcher' from the list. The molecule is drawn in using the tools in the card. The view of the molecule is rotated using the right mouse button, translated with the middle button and sized by pressing shift and the middle mouse button together.

2.1.2 Polymer Builder

Building polymers in the Cerius[2] program consists of drawing in the repeat unit, transforming it into a "monomer" suitable for the program and then into a polymer. Before the repeat unit in the window can be considered a "monomer" by the program, a head and tail must be defined by choosing 'Edit' then 'Monomer' on the 'Polymer Builder' card. The atoms defined as the head and tail between repeat units are eliminated upon "polymerization".

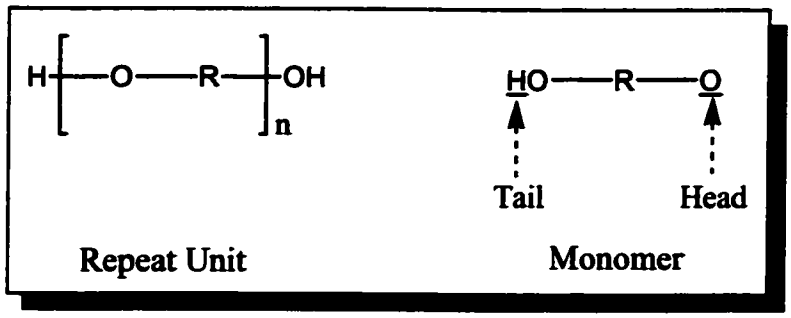

Figure 2. 2. Head and Tail Definitions for a Diol Polymer

Using the polymerization of a diol as an example (Figure 2. 2), the proton and oxygen indicated would be defined as the head and tail of the monomer. The proton that would be attached to the head is eliminated from the "monomer" so as to prevent "floating" or non-attached hydrogens in the polymer model. It is good practice to save the "monomer" model at this point since the model will be lost upon polymerization. In order to model norbornene and norbornadiene systems, the true monomer had to be ring-opened to create an artificial monomer for the program (Figure 2. 3).

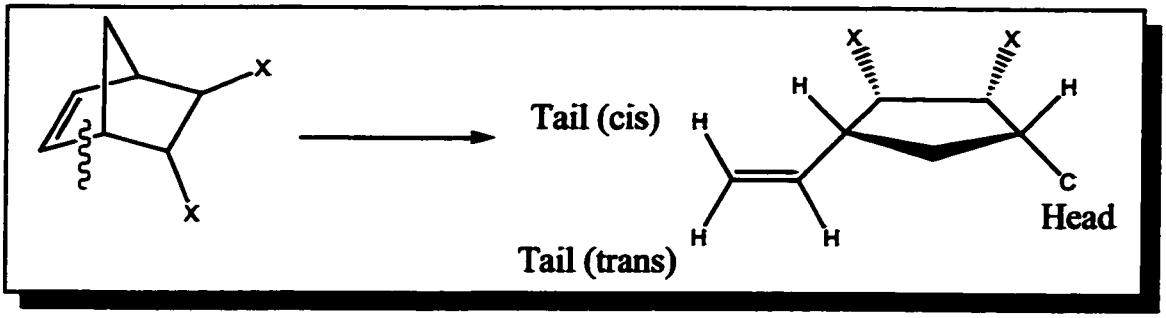

Figure 2. 3. Ring-Opened Norbornene/Norbornadiene Monomer in Cerius[2]

After minimizing the "monomer" model structure to its lowest energy through repeated dynamics/minimization cycles as described in the following sections, the polymer is built by opening the 'Homopolymer' module in the 'Polymer Builder' card and entering the number of "monomers" to be joined together.

2.1.3 Force Field Minimization

When drawn, most models are not in their most favourable conformation and their energy must be minimized. The Open Force Field (OFF) method of energy minimization finds the conformation of lowest energy. Cerius[2] uses the Universal Force Field (UFF) described in a series of papers by Rappé, Casewit, Colwell, Goddard, Skiff and Castonguay as a default. [1-3] This standard force field approximates the structure of the molecule within 0.1Å bond distance and 5-10° bond angle. The 'Energy Minimizer' module is under the 'OFF Methods' card. The minimization is re-started until the energy no longer changes. The number of iterations depends on the size of the molecule, and how distorted the starting structure is from its lowest-energy conformation.

2.1.4 Dynamics Simulation

A structure minimized by the OFF method may not necessarily lie in the global minimum of its energy curve but in a local minimum of higher energy. In order to find the global minima for the structure, the structure must be perturbed from the local minimum by applying a dynamics cycle. The 'Dynamics Simulation' module is also under the 'OFF Methods' card and it uses the same Universal Force Field (UFF) protocol described by Rappé et al. [1-3] The temperature is varied from 300 K to 1000 K in order to give the molecule enough perturbation to move out of the local minimum.

2.1.5 First Method of Polymer Survey

The repeat unit or "monomer" structures shown in Figure 2. 3 and Figure 2. 4 were subjected to several dynamics/minimization cycles until no further change in energy and conformation were observed. If the repeat unit is assembled in a simple head-to-tail manner, the result is an isotactic polymer. Syndiotactic structures can be broken down into regularly repeating dyads. In these cases, the racemic dyads are drawn and treated as monomers for the purpose of producing models of these oligomers (Figure 2. 4). Models were built with either 25 or 50 repeat units by using the polymer builder. The resulting oligomer model was then minimized using the standard UFF. Once the oligomers had been minimized, measurements such as number of repeat units per helical turn, helical pitch, inner diameter and length were made (Figure 2. 5).

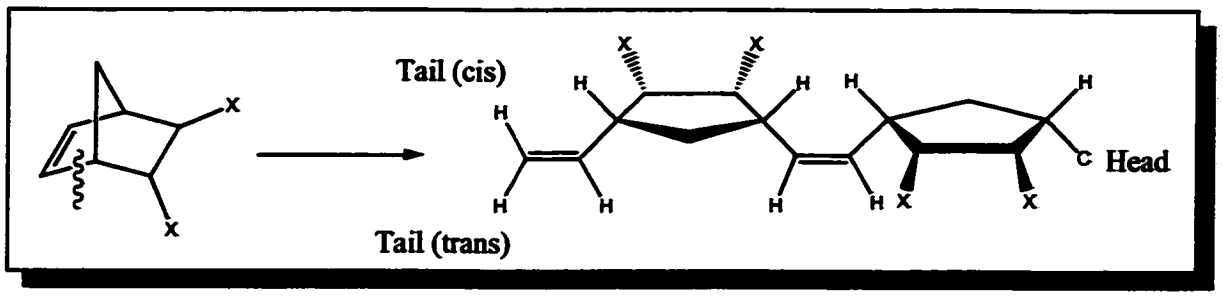

Figure 2. 4. Repeat Unit (Dyad) for Non Cis-Isotactic Polymers of Norbornene/Norbornadiene

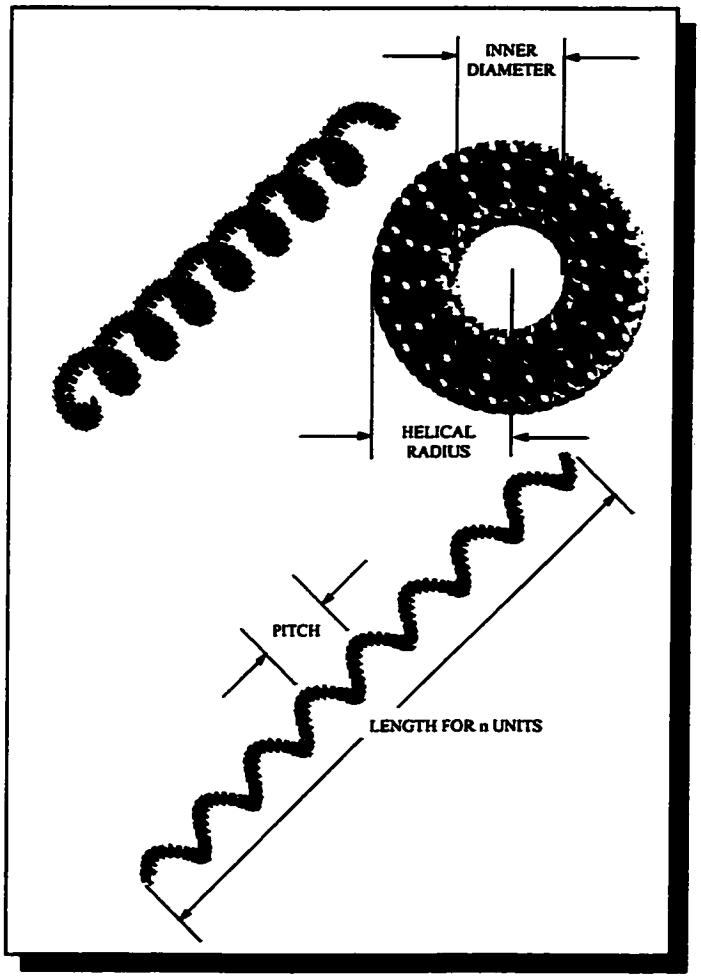

Figure 2. 5. Definition of Helical Parameters for a General Helix

2.1.6 Second Method of Polymer Survey

The most promising candidates from the first survey were more rigorously modeled through consideration of internal torsion angles of polymer dyads.

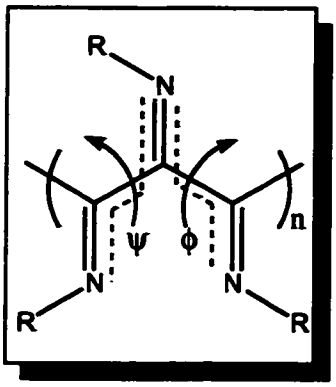

Figure 2. 6. Torsion Angle Definitions on Poly(isocyanide)

All helical polymers can be described by the main chain torsion angles ψ and ϕ which repeat regularly throughout the polymer chain. Polymer systems where the main chain torsion angles pivot about a single atom (central C in Figure 2. 6) have been studied at length and are well understood. Helical parameters can be calculated for a given set of torsion angles ψ and ϕ by using the relations produced from previous studies. Norbornene and norbornadiene polymers are more complex because of the double bond that separates the two torsion angles (Figure 2. 7). Previously used relations for simple polymers whose torsion angles are only separated by a single atom do not apply to these more complicated polymers.

The appropriate ring-opened dimer (Figure 2. 4) is drawn using the sketcher tools. By repeating the dynamics/minimization cycle, the dimer's lowest energy conformation is determined. The two internal torsion angles ψ and ϕ (Figure 2. 7) located around the central double bond are then determined.

In order to form a regularly repeating structure, the two torsion angles measured from the dyad must repeat regularly throughout the main chain. Therefore, the torsion angle ϕ at f-g-h-i (Figure 2. 7) was measured, and that defined by a-b-c-d was set to ϕ by using the torsion rotation tool. An oligomer with regularly repeating torsion angles was built using the Polymer Builder by setting the polymer torsion angle variable to ψ. The resulting polymer was minimized using the standard UFF and measurements made.

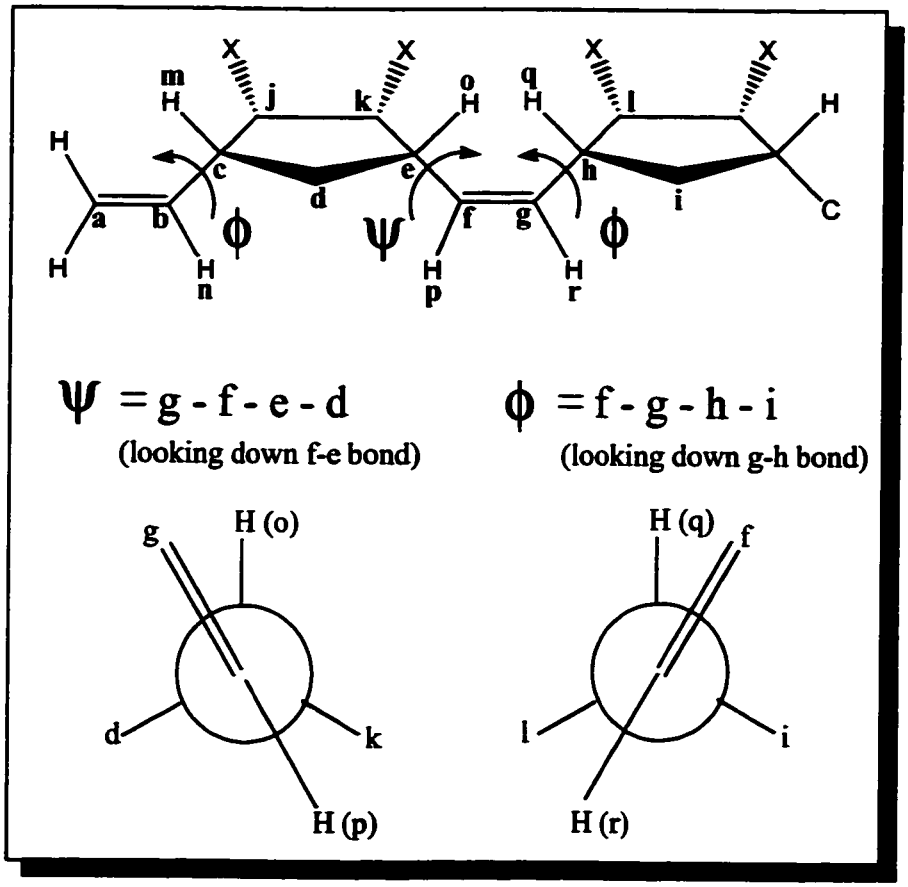

Figure 2. 7. Definition of Torsion Angles for Norbornene/Norbornadiene Polymers

2.2 Materials

Spectral grade and chromatography grade dichloromethane were purchased from Omni-Solv and used without further purification. Deuterated chloroform ($CDCl_3$) was obtained from Canadian Isotopes and used directly. All monomers, catalysts and polymers (listed in Table 1. 2 and Figure 1. 23) produced for this thesis were kindly synthesized by Jennifer L. Snelgrove of this laboratory.

2.3 Instrumentation

Nuclear magnetic resonance (NMR) spectra were recorded on a Varian Gemini 200, Bruker AMX300 or Bruker AMX500 spectrometer, using internal standards or the residual proton or carbon (for ^{1}H and ^{13}C NMR spectra) signals of the solvent. Downfield shifts were taken as positive for all nuclei.

Gel permeation chromatography/light scattering (GPC/LS) was obtained with chromatography grade dichloromethane as eluent at a flow rate of 1.00 mL/min and a sample concentration of approximately 1.0 mg/mL. The high pressure liquid chromatography (HPLC) system was equipped with a Waters model 610 pump, a Rheodyne model 7125 injector with a 200 μL injection loop, Waters HR-4 and HR-3 columns in series, and a Waters model 410 diffraction refractometer. Molecular weights and polydispersities are reported versus commercially available polystyrene standards ranging from 1.3×10^3 to 3.15×10^6 g/mol MW. (laser wavelength is 633nm)

Ultraviolet-visible (UV-vis) spectra were recorded on a Varian Cary 1E spectrophotometer. Circular dichroism (CD) spectra were collected on an Aviv 202 spectrometer with a 450W xenon lamp light source. The cell path length was 1 cm and the solvent was either spectral grade dichloromethane or acetonitrile. Optical rotations were measured on a Perkin-Elmer 241 polarimeter using a sodium lamp of wavelength 589 nm as a light source. All computer simulations were carried out on a Silicon Graphics Inc. (SGI) Octane^2 workstation operating on an IRIX6.4 or IRIX6.5 platform. The Cerius^2 program (version 4.5MS) by Molecular Simulations Inc. (MSI) was used for all modelling work.

2.4 Nuclear Magnetic Resonance Spectroscopy (NMR)

Nuclear magnetic resonance spectroscopy (NMR) has become an indispensable tool for chemical analysis because it is quick, informative and non-destructive. ^{1}H NMR was used to probe the microstructure of synthesized polymers.

^{1}H NMR experiments were also used to verify completion of the polymerization by comparison of the monomer spectrum with that of the polymer. ^{1}H NMR assignments are listed in Table 2. 1. Complete spectra are in appendix A.

•Poly(2,3-dicarbomethoxynorbornadiene) : ^{1}H NMR ($CDCl_3$) δ 5.45 ppm (br, Ha), 3.90 ppm (m, Hc or Hc'), 3.71 ppm (s, CO_2CH_3), 3.52 ppm (m, Hc or Hc'), 2.43 ppm (m, Hb or Hb'), 1.47 ppm (m, Hb or Hb')

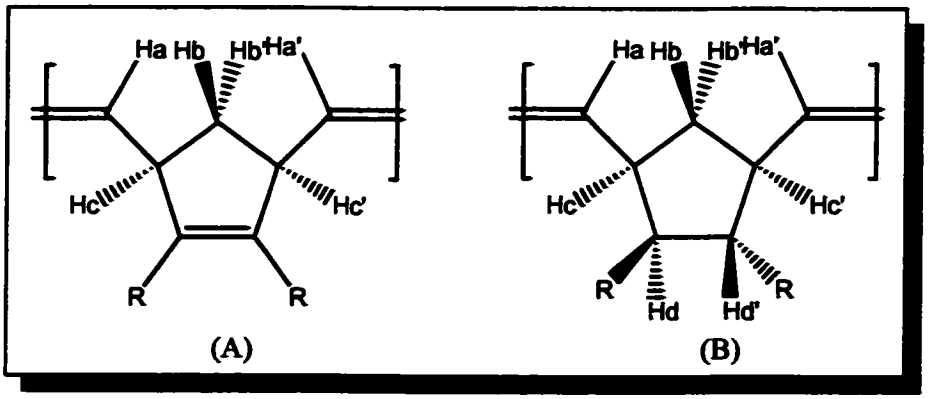

Figure 2. 8. ^{1}H Labelling Scheme for Table 2. 1.

Table 2. 1 ^{1}H NMR Peak Assignments for Norbornadiene (A) and Norbornene (B) Polymers

	A, R=Me		A, R=^{t}Bu	A, R=Menthyl		B, R=Menthyl
	1A (ppm)	1B (ppm)	2A (ppm)	3A (ppm)	3B (ppm)	4A, 4B, 4C (ppm)
Ha, Ha'	5.4	5.4	5.5	5.5, 5.4	5.6	5.5
Hb, Hb'	2.5, 1.5	2.5, 1.5	3.5, 2.5	2.3, 2.0	2.3, 2.0	1.9
Hc, Hc'	3.9, 3.55	3.55	3.8	3.9, 3.8	3.5	3.2, 3.0
Hd, Hd'						2.8, 2.7
R	3.7		1.4	4.6, 1.5,1.4, 1.0, 0.7		4.6, 1.5,1.4, 1.0, 0.7

Proton-decoupled ^{13}C NMR was used extensively for microstructure analysis. Cis/trans ratios can be determined from the olefinic and allylic carbon signals (Ha and Hc respectively, in Figure 2. 8). The allylic carbons have two distinctive and well separated signals for the cis (~45 ppm) and trans positions (~50 ppm). Fine structure can also arise for polymers made from enantiomerically pure unsymmetrical monomers due to head-tail effects.[4] Analysis of fine structure are indirect measures of tacticity in these systems. ^{13}C{^{1}H} NMR assignments are listed in Table 2. 2. Complete spectra are in appendix A.

•Poly(2,3-dicarbomethoxynorbornadiene) : ^{13}C{^{1}H} NMR ($CDCl_3$) δ 165.6 ppm (CO_2CH_3), 142.5 ppm (C_5 and C_6), 132.7 ppm (C_2 and C_3 trans), 131.8 ppm (C_2 and C_3 cis), 52.4 ppm (CO_2CH_3), 49.4 ppm (C_1 and C_4 trans), 44.6 ppm (C_1 and C_4 cis), 38.363 ppm (tr, C_7)

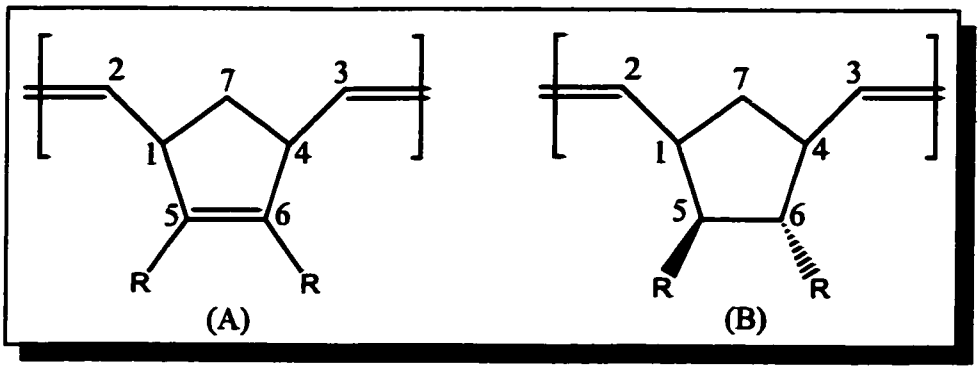

Figure 2. 9. $^{13}C\{^1H\}$ Labelling Scheme for Table 2. 2.

Table 2. 2. $^{13}C\{^1H\}$ NMR Peak Assignments for Norbornadiene (A) and Norbornene (B) Polymers

	A, R=Me		A, R=^{t}Bu	A, R=Menthyl		B, R=Menthyl
	1A (ppm)	1B (ppm)	2A (ppm)	3A (ppm)	3B (ppm)	4A, 4B, 4C (ppm)
CO_2	165.6	165.4	164.6	165, 164.3	164.7, 164.6	173.9
C_2, C_3	132.7 trans 131.8 cis	132.5 trans 131.5 cis	132.8 trans 132.0 cis	132.6, 131.5 cis	132.1 trans	133.7 trans, 131.1,129.9 cis
C_1, C_4	49.4 trans 44.6 cis	49.2 trans 44.2 cis	49.9 trans 44.9 cis	45.6, 44.8 cis	49.4, 49.2 trans	53.4, 52.5 trans 46.3 cis
C_5, C_6	142.6	142.2	142.5	143.8, 140.8	142.7, 141.4	54.4
C_7	39.1 mm 38.4 mr/rm 38.2 rr	38.4 mm 38.1 mr/rm 37.8 rr	40.0 mm 38.7 mr/rm 38.1 rr	39.7	37.9	40.6 (br)
R	52.4		82.0, 28.6	75.4, 47.0, 34.7, 31.9, 25.9, 23.5, 22.5, 21.4, 16.4		

^1H-^1H COSY NMR was used to determine tacticity of polymers made from unsymmetrical monomers. Cross-peaks between olefinic protons indicated isotacticity whereas lack of the cross-peaks indicated syndiotacticity. Results are listed in Table 2. 3. Complete ^1H-^1H COSY NMR spectra are in appendix A.

Table 2. 3. Tacticity Assignments Found by ^{1}H-^{1}H COSY NMR

Polymer	*Tacticity*	*Literature Assignment*	*Reference*
3A	Isotactic	Isotactic	5
3B	Syndiotactic	Syndiotactic	5
4A	Syndiotactic	---------	
4B	Syndiotactic	---------	
4C	Syndiotactic	---------	

2.5 Gel Permeation Chromatography/Light Scattering (GPC/LS)[6-8]

The following discussion is adapted from several polymer texts referenced above. Polymer chains fractionated by GPC are detected by light scattering (LS) and by refractive index (RI) as they are eluted. The measurements of molecular mass (by LS) and specific refractive index increment (dn/dc) by (RI) allow for absolute determination of molecular mass.

By measuring the intensity of scattered light at different angles and hence the Rayleigh ratio (R_θ) for the polymer, the molecular mass of the polymer is calculated using Equation 10. All other variables in the equation are known, given that the differential refractive index (dn/dc) is measured by the RI detector, and we assume that the polymer is in its theta state (or polymer's natural state) in solution. A_2 is thus equal to zero.

$$\frac{Kc}{R_\theta} = \frac{1}{M} + 2A_2c$$

Equation 10

$$K = \frac{4\pi^2 (dn/dc)^2 n_o^2}{N_A^2 \lambda_o^4}$$

Equation 11

K - constant (encompasses all constant parameters for an experiment)
R_θ - Rayleigh ratio (describes the fraction of light scattered at an angle θ)
M - molecular mass of the polymer
A_2 - second virial coefficient (measure of solute-solvent interactions)
c - concentration
n - refractive index

The molecular weight measured by LS is an absolute value because the dn/dc value is measured by the RI detector. As the polymer chains increase in size and become greater than $\lambda/20$ in dimension, destructive interference becomes significant. A particle scattering factor $P(\theta)$ is introduced into the equation to reflect this change.

$$\frac{Kc}{R_\theta} = \frac{1}{MP(\theta)} + 2A_2c$$

Equation 12

$$P(\theta) = 1 + \frac{16\pi^2}{3\lambda^2}\langle r_g \rangle^2 \sin^2(\theta/2)$$

Equation 13

There are limiting cases where this equation can be simplified in order to calculate the molecular weight. For low angle scattering ($\theta = 0$), $P(\theta)$ becomes 1, eliminating the effect of intramolecular scattering. If the solution is infinitely dilute ($c = 0$), intermolecular scattering effects are removed. In essence, one single polymer chain is observed, thus scattering can be described by Equation 14.

$$\frac{Kc}{R_\theta} = \frac{1}{MP(\theta)}$$

Equation 14

A polymer chain in solution can adopt conformations varying from a random coil, to a rod or a sphere. Light scattering, measures the average distance between the two chain ends, and thus gives a partial idea of the chain dimensions. The radius of gyration ($\langle r_g \rangle$), or the root mean square (rms) radius of the polymer, measures the mass distribution of the polymer about its center of mass.

$$\langle r_g \rangle^2 = \sum \frac{r_i^2 m_i}{M}$$

Equation 15 Root Mean Square (rms) Radius

In order to measure the solution conformation of a polymer, the polymer chains must be longer than 10 nm. At shorter lengths, polymer chains do not scatter evenly, which is a condition for measurement of $\langle r_g \rangle$. The conformation of the polymer is deduced from the slope of a log-log plot of $\langle r_g \rangle$ vs M_w, with a slope of 1 indicating a rod, 0.5-0.6 a random coil, and 0.3 a sphere. For example, this technique was used to judge the change of poly(guanidine) conformation from random coil to a rigid rod upon increase of steric bulk in the side chains.[9] The information from the slope and the value of r_g can be combined with Equations 16-19 listed below to give dimensions of the polymer in solution.

Sphere $r = \sqrt{5/3}\, r_g$ **uniform density sphere**

Equation 16

$r = r_g$ **hollow sphere**

Equation17

Random Coil $L = \sqrt{6} r_g$ **average end to end length**

Equation 18

Rigid Rod $L = \sqrt{12} r_g$

Equation 19

2.6 Optical Rotatory Dispersion (ORD)[10]

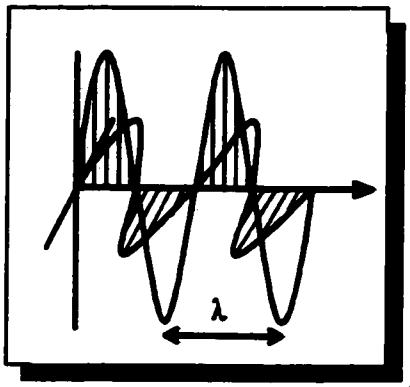

Figure 2. 10. Electromagnetic Radiation

Electromagnetic radiation is composed of electric and magnetic waves that oscillate perpendicular to each other as depicted in Figure 2. 10. Linearly polarized light is obtained by passing light propagating in all directions through a polarizer which selects one plane of light (Figure 2. 11) that has constant direction and varying magnitude.

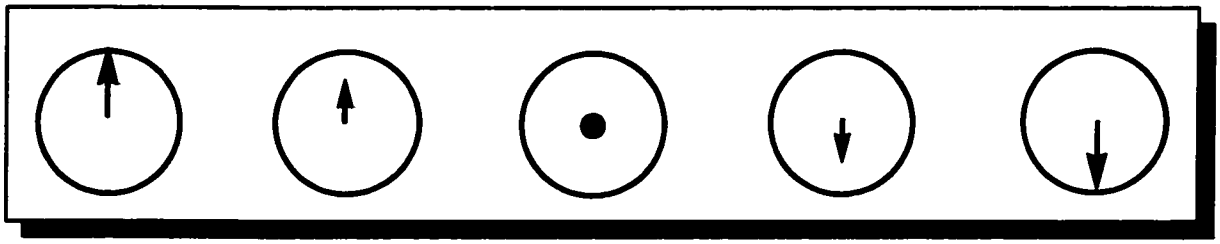

Figure 2. 11. Linearly Polarized Light

Light will interact with molecules to change the direction and/or magnitude of the light. If a sample is chiral or asymmetric, the linearly polarized light will be transformed to an ellipse with the major axis rotated by an angle of ϕ from the incident light as depicted in Figure 2. 12. The ellipse traced out by rotation of the plane of polarized light can also be described as two circularly polarized components with different intensities and refractive indexes (Equation 20).

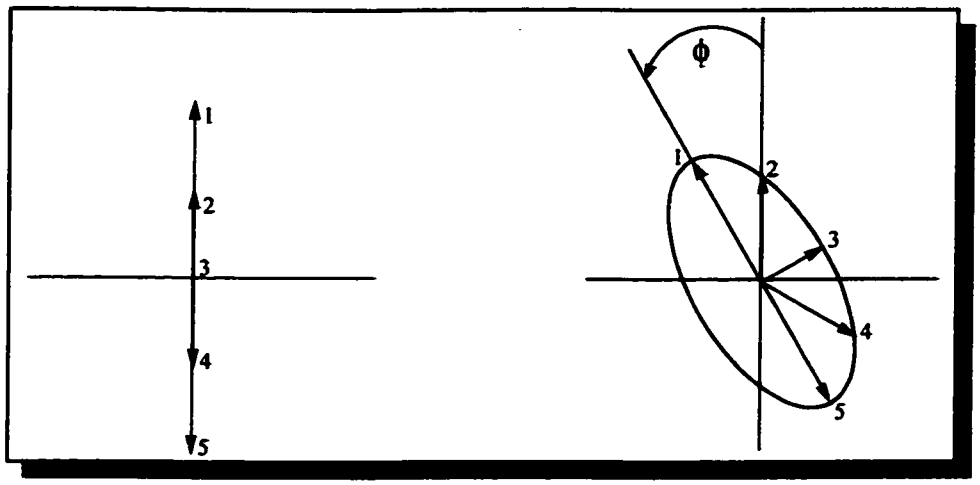

Figure 2. 12. Rotation of Linearly Polarized Light by an Angle ϕ

$$\phi = \frac{180(n_L - n_R)}{\lambda}$$

Equation 20 Angle of Rotation

$$[\phi] = \frac{100\phi}{cl}$$

Equation 21 Optical Rotation

ϕ = angle of rotation
n_L = refractive index (left-hand component
n_R = refractive index (right-hand component
c = concentration
l = length of sample cell

The rotation by the angle ϕ (measured by a polarimeter) can be described in terms of the difference of refractive index between the right and left hand components (n_L and n_R) of the circularly polarized light. Optical rotation, as illustrated by Equation 21, normalizes the rotation to sample concentration (c) and length of the polarimeter cell (l).

2.7 Ultra-Violet-visible (UV-vis) Spectroscopy[11]

UV-vis spectroscopy was not performed, but its discussion is necessary to the understanding of circular dichroism (CD) spectroscopy. Electromagnetic radiation

passing through a sample may be absorbed by that sample from excitation of ground state electrons to an excited state. Typically, the transition is from the highest occupied molecular orbital (HOMO) to the lowest unoccupied molecular orbital (LUMO). The difference between the ground and excited energy states is described by Equation 22. As the energy difference between the two orbitals increases, the wavelength of light absorbed will diminish (move to higher energy).

$$\Delta E = E_{excited} - E_{ground} = h\nu = \frac{hc}{\lambda}$$

h = Planck's constant
c = speed of light
ν = frequency
λ = wavelength

Equation 22

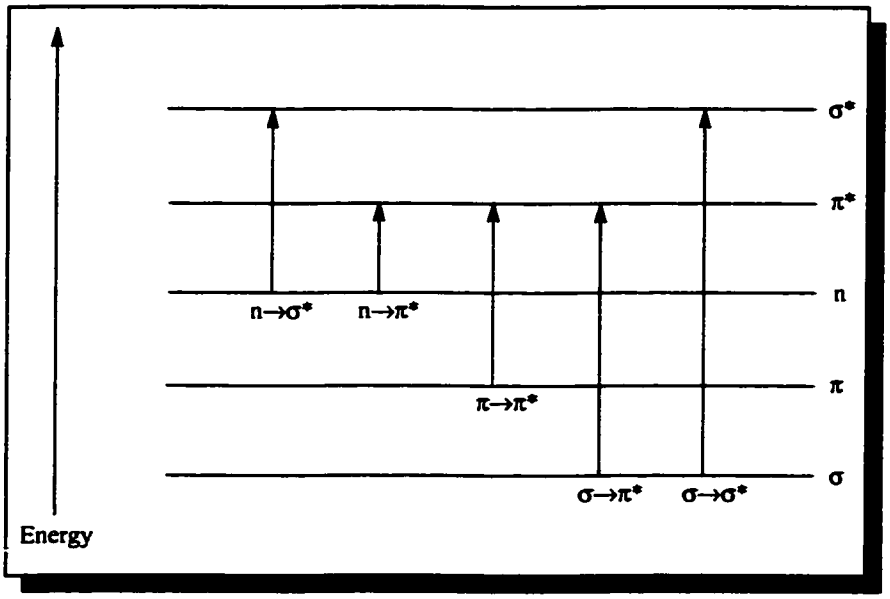

Figure 2. 13. Electronic Energy Levels and Transitions

A given chromophore has unique orbital energy levels resulting from its electronic configuration. Thus, absorption patterns are unique to a particular group of atoms in a molecule and sensitive to changes in structure. Spectra of conjugated systems are typically red-shifted because electron sharing between orbitals results in lower transition

energies. Solvent transparency becomes an issue at very low absorption wavelengths, since the transitions of the solvent may mask those due to the sample.

Alkanes	$\sigma \rightarrow \sigma^*$
Alkenes, Alkynes	$\pi \rightarrow \pi^*$
Alcohols, Ethers, Amines	$n \rightarrow \sigma^*$
Carbonyls	$\pi \rightarrow \pi^*$ and $n \rightarrow \pi^*$

The norbornene and norbornadiene base systems as shown in Figure 2. 14 have very few transitions because of the lack of chromophores. The energy differences between the alkane $\sigma \rightarrow \sigma^*$ and alkene $\pi \rightarrow \pi^*$ orbitals are large, and very low wavelengths are thus observed (180-200 nm). In most cases, the polymers are only soluble in dichloromethane which is only transparent above 230 nm. Thus the solvent masks any alkane/alkene transitions.

Substituents marked as X in Figure 2. 14 would ideally contain chromophores that would absorb light at longer wavelengths than 230 nm, thus shifting transitions into a more readily probed window (250-900 nm). Conjugated carbonyl functionalities, for example, should exhibit transitions outside the CH_2Cl_2 solvent region.

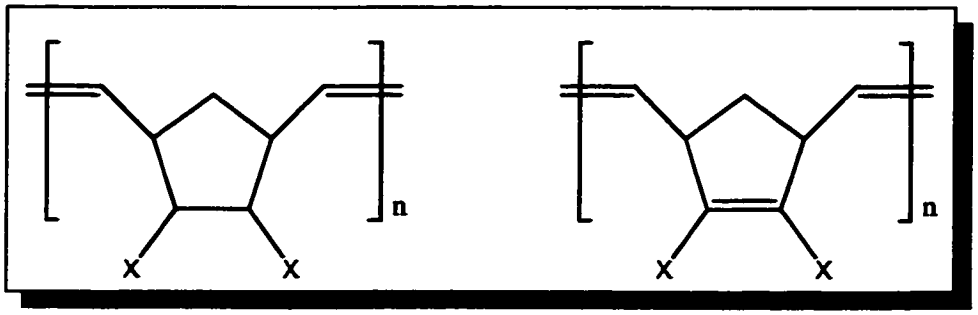

Figure 2. 14. Repeat Units for Norbornene and Norbornadiene Systems

2.8 Circular Dichroism (CD) Spectroscopy[12]

Circular dichroism spectroscopy has traditionally been used to probe biological systems for asymmetry. The rigid structures pertaining to biomacromolecules such as α-helices and β-sheets have distinct spectra which are useful in characterization. CD spectroscopy has also been applied to synthetic macromolecular systems such as poly(isocyanides) and poly(methacrylates) that display optical activity.

In contrast to linearly polarized light, circularly polarized light has varying direction and constant magnitude as represented in Figure 2. 15. Circularly polarized light is made up of right-handed and left-handed components. An asymmetric sample will interact differently with the two hands of circularly polarized light resulting in an ellipse as shown in Figure 2. 12. The difference in absorbance (A) between the two hands of light describes ellipticity.

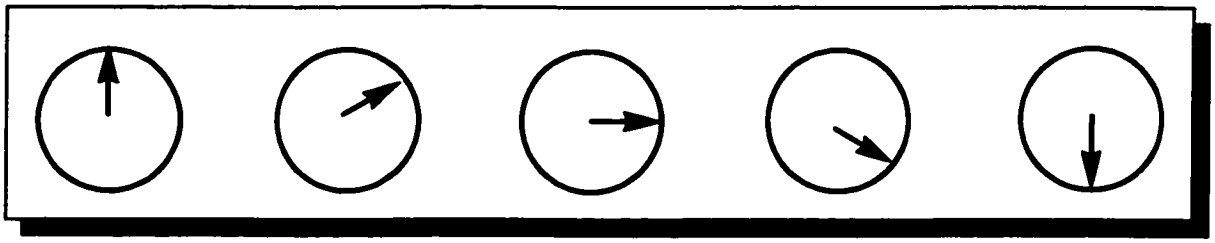

Figure 2. 15. Right-Handed Circularly Polarized Light

$$\theta = \frac{2.303(A_L - A_R)180}{4\pi}$$

A_L=absorption of left-handed circularly polarized light
A_R=absorption of right-handed circularly polarized light

Equation 23 Ellipticity

$$[\theta] = \frac{100\theta}{cl}$$

θ = ellipticity
c = concentration (mol/L)
l = polarimeter cell length (cm)

Equation 24 Molar ellipticity

$$\Delta\varepsilon = \frac{[\theta]}{3298}$$

Equation 25 Differential dichroic absorption

$$[\theta] = \frac{\text{CD signal}}{(\#\text{ repeat units})(\text{conc.})(\text{cell length in cm})(10)}$$

Equation 26

$$\Delta\varepsilon = \frac{\text{CD signal}}{(\text{conc.})(\text{cell length in cm})(32\,980)}$$

Equation 27

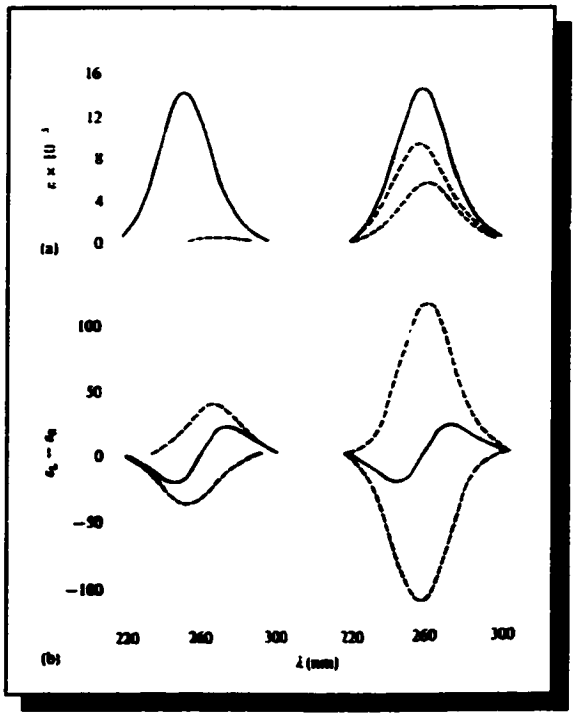

Figure 2. 16 Comparison of UV-vis Absorbance and CD Spectra for a Single Chromophore (dashed line) and dimer (solid line) [(a) UV-vis Absorbance, (b) CD Spectra][12]

The numerical values of 3298 and 32980 in Equation 25 and Equation 27 are constants. In practice, molar ellipticity ([θ]) is used for comparing polymers with different numbers of repeat units because it is a measure of optical activity per repeat unit. Differential dichroic absorption (Δε), in contrast, is directly comparable to the absorption spectrum. A band in the CD spectrum will usually have the same shape as its corresponding absorption spectrum, since

both rely on absorption from chromophores. If a chromophore is exposed to both hands of circularly polarized light and does not absorb both equally, a positive or negative CD exciton band will be observed. If asymmetry in the sample arises from a chiral structure such as a helix, the chromophores will interact and split the single exciton band into an exciton couplet. This is otherwise known as the Cotton effect.[13]

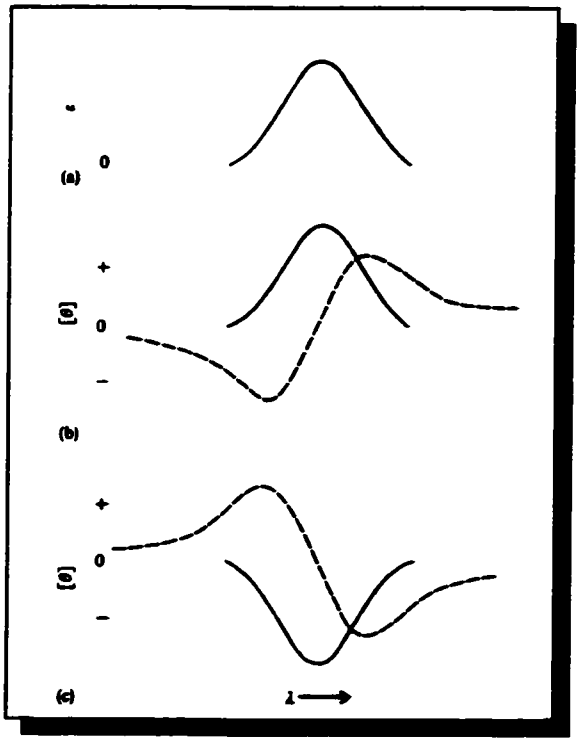

Figure 2. 17. Comparison of CD (dashed line) and ORD (solid line) Spectra [(a) UV-vis Absorbance, (b) Positive ORD (c) Negative ORD][12]

As stated above (Section 2.7), light is composed of electric and magnetic components. Pure absorption properties are dominated by electric effects while optical activity is a product of magnetic and electric effects (Figure 2. 17). The Cotton effect arises when the incident light impinging on a asymmetric structure induces a helical charge circulation. If the left-handed and right-handed helices are present in equal concentration, no signal will be observed because the two helical charge circulations will cancel out.

An example of CD analysis is shown below, for resolved poly(tert-butyl isocyanide) helices. The two resolved hands of the polymer had equal, but opposite optical rotation as measured by polarimetry. The CD spectra of the two samples exhibited signals that

were equal in differential dichroic absorption (Δε), but opposite in signal (Figure 2. 18.). The exciton couplet arises from the interaction of the imino chromophores with main-chain chirality.

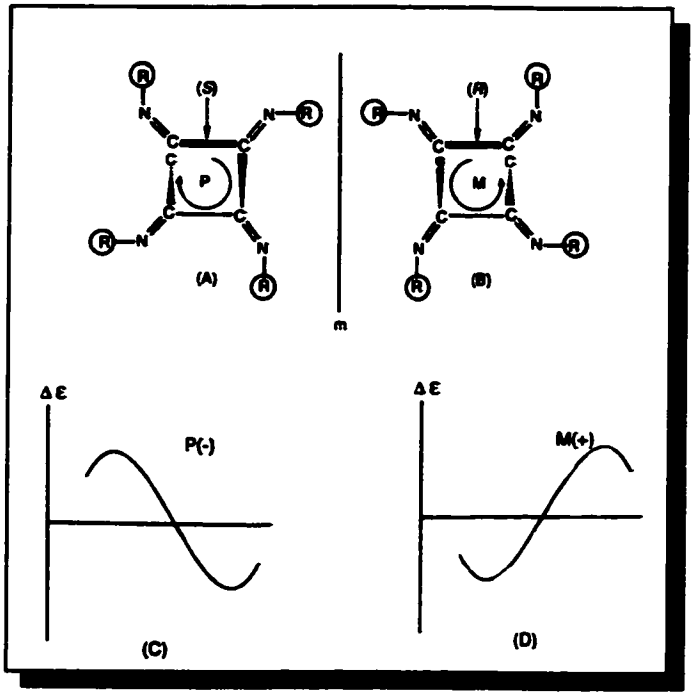

Figure 2. 18. Right-Handed (A) and Left-Handed (B) Poly(isocyanide) Helices and their Corresponding Circular Dichroism Spectra (C and D respectively)[14]

It also may be possible to include dyes either as the substituent or in solution to determine polymer helicity. As outlined in a recent paper, a helical conformation can be imposed on a dye by binding to DNA strands. The composite thus formed exhibits a couplet in the CD spectrum.[15] This technique could be extended to judge helicity in our systems. Dyes that are soluble in organic solvents which could be bound to the helical polymer (via a suitable monomer), should permit shifting of the CD transition well above the solvent region if the polymer is in a helical arrangement.

2.9 References

1. Rappe, A.K., Casewit, C.J., Colwell, K.S., Goddard, W.A.,Skiff, W.M. *J. Am. Chem. Soc.*, **1992**, *114*, 10024

2. Casewit, C.J., Colwell, K.S.,Rappe, A.K. *J. Am. Chem. Soc.*, **1992**, *114*, 10035

3. Casewit, C.J., Colwell, K.S.,Rappe, A.K. *J. Am. Chem. Soc.*, **1992**, *114*, 10046

4. Hamilton, J.G. *Polymer*, **1998**, *39*, 1669

5. O'Dell, R., McConville, D.H., Hofmeister, G.E.,Schrock, R.R. *J. Am. Chem. Soc.*, **1994**, *116*, 3414

6. Stevens, M.P. *Polymer Chemistry: An Introduction, 2nd Edition*, Oxford University Press, New York, **1990**, p.53

7. Cowie, J.M.G. *Polymers: Chemistry and Physics of Modern Materials, 2nd Edition*, Blackie Academic & Professional, New York, **1997**, p.196

8. Carraher, C.E. *Polymer Chemistry: 5th Edition, Revised and Expanded*, Marcel Dekker Inc., New York, **2000**, p.72

9. Nieh, M.-P., Goodwin, A.A., Stewart, J.R., Novak, B.M.,Hoagland, P.A. *Macromolecules*, **1998**, *31*, 3151

10. Ege, S.N. *Organic Chemistry: Structure and Reactivity*, D.C. Heath and Company, Toronto, **1994**, p.204

11. Ege, S.N. *op. cit.*, **1994**, p.759

12. Cantor, C.R.,Schimmel, P.R. *Biophysical Chemistry, Part II:Techniques for the Study of Biological Structure and Function*, W.H. Freeman and Company, San Francisco, **1980**, p.409

13. Cantor, C.R.,Schimmel, P.R. *op. cit.*, **1980**,p.414

14. Nolte, R.J.M. *Chem. Soc. Rev.*, **1994**, 11

15. Cosa, G., Focsaneanu, K.-S., McLean, J.R.N., McNamee, J.P.,Scaiano, J.C. *Photochem. Photobiol.*, **2001**, *73*, 585

CHAPTER 3

RESULTS

3.1 Computer Modelling

Poly(norbornenes) and poly(norbornadienes) were studied by computer modelling in order to determine the effect on polymer topology of specific structural features in the repeat unit. Our target macrostructural form is a helix with varying radius, resembling a tube. Polymers of norbornenes and norbornadienes represent a unique opportunity to tune helical parameters through variation of substituents on the monomer. In comparison, existing examples of synthetic helical polymers (such as poly(isocyanides) and poly(methacrylates)) have fixed conformations: these structures can only lead to rods (rather than tubes).[1,2] The effect of the following variables was assessed:

- Monomer type (norbornadiene vs. norbornene)
- Monomer substituents (4,5-positions)
- Tether (ester vs. ether, group that links the substituent to the monomer)
- Type of C_7 bridge (methylene vs. oxygen)

All norbornene monomer were constrained to an ego, endo substitution pattern, because the tacticity of such polymers are readily identifiable by NMR methods (Section 1.2.4).

Two computer modelling methods were used to survey polymer topology. The first survey examined energy-minimized polymer models created from 25 or 50 repeat units. Although this method was rapid for small substituents (such as methyl), it was time-

consuming for larger substituents. Most models displayed flexibility in the chain ends, causing irregularity of the helix and helical parameters. The second method constrained the internal torsion angles (ψ and ϕ) that repeat regularly throughout any helical polymer. Models made using this method were much more regular, and did not display the motional flexibility of the chain ends observed in the first survey. The second method was sometimes more time-consuming than the first but produced more precise results.

In most models represented throughout this chapter, olefinic and C_7 carbons are coloured in green (see repeat unit Figure 3. 1). The "tail" atom was marked in blue, while the "head" atom was coloured pink to distinguish their positions in the polymer model. All other atoms were coloured according to standard chemical conventions (carbon = grey, hydrogen = white, oxygen = red, nitrogen = blue, etc.)

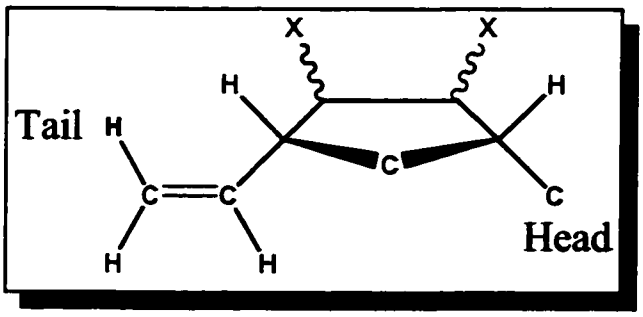

Figure 3. 1. Colour Scheme of Monomer Repeat Units in Cerius[2]

Typical helices appear as "twisted ribbons", and so the helical parameters are reported in terms of helical turn, radius and pitch (Figure 2. 5).[3, 4] The norbornene and norbornadiene polymer models studied in this work resembled tubes, and required other helicity measurements in order to assess and compare them. The helical measurements made were (Figure 2. 5):

- Helical Turn (number of repeat units/1 turn of the helix)
- Inner diameter
- Helical Pitch (translational distance for one turn of the helix)
- Length (for 50 repeat units)

The inner diameter of the void was measured in order to assess effect of variables on this feature. As a polymer helix of interest as a possible protective Trojan horse for transporting small molecules through harsh environments, the size of the void is of interest.

Comparison of helices can be described in terms of elongation and compression, just as for springs. Elongations are characterized by increased helical pitch and length, whereas compressions are the opposite.

3.2 First Polymer Modelling Survey

3.2.1 Unsubstituted Monomers

Norbornene and norbornadiene polymers were examined in this study. The longer pitch and length for the poly(norbornadiene) model (Table 3. 1) indicates elongation of the helix compared to poly(norbornene) (Figure 3. 2).

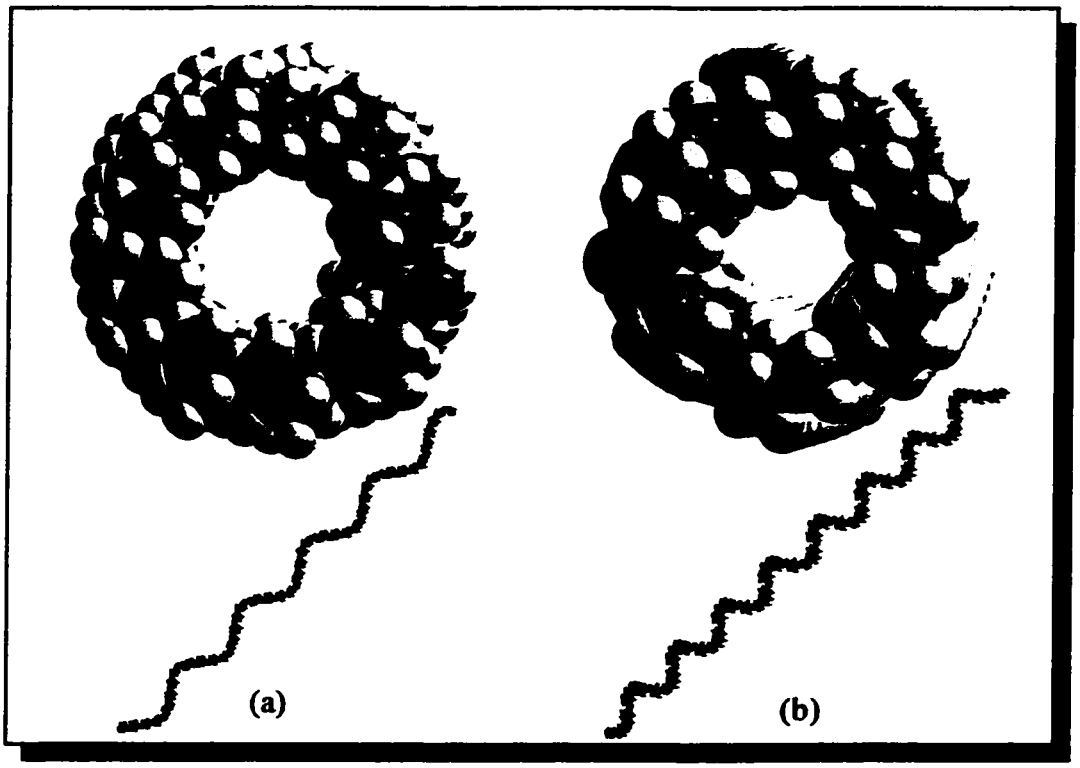

Figure 3. 2. Computer Models of Unsubstituted cis/iso (a) Poly(NBD) and (b) Poly(NBE)

Table 3. 1. Comparison of Unsubstituted Cis/Isotactic Poly(NBD) and Poly(NBE) (First Survey Results)

Helical Turn Inner Diam. (Å) Pitch (Å) Length (Å) Figure	10/1 7 45 205 3.3(a)	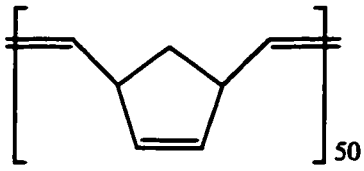
Helical Turn Inner Diam. (Å) Pitch (Å) Length (Å) Figure	6/1 5 25 185 3.3(b)	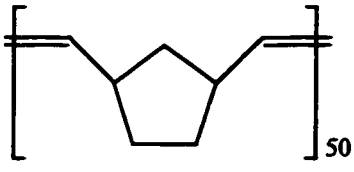

3.2.2 Tactic Combinations

Since norbornene (NBE) and norbornadiene (NBD) polymers can be described by the four tactic dyads, all eight oligomers were modelled (Table 3. 2). Polymers were

modelled using a tert-butyl group as a standard substituent, since this group is intermediate three-dimensional bulk between methyl (small) and adamantyl (large).

Both poly(NBE) and poly(NBD) display helices for all four possible tactic arrangements. The cis/isotactic and trans/syndiotactic structures are loosely wound helices (Figure 3. 3 (a) and (d)), though the former is elongated relative to the latter (Table 3. 2). In contrast, the trans/isotactic and cis/syndiotactic models can be viewed as rods rather than tubes (Figure 3. 3(b) and (c)). The trans/isotactic model resembles a flat, twisted ribbon, or an elongated helix. However the cis/syndiotactic model has no void, this being filled by the substituents (see end-on view in Figure 3. 3(c)).

Table 3. 2. Effect of Tacticity on Poly(NBD) and Poly(NBE) (First Survey Results)

	Cis/iso	*Tr/iso*	*Cis/syndio*	*Tr/syndio*	
Helical Turn	10/1	7/1	8/1	17/1	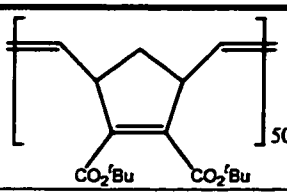
Inner Diam. (Å)	5	0.2	0	14	
Pitch (Å)	45	75	35	50	
Length (Å)	220	240	210	195	
Helical Turn	10/1	17/1	10/1	20/1	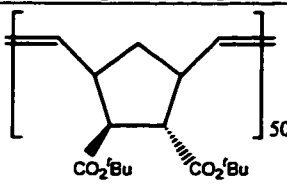
Inner Diam. (Å)	5	0	0	18	
Pitch (Å)	45	90	35	20	
Length (Å)	220	260	210	70	
Figure	3.4(a)	3.4(b)	3.4(c)	3.4(d)	

Although both cis/isotactic and trans/syndiotactic models resulted in tube-like helices, the cis/isotactic arrangement was used exclusively for the remainder of the modelling work. The latter structure is attractive for the increased potential of steric interaction between substituents on neighbouring substituents (Figure 3. 4), which is expected to promote formation of a helical macrostructure.

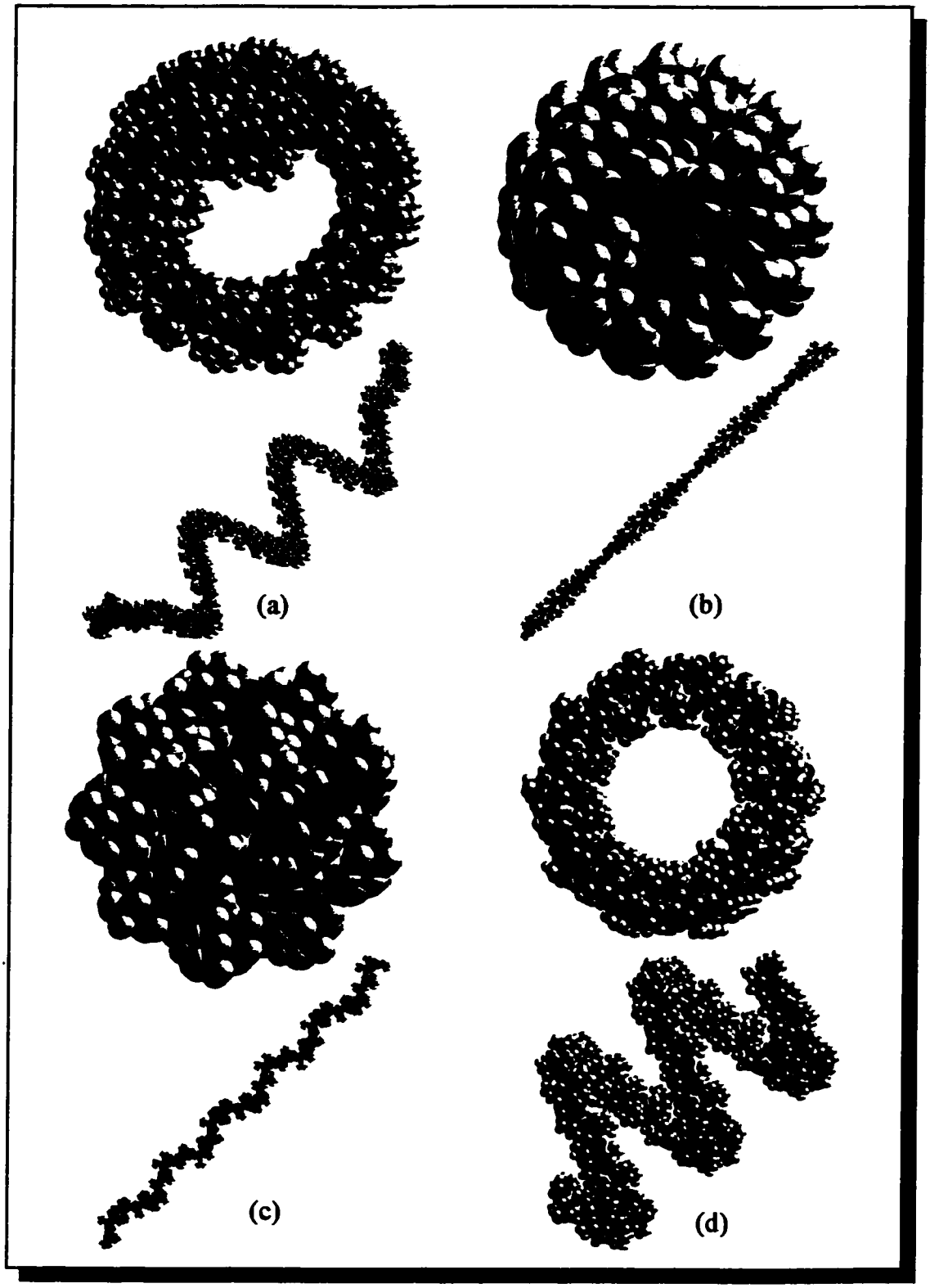

Figure 3. 3. Computer Models of Poly(Exo,Endo NBE($CO_2{}^tBu)_2$) (50 units) (a) cis/isotactic, (b) trans/isotactic, (c) cis/syndiotactic, (d) trans/syndiotactic

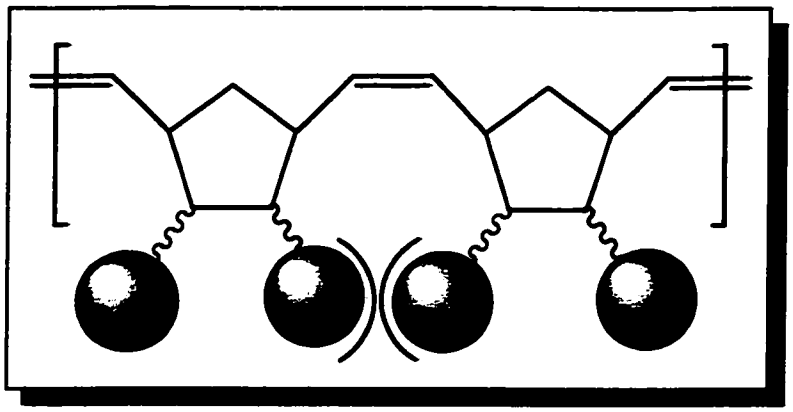

Figure 3. 4. Steric Hindrance Between Bulky Substituents on a Cis/Isotactic Dyad

3.2.3 Three-Dimensional Bulk

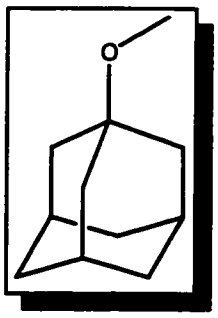

Figure 3. 5. Adamantyl

Polymers made of unsubstituted NBE and NBD are unlikely to exist as helices in solution, but as random coils. We wished to explore the possibility that substituents present on the repeat unit would stabilize a helical structure. An enhanced capacity for "tuning" helical parameters is anticipated as a secondary result. Consistent with this, a slight helix elongation is found in increasing the bulk of poly(NBE) or poly(NBD) (methyl to tert-butyl to adamantyl (Figure 3. 5)). The length of a standard 50-mer increases with increasing bulk, while the helix radius decreases (Table 3. 3).

Table 3. 3. Effect of Increase in Three-Dimensional Bulk on Cis/Isotactic Poly(NBE) and Poly(NBD) (First Survey Results)

R=	*Me*	*^{t}Bu*	*Ad*	
Helical Turn	10/1	10/1	10/1	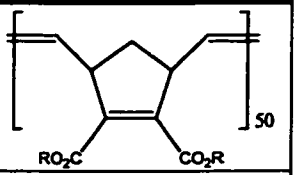
Inner Diam. (Å)	5	5	4	
Pitch (Å)	37	45	40	
Length (Å)	200	220	220	
Helical Turn	16/1	16/1	14/1	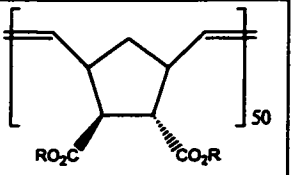
Inner Diam. (Å)	18	16	8	
Pitch (Å)	40	35	40	
Length (Å)	130	135	145	
Figure		3.7(a)	3.7(b)	

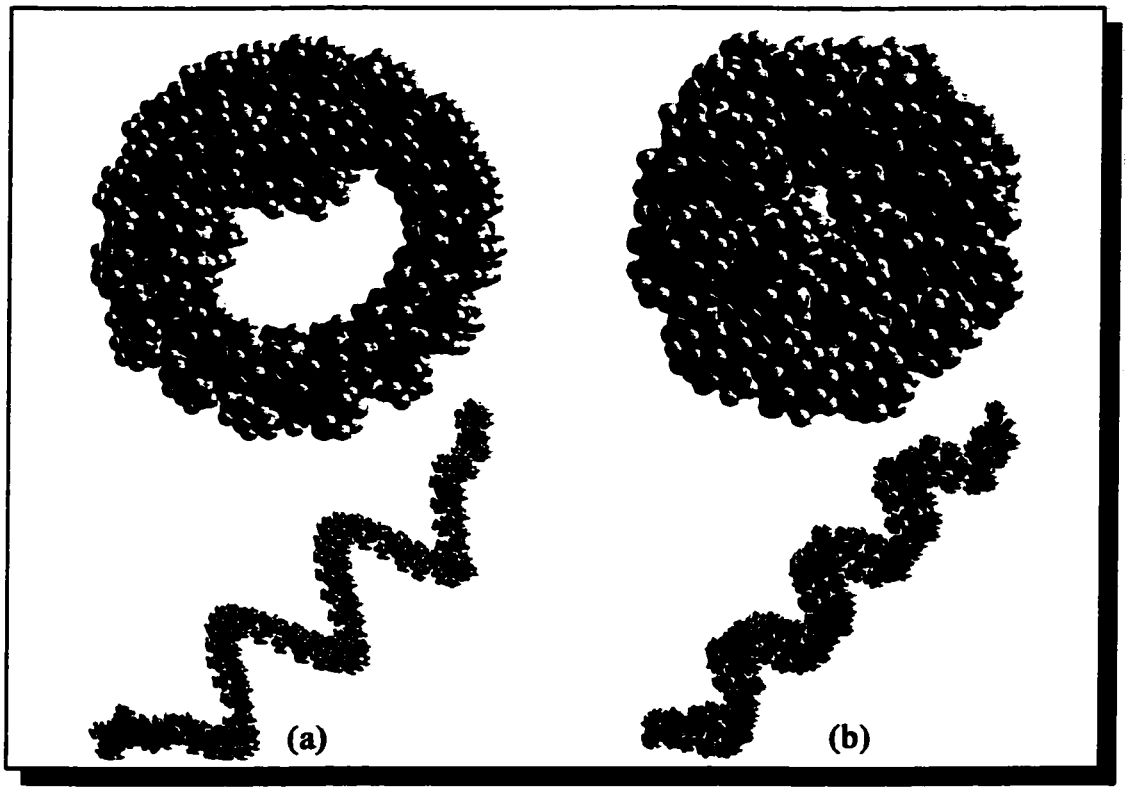

Figure 3. 6. Computer Models of Cis/Isotactic Poly(Exo,Endo NBE($CO_2R)_2$) (a) R = ^{t}Bu, (b) R = Ad

3.2.4 Tether Type

The type of tether that links the substituent to the cyclopentene or cyclopentene repeat unit may affect the helical parameters by changing the extent of interaction between neighbouring substituents. An ester is frequently the tether used to bind substituents to norbornenes and norbornadienes. In certain cases, monosubstituted and disubstituted norbornenes with ether tether groups have been reported.[5, 6]

Table 3. 4. Effect of Tether Type on Cis/Isotactic Poly(NBD) (First Survey Results)

R=	*Me*	*^{t}Bu*	*Ad*	*Ph*	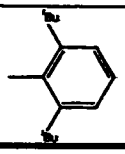	
Helical Turn	10/1	10/1	10/1	10/1	10/1	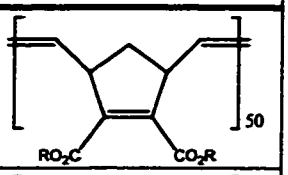
Inner Diam. (Å)	5	5	4	8	6	
Pitch (Å)	37	45	40	40	48	
Length (Å)	200	220	220	215	220	
Helical Turn	10/1	10/1	10/1	10/1	10/1	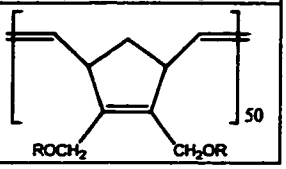
Inner Diam. (Å)	6	4	5	5	6	
Pitch (Å)	40	45	40	40	45	
Length (Å)	190	220	220	210	220	

Table 3. 5. Effect of Tether Type on Cis/Isotactic Poly(NBE) (First Survey Results)

R=	*Me*	*^{t}Bu*	*Ad*	*Ph*	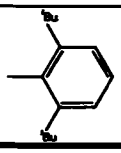	
Helical Turn	16/1	16/1	14/1	16/1	15/1	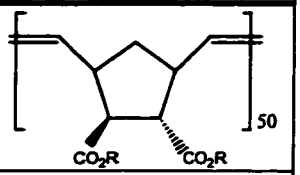
Inner Diam. (Å)	18	16	8	1	16	
Pitch (Å)	40	35	40	40	42	
Length (Å)	130	135	145	150	150	
Helical Turn	14/1	12/1	14/1	14/1	13/1	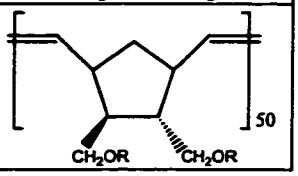
Inner Diam. (Å)	17	16	8	16	14	
Pitch (Å)	35	32	40	30	30	
Length (Å)	130	135	150	110	130	

Although the ether tethers should offer more flexibility and more interaction between substituents, the tether type has little effect on helix parameters: the inner diameter, helical turn, pitch and length (Table 3. 4 and Table 3. 5). Slight compression of the ether helices is manifested in their shorter lengths, and in their tighter pitch. Inner diameters are fairly comparable. Anomalous is this series is the phenyl substituted poly(NBE), which displays an increased inner diameter, and a decreased in helical pitch and length (Table 3. 5), possibly due to greater interaction between phenyl substituents.

3.2.5 Tether Length

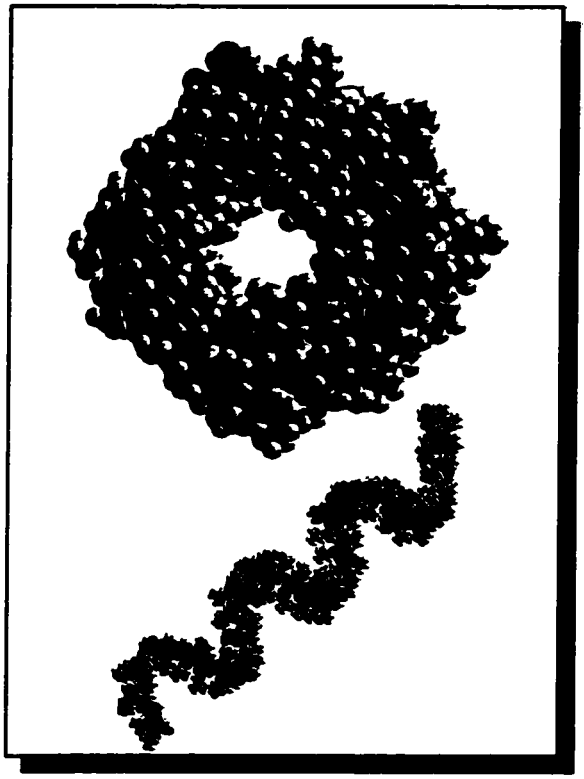

Figure 3. 7. Computer Model for Cis/Isotactic Poly(Exo, Endo NBE($CO_2CH_2{}^tBu$)$_2$)

The proximity of substituent steric bulk to the poly(NBE) or poly(NBD) backbone may affect helical parameters. This effect was examined by inserting hydrocarbon chains between the tether and the substituent. While other helix parameters are largely unaffected (Table 3. 6), the inner diameter decreases progressively with increasing hydrocarbon "linker" chains. This is attributed to bending of long substituents toward the middle of the helix and between each turn of the helix. A greater "ribbon" width, as well as a smaller inner diameter, are observed by contrasting Figure 3. 3(a) and Figure 3. 7.

Table 3. 6. Effect of Proximity of Steric Bulk to Cis/Isotactic Poly(NBE) Backbone (First Survey Results)

# of (CH_2) groups (X)	*0*	*1*	*2*	*3*	
Helical Turn	16/1	14/1	16/1		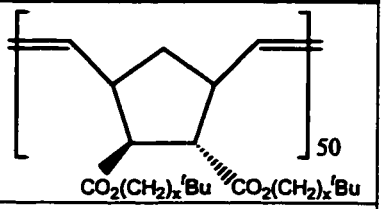
Inner Diam. (Å)	16	8	5		
Pitch (Å)	35	35	40		
Length (Å)	135	120	140		
Figure		3.7			
Helical Turn	12/1	11/1	10/1	12/1	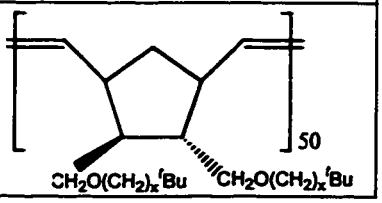
Inner Diam. (Å)	16	12	11	9	
Pitch (Å)	32	25	30	35	
Length (Å)	135	135	145	150	

3.2.6 Hydrocarbon vs. Oxygen-Containing Rings

As the olefinic protons and the C_7 atom form the interior sheath of the helix in many of the polymers modelled, we considered the possibility of modulating the electronic characteristics of that interior by replacing the carbon of C_7 with an oxygen atom. Oxananorbornenes and oxananorbornadienes were compared with their hydrocarbon counterparts.

The oxygen of the heterocyclic ring points into the interior of the helix, as also observed for C_7 in the hydrocarbon counterparts. Little perturbation of helical parameters is observed (Table 3. 7). The helical pitch and length are very slightly larger, and inner diameters are slightly smaller.

Table 3. 7. Effect of Oxygen Bridge on Cis/Isotactic Poly(NBD) and Poly(NBE) (First Survey Results)

	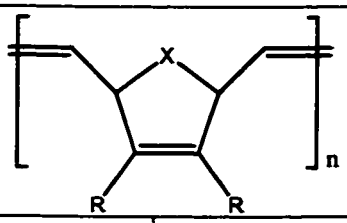		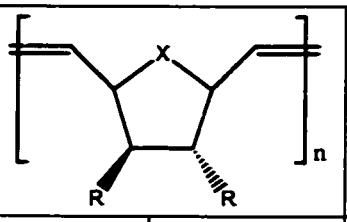		
R=	***CO_2Me***	***CH_2OMe***	***CO_2Me***	***CH_2OMe***	***C_7 Atom***
Helical Turn	10/1	10/1	16/1	14/1	***CH_2***
Inner Diam. (Å)	5	6	18	17	
Pitch (Å)	37	40	40	35	
Length (Å)	200	190	130	130	
Figure	3.9(a)		3.9(c)		
n	25		50		
Helical Turn	10/1	8/1	16/1	16/1	***O***
Inner Diam. (Å)	5	5	18	15	
Pitch (Å)	40	45	50	60	
Length (Å)	240	240	160	180	
Figure	3.9(b)		3.9(d)		
n	25		50		

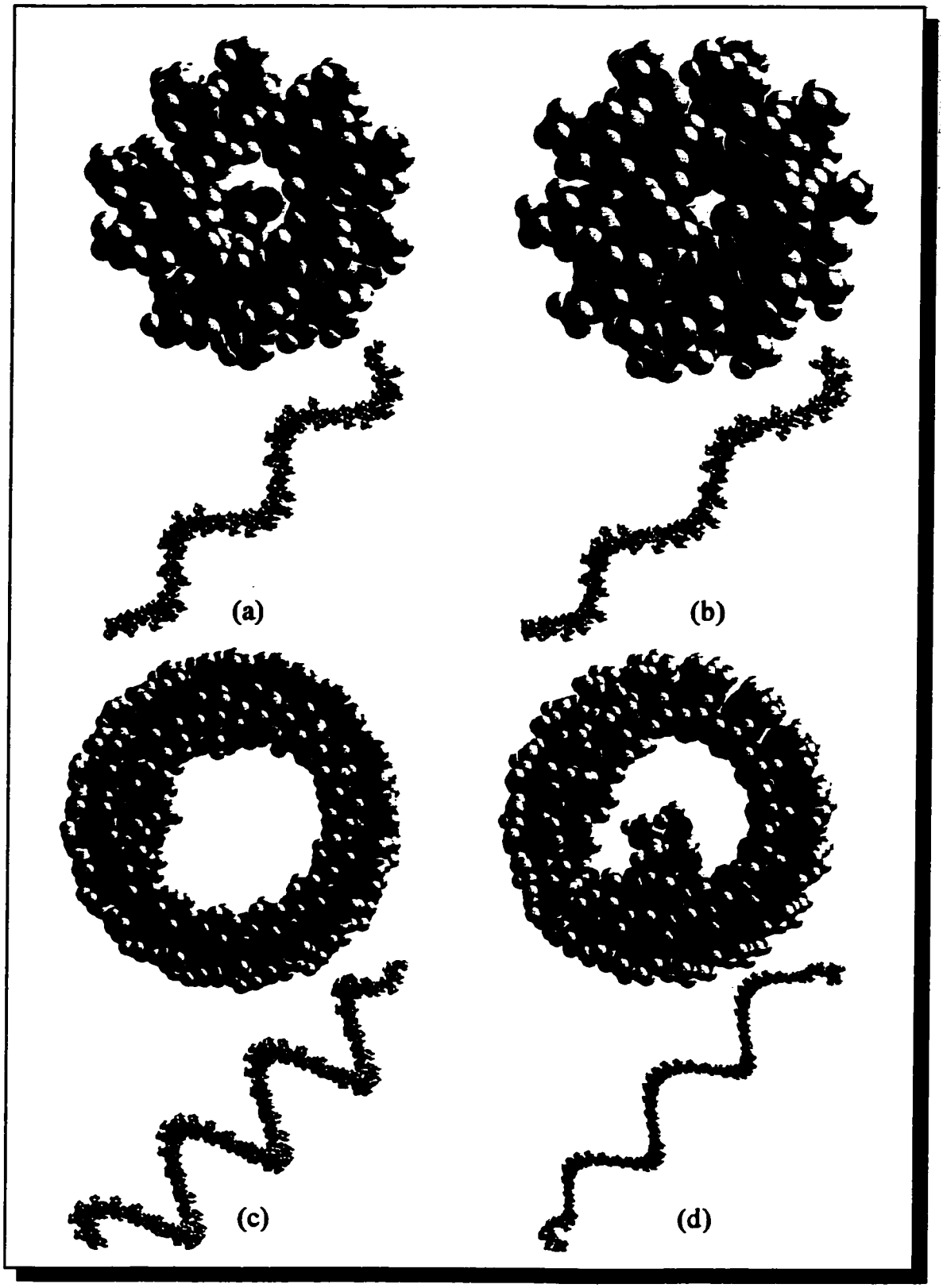

Figure 3. 8. Computer Models of Cis/Isotactic Poly(NBD) {(a) and (b)} and Poly(NBE) {(c) and (d)}, CO_2Me substitution

3.2.7 Summary of First Survey Results

Results from the first survey indicate that all four tactic arrangements yield helical structures, but that only cis/isotactic and trans/syndiotactic result in tube-like helices with measurable inner diameters. We are interested in poly(norbornenes) and poly(norbornadienes), in view of the ability to affect their helical parameters through judicious choice of substituents. Cis/isotactic polymers were considered given the greater likelihood of steric interaction between substituents of neighbouring repeat units and, therefore greater tunability of helical parameters. Models of poly(norbornenes) tend to be compressed in comparison with poly(norbornadienes). Addition of three-dimensional bulk causes slight elongation of the helix; the nature of the tether group, however has little effect on the helical parameters. Lengthening the tether with hydrocarbon chains decreases the inner diameter, and increases the width of the "ribbon" from the folding of substituents into the helix. Poly(oxananorbornenes) and poly(norbornadienes) are closely similar in structure to the parent hydrocarbon polymers.

Limitations of this first survey method can be seen on closer examination of the figures. The chain ends of Figure 3. 3(a), Figure 3. 7(a) and Figure 3. 10(c) and (d) display irregularity with the central parts of the models. The first method of computer modeling while useful for approximating of idealized structures for poly(norbornenes) and poly(norbornadienes), is of limited value as main chain torsion angles were not considered. Inconsistencies between helical turn and pitch measurements are possible, due to difficulty in defining the edges of helical turns.

3.3 Second Polymer Computer Modelling Survey

As discussed in Section 2.1.6, any regularly repeating polymer can be described in terms of two torsion angles (ψ and ϕ). With the intention of closer inspection of the helical parameters, we undertook the second survey in which the dyads were drawn, minimized and their internal torsion angles measured. The models (50 repeat units) were created by constraining ψ and ϕ to their optimized values, and imposing retention of these values during the simulated polymerization.

Typically, the pre-minimization models have potential energies and conformations near their minimum values (40 – 100 kcal/mol·monomer). Before and after energy minimization, the green olefinic and bridgehead carbons point into the helix interior, and the substituents face the exterior (consistent with the steric demand of the latter). The low pre-minimization energies are plausible because the chains and substituents are already in their less sterically encumbered conformations. In contrast, unoptimized models of the first survey had very high energies ($10^{10\text{-}20}$ kcal/mol·monomer). As for the first survey, helical parameters were measured (inner diameter, helical turn, pitch, length for 50 repeat units). In addition, the torsion angles (ψ and ϕ) were measured and tabulated in Tables 3. 9 to 3. 15.

General trends for torsion angles emerge within each tacticity type (Table 3. 9). Isotactic dyads have one positive and one negative torsion angle, whereas both are negative for

syndiotactic dyads. On average, cis dyads have one angle less than 90°, and one greater than 90°. Torsion angles for trans dyads are typically greater than 90°.

Table 3. 8. General Torsion Angle Rules for Tactic Dyads

Double Bond Type	*Requirements*	*Tacticity*	*Requirements*
Cis	one angle > 90° other angle < 90°	isotactic	one positive angle one negative angle
trans	both angles > 90°	syndiotactic	both negative angles

3.3.1 Tactic Combinations

All four possible tactic arrangements were studied for both poly(norbornadiene) and poly(norbornene). As with the first survey, tert-butyl group was used as a standard substituent.

Table 3. 9. Effect of Tacticity on Poly(NBD) and Poly(NBE) (Second Survey Results)

	Cis/iso	*Tr/iso*	*Cis/syndio*	*Tr/syndio*	
Helical Turn	4/1	22/1	115/1	50/3	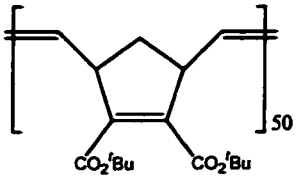
Inner Diam. (Å)	2	0	58	13	
Pitch (Å)	10	120	500	35	
Length (Å)	90	250	230	105	
ψ	-73.5°	-125°	-85°	-135°	
ϕ	122.7°	165°	-110°	-150°	
Figure	3.11(a)	3.11(b)	3.11(c)	3.11(d)	
Helical Turn	19/4	41/3	10/1	25/2	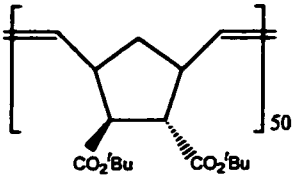
Inner Diam. (Å)	0	8	2.5	15	
Pitch (Å)	14	40	18	10	
Length (Å)	150	150	95	50	
ψ	-140°	-121°	-170°	-125°	
ϕ	88.5°	163°	-120°	-132.5°	
Figure				3.10	

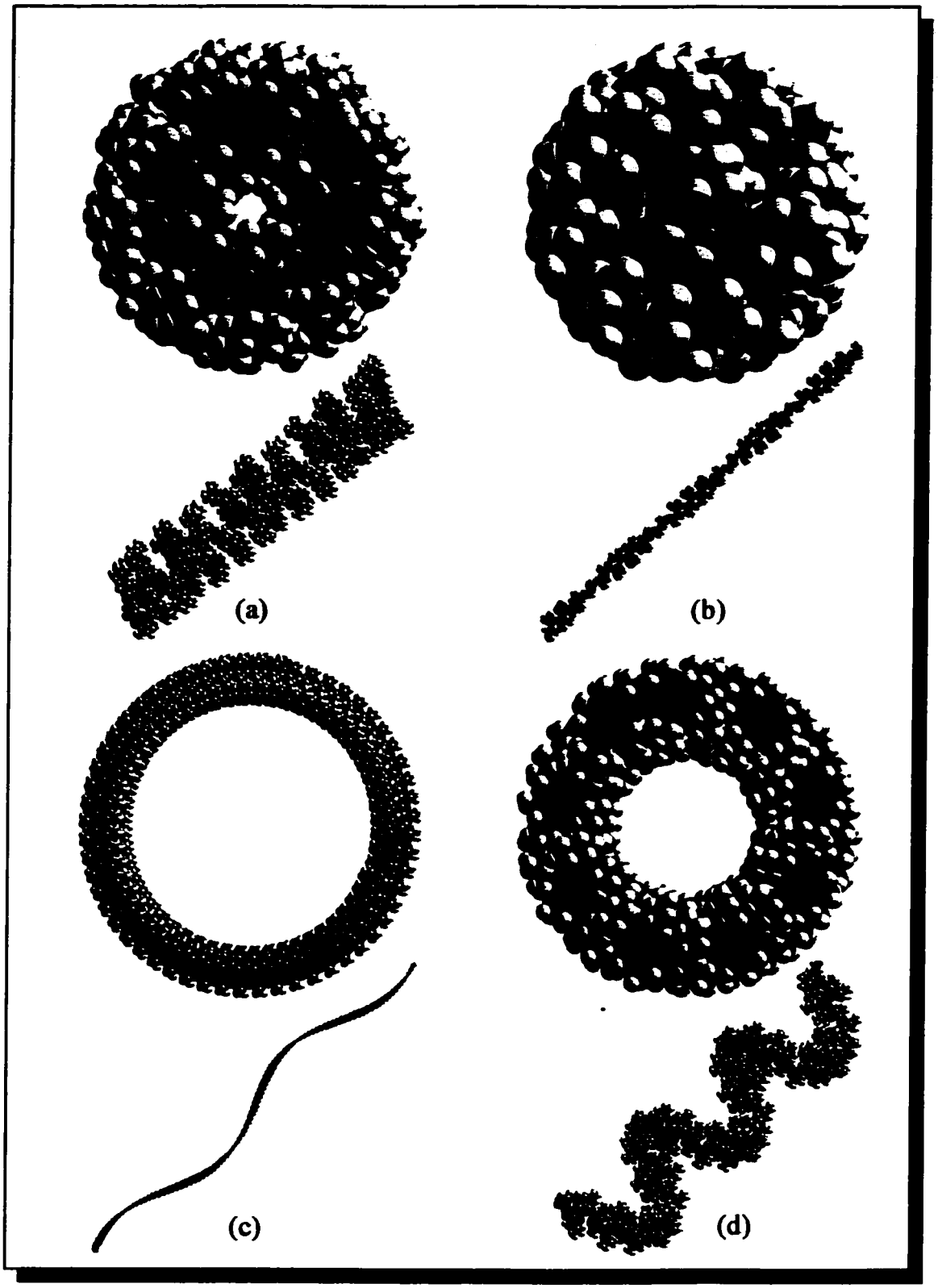

Figure 3. 9. Computer Models of Poly(NBD(CO_2tBu)$_2$) (50 units except (c) 200 units) (a) cis/isotactic, (b) trans/isotactic, (c) cis/syndiotactic, (d) trans/syndiotactic

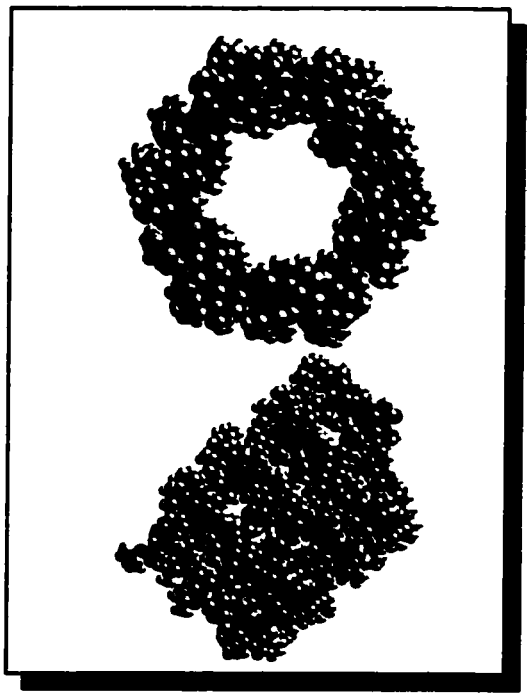

Figure 3. 10. Computer Model of Trans/Syndiotactic Poly(Exo, Endo NBE($CO_2{}^tBu)_2$) 50 units

The four tactic models of poly(NBD) and poly(NBE) all displayed helical structures (Figure 3. 10 and Figure 3. 9). Both the cis/isotactic and trans/syndiotactic models appear as more compact structures than for the first survey, as seen by the shorter pitch and lengths (Table 3. 9). The most dramatic change is manifested in the cis/syndiotactic model, which appears as a loose and open helix (Figure 3. 9(c)). The cis/isotactic arrangement gives rise to the most compressed helix. Unlike their poly(NBD) counterparts, all four tactic models of poly(NBE) display helices of shorter helical pitch and lengths, with trans/syndiotactic being the most compact.

3.3.2 Three-Dimensional Bulk and π - Stacking

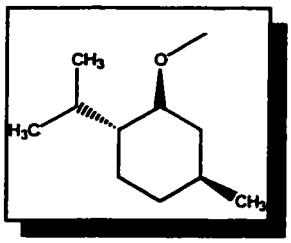

Figure 3. 11 Menthyl

Although the models for unsubstituted poly(NBD) and poly(NBE) predict tightly wound helices, such structures are not expected to retain helicity in solution. This part of the first study was repeated in order to determine if the observations were the same. Another group, the menthyl ester, was studied since it is synthetically accessible.[5] This group is not of uniform bulk like the other three examples (methyl, tert-butyl and

adamantyl). Instead, it is longer along the axis of the methyl and isopropyl substituents, and (as compared to the adamantyl group) it is comparatively flat.

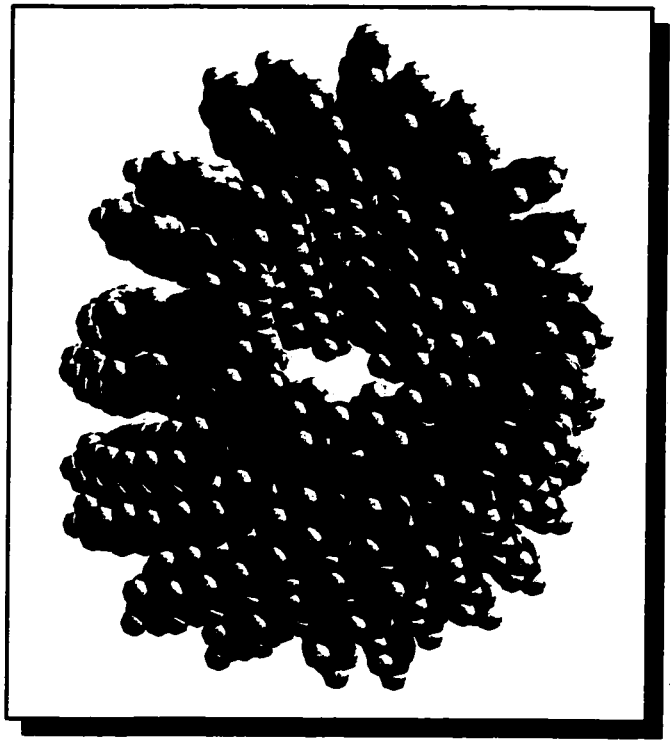

Figure 3. 12. Computer Models of Cis/Isotactic Poly(Exo, Endo NBE(CO_2Ph_2)

In contrast with the results from the first survey, helical pitch and length increase with increasing bulk, and the inner diameter remains constant (Table 3. 10). Larger substituents are associated with elongated helices. The exception to these generalizations is the phenyl ester-functionalized poly(norbornene), in which the inner diameter is dramatically larger. We ascribe these changes to π-stacking interactions between phenyl groups on neighbouring repeat units (Figure 3. 12). There is no evidence of π-stacking between turns of the helix because of the large pitch distance (20Å) since π-stacking interactions are characterized by distance of 3 to 5 Å.[7] However, it is possible that such interactions could enforce a compression of the helix to form a tube-like structure. Such forces are also responsible for supramolecular self-assembly of helical macrostructures as studied by Lehn and co-workers.[8, 9]

Table 3. 10. Effect of Increase in Three-Dimensional Bulk on Cis/Isotactic Poly(NBE) and Poly(NBD) (Second Survey Results)

R=	*Me*	*^{t}Bu*	*Ad*	*Menthyl*	*Ph*	
Helical Turn	4/1	4/1	5/1	13/3	4/1	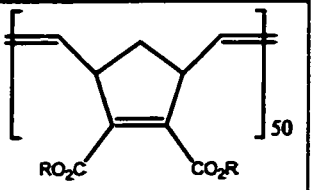
Inner Diam. (Å)	2	2	3	1	2	
Pitch (Å)	5	10	10	9	8	
Length (Å)	65	90	110	100	65	
ψ	-74°	-73.5°	-72.5°	-67.5°	-76°	
ϕ	111°	123°	130°	120°	112.5°	
Helical Turn	21/4	19/4	11/2	6/1	9/1	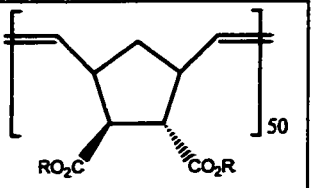
Inner Diam. (Å)	3	0	2.5	3.5	9	
Pitch (Å)	12	14	20	14	20	
Length (Å)	110	150	165	115	115	
ψ	-79°	-88.5°	-90°	-72°	-92.5°	
ϕ	125°	140°	135°	137°	145°	
Figure					3.13	

3.3.3 Hydrogen Bonding

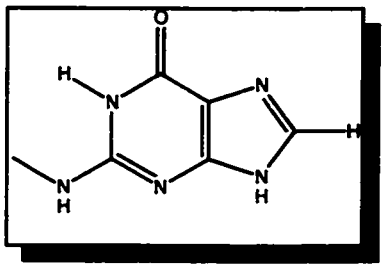

Figure 3. 13. Guanine

Hydrogen-bonding presents another potential means of enforcing helical rigidity in solution. DNA is the prototypical case. Guanine was selected as a substituent since it can form up to three hydrogen bonds between neighbouring guanine groups (Figure 3. 13).

The guanine-substituted helices are highly regular, with parameters comparable to models previously examined. A remarkable feature of the new polymers, however, is the alignment of guanine groups on neighbouring repeat units (Figure 3. 14). The observed order cannot be due to hydrogen-bonding because the computer modelling software does not support this parameter. Hydrogen-bonding may be indeed be possible, despite the large pitch (14-25 Å), given that the separation between substituents on neighbouring

repeat units is 3-5 Å, and typically hydrogen-bonding is 2 to 4 Å.[10] Once synthesized, the helix may compress because of hydrogen bonding between the turns of the helix.

Table 3. 11. Second Survey Results for Comparison of Amide and Amine Linked Poly(NBD) and Poly(NBE) (R = Guanine)

	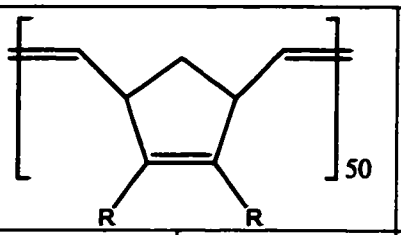		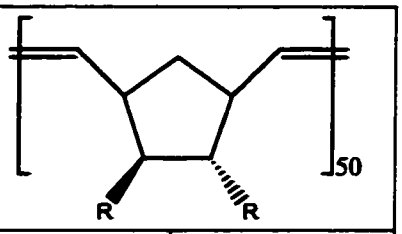	
R=	***CO_2Guanine***	***CH_2OGuanine***	***CO_2Guanine***	***CH_2OGuanine***
Helical Turn	6/1	21/4	20/3	25/4
Inner Diam. (Å)	4	3	4.5	3
Pitch (Å)	18	14	25	20
Length (Å)	140	115	160	190
ψ	-82.5°	-77.5°	-95°	-104°
ϕ	140°	130°	147.5°	158°
Figure	3.15			

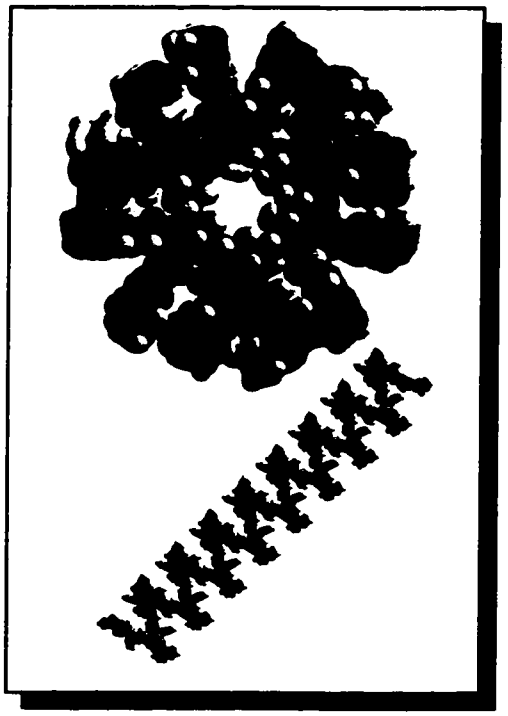

Figure 3. 14. Computer Model for Cis/Isotactic Poly(NBD(COGuanine)$_2$)

3.3.4 Tether Type

The tether type did not greatly affect helical parameters as observed in the first survey. This study was repeated using the second method, given the differences already observed using this method. Generally, the type of tether does not affect the helical parameters with the exception of phenyl-substituted models (Table 3. 12 and Table 3. 13). These polymers display an elongation through the increase in helical pitch and length.

Table 3. 12. Effect of Tether Type on Cis/Isotactic Poly(NBD) (Second Survey Results)

R=	*Me*	*^{t}Bu*	*Ad*	*Menthyl*	*Ph*	
Helical Turn	4/1	4/1	5/1	13/3	4/1	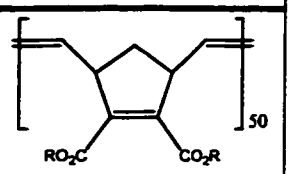
Inner Diam. (Å)	2	2	3	1	2	
Pitch (Å)	5	10	10	9	8	
Length (Å)	65	90	110	100	65	
ψ	-74°	-73.5°	-72.5°	-67.5°	-76°	
ϕ	111°	123°	130°	120°	112.5°	
Helical Turn	21/4	19/4	14/3	19/4	7/1	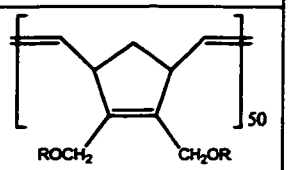
Inner Diam. (Å)	3	2	2	2.5	6	
Pitch (Å)	13	10	10	12	20	
Length (Å)	110	95	105	130	150	
ψ	-77.5°	-73°	-70°	-70°	-90°	
ϕ	130°	122°	125°	130°	140°	

Table 3. 13. Effect of Tether Type on Cis/Isotactic Poly(NBE) (Second Survey Results)

R=	*Me*	*^{t}Bu*	*Ad*	*Menthyl*	*Ph*	
Helical Turn	21/4	19/4	11/2	6/1	9/1	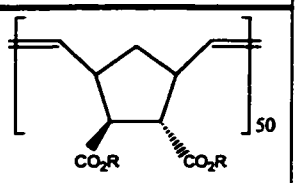
Inner Diam. (Å)	3	0	2.5	3.5	9	
Pitch (Å)	12	14	20	14	20	
Length (Å)	110	150	165	115	115	
ψ	-79°	-88.5°	-90°	-72°	-92.5°	
ϕ	125°	140°	135°	137°	145°	
Helical Turn	5/1	11/2	5/1	6/1	11/2	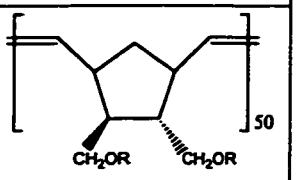
Inner Diam. (Å)	2.5	3.5	3	4	0	
Pitch (Å)	12	16	12	18	23	
Length (Å)	110	140	115	150	185	
ψ	-82°	-90°	-73.5°	-92.5°	-110°	
ϕ	127°	135°	136°	138°	160°	

3.3.5 Hydrocarbon vs. Oxygen-Containing Rings

As in the first survey, polymer topology is conserved in changing the C_7 atom for an oxygen atom. The helices containing heterocyclic rings are slightly elongated as compared to hydrocarbon rings, however the substitution brings about little change in structure (Table 3. 14).

Table 3. 14. Effect of Oxygen Bridge on Cis/Isotactic Poly(NBD) and Poly(NBE) (First Survey Results)

	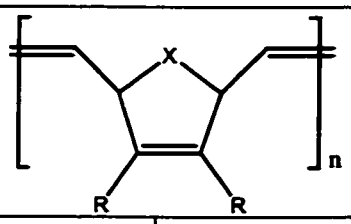		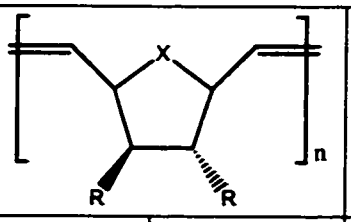		
R=	***CO_2Me***	***CH_2OMe***	***CO_2Me***	***CH_2OMe***	***C_7 Atom***
Helical Turn	4/1	21/4	21/4	5/1	***CH_2***
Inner Diam. (Å)	2	3	3	2.5	
Pitch (Å)	5	13	12	12	
Length (Å)	65	110	110	110	
ψ	-74°	-77.5°	-79°	-82°	
ϕ	111°	130°	125°	127°	
Helical Turn	4/1	14/3	4/1	13/3	***O***
Inner Diam. (Å)	2.5	3	1	2.5	
Pitch (Å)	6	12	10	12	
Length (Å)	70	115	115	135	
ψ	-67.5°	-70°	-70°	-75°	
ϕ	110°	130°	120°	127.5°	

3.3.6 Dynamics Simulation of a Model Helix

Computer models obtained above represent idealized gas-phase structures. Dynamic solution behaviour is unaccounted for in this analysis. In an effort to assess the stability of these helical conformations, a model was subjected to 5 × 50 ps of dynamics simulation at 300 K. The choice of model stemmed from characterization results of a polymer {poly(NBE(CO_2Menthyl)$_2$)}with cis/syndiotactic structure.

The chain starts to collapse at 50 ps (Figure 3. 16(a)); the helix collapses into a ball by 100 ps (Figure 3. 16(b)), following which little change is observed. The cis/syndiotactic structure of poly(NBE(CO_2Menthyl)$_2$) is a typical helix where there are large gaps between each turn of the helix (Figure 3. 15). Rapid collapse of the helical structure may arise from the lack of bonding interactions between the large aliphatic (menthyl) groups and the loose helical structure. However negative these results are, this dynamics simulation was conducted under harsh conditions and would likely cause the collapse of polymer helices known to be stable. Future experiments should focus on models capable of π-stacking and hydrogen-bonding to determine if these aid in stabilizing the structure.

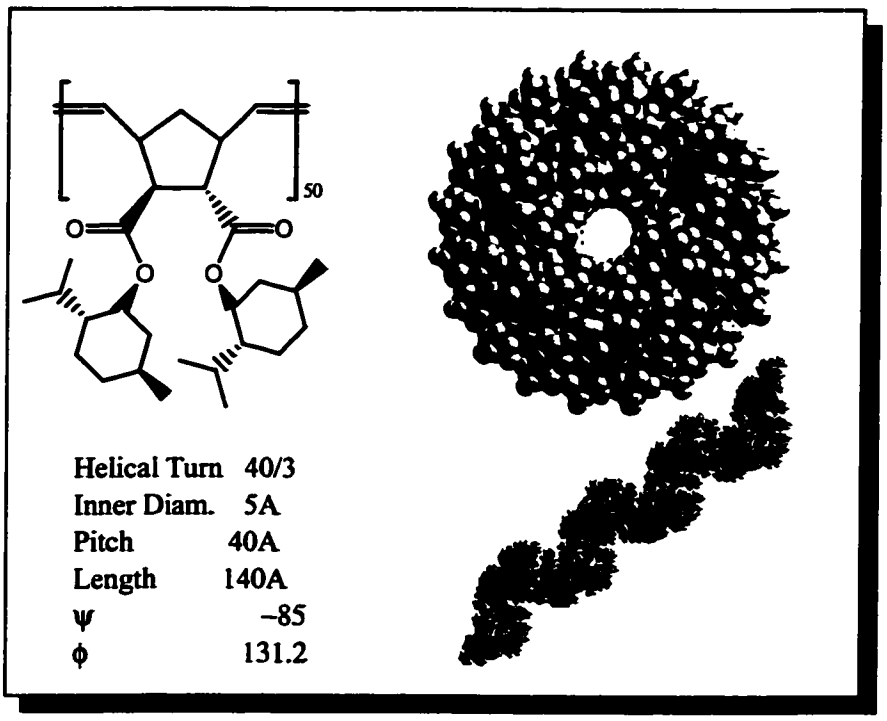

Figure 3. 15. Computer Model for c/s Poly(NBE(CO_2Menthyl)$_2$) 50 units

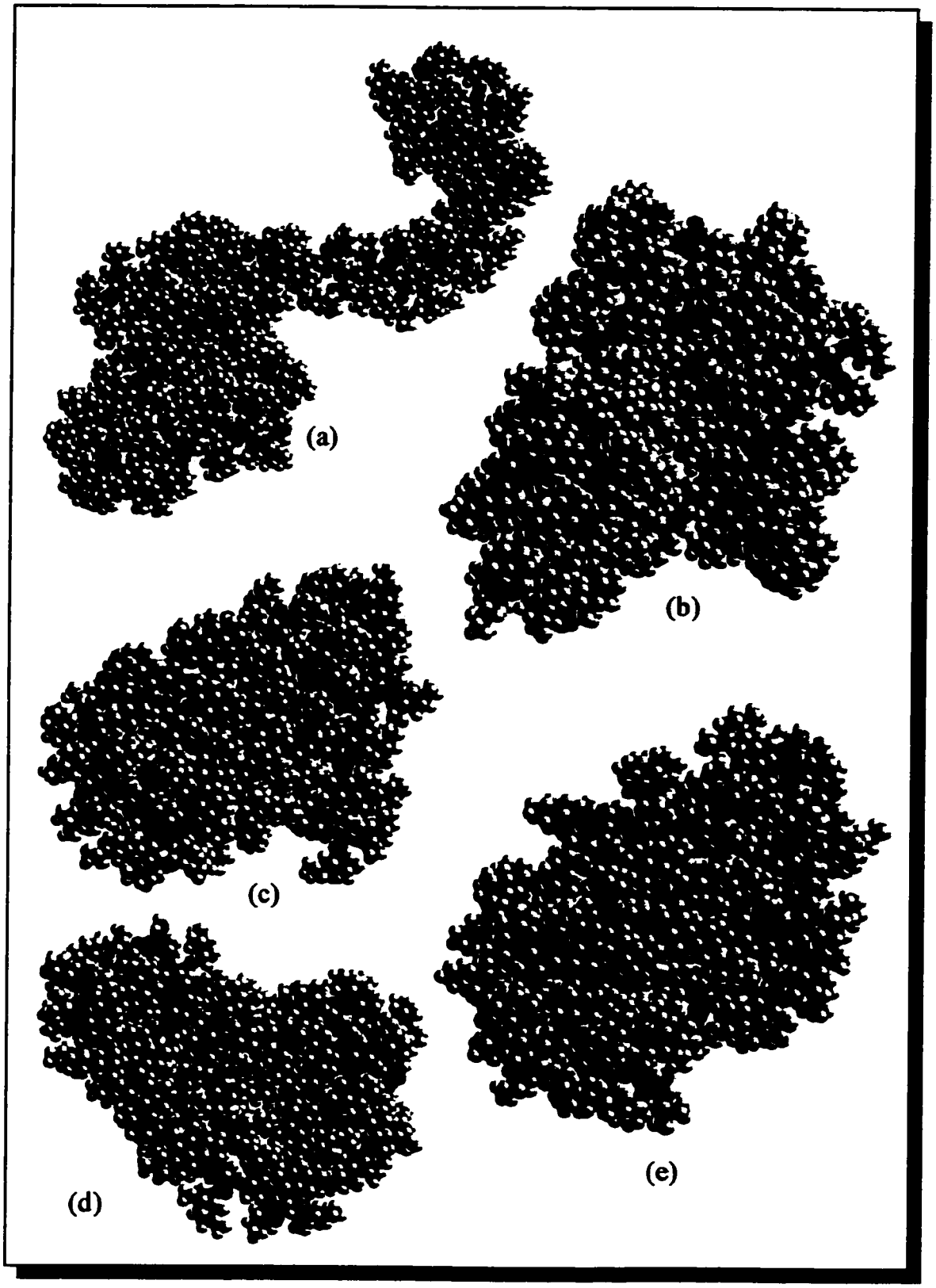

Figure 3. 16. Computer Models for Dynamics Simulation of Poly(NBE(CO_2Menthyl)$_2$) 50 units (a) 50 ps, (b) 100 ps, (c) 150 ps, (d) 200 ps, (e) 250 ps

3.3.7 Summary and Conclusions

Qualitative agreement between the two survey methods exists, although models produced by the second method are more compressed than counterparts from the first survey. All four possible tactic arrangements result in helical structures. Cis/isotactic poly(NBD) and trans/syndiotactic poly(NBE) display the shortest pitch lengths, and hence most tube-like structures (Figure 3. 9 and Figure 3. 10). The results of the second survey permit us to define certain general rules for the torsion angles required to attain a particular double bond geometry and tacticity (Table 3. 8). Inconsistencies between helical turn and pitch measurements may arise from the difficulty in defining the edges of helical turns.

As can be seen from Figures 3. 9, 10, 11 and 13, models from the second study have much more regular helices, without the motional flexibility of the chain ends. However, the dynamics simulation of a helical polymer model predicted collapse of the structure. Chains without π-stacking or hydrogen-bonding interactions would be expected to "unwind" and lose helicity.

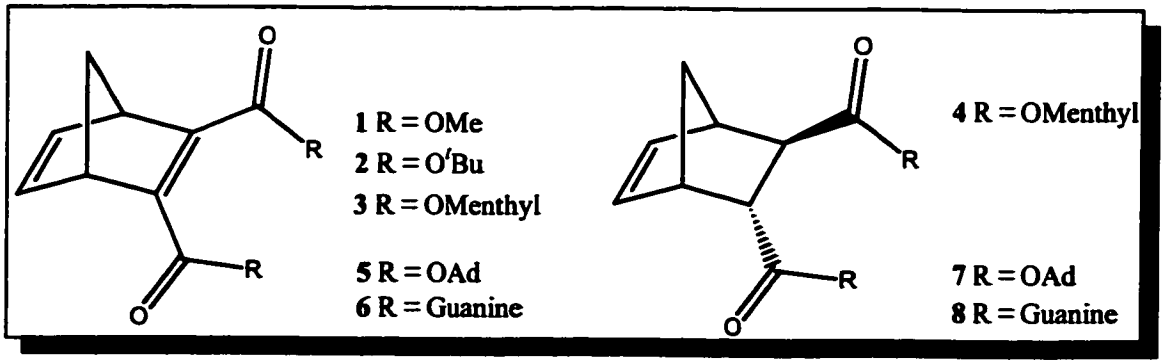

Figure 3. 17. Target Momomers for Synthesis

Key targets emerging from these modelling studies are listed in Figure 3. 17, some of which have been reported in the literature (**1**[11], **2**[12] ,**3**[5]). Although the modelling results do not indicate that polymers of **1** or **2** will generate the desired tube-like structures, they have been previously synthesized and characterized and will serve as reference compounds. Modelling has indicated that large 3D steric bulk, π-stacking and/or hydrogen-bonding may enforce a helical macrostructure in solution through substituent interactions. Other monomer targets should display the effect of steric bulk (adamantyl and menthyl) as well as hydrogen-bonding (guanine) on polymer topology.

3.4 Spectroscopic Characterization of Polymers

Of the eight targets listed in Figure 3. 17., four were kindly synthesized and polymerized by J. Snelgrove of this laboratory (**1**, **2**, **3** and **4**). Polymerizations were carried out using catalysts **A**, **B** or **C** (Figure 3. 18). On the basis of literature results, these were expected to yield cis/isotactic, trans/syndiotactic and atactic polymers respectively. Polymers are numbered according to the monomer number and catalyst letter. Polymerization details are summarized in Table 3. 15.

Table 3. 15. Polymer Properties

Polymer	*[Mon.]/[Cat.]*	*% yield*
1A	500	77
1C[13]	200	79
2A[12, 14]	500	91
3A[5]	500	
3B[5]	500	59
4A	500	77
4B	500	71
4C	500	95

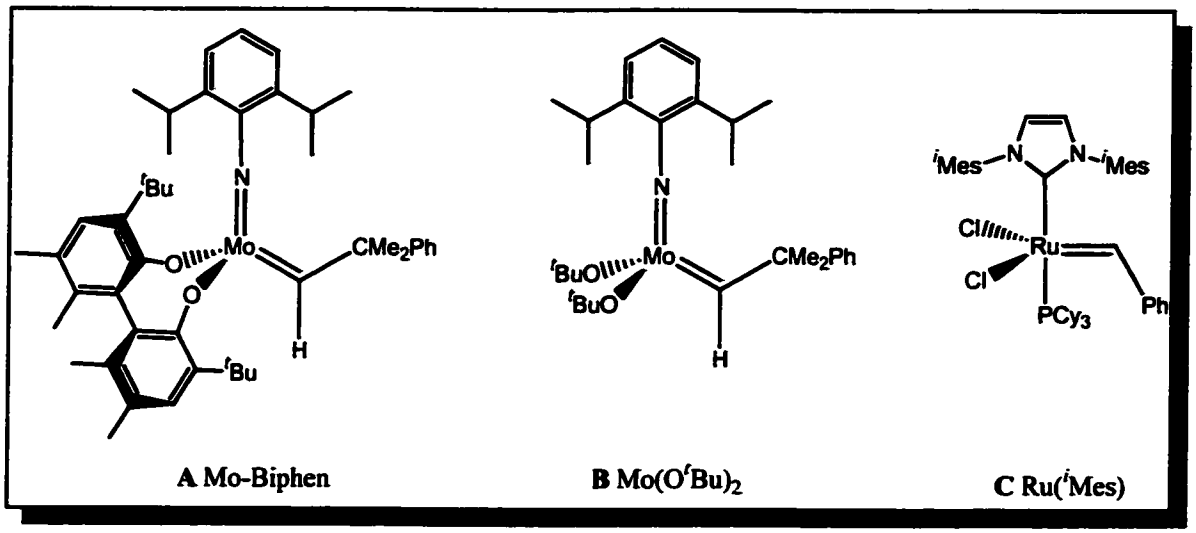

Figure 3. 18. Polymerization Catalysts Used

3.4.1 Cis/Trans and Tacticity Analysis

$^{13}C\{^1H\}$ NMR spectra provide critical insight into cis/trans ratios and tacticity. Ratio of cis/trans double bond can be calculated from the relative integrations of the allylic carbon signals ($\delta_{C1,4}$ trans ≈50 ppm, $\delta_{C1,4}$ cis ≈45 ppm) for both poly(norbornenes) and poly(norbornadienes) (Figure 3. 20). This ratio can be confirmed from the olefinic carbon signals ($\delta_{C2,3}$ trans ≈132.5 ppm, $\delta_{C2,3}$ cis ≈132 ppm) for poly(norbornadienes) (Figure 3. 19). However, the olefinic carbon signals for poly(norbornenes) are complicated by fine structure due to tacticity (see Section 1.4.2).

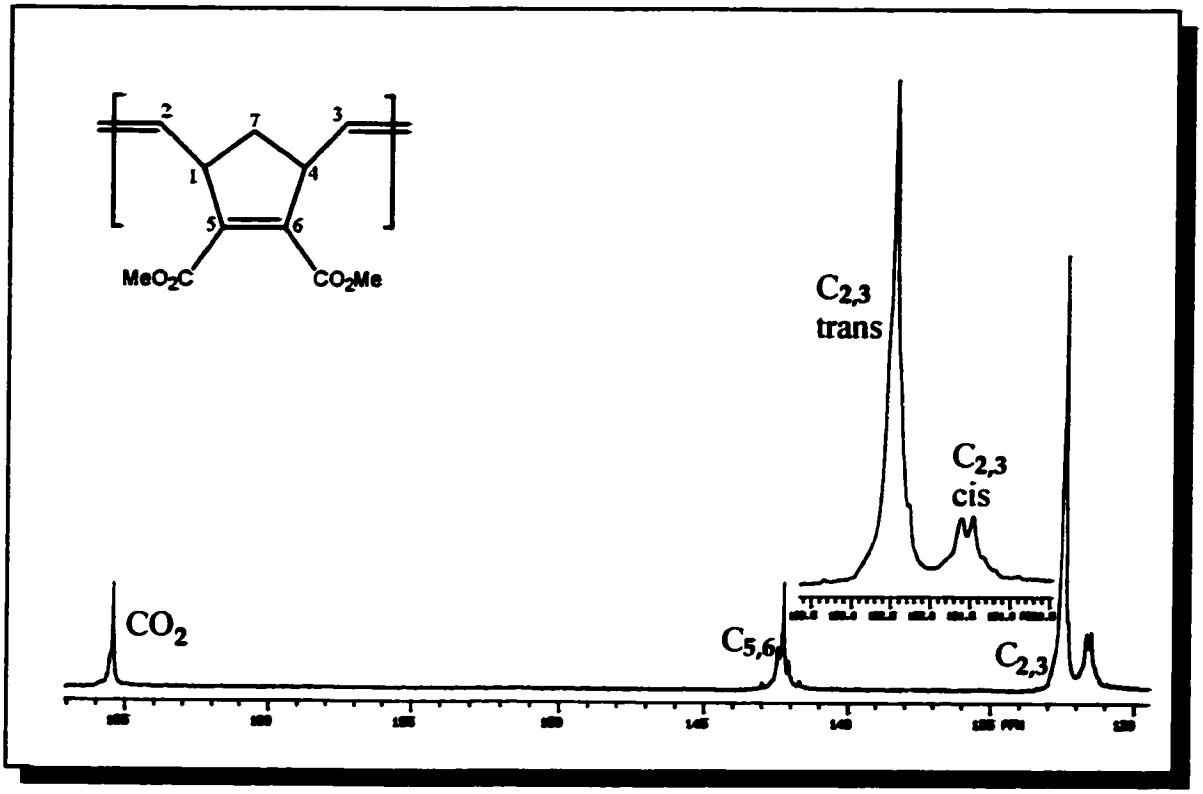

Figure 3. 19. Expansion of Olefinic Region of $^{13}C\{^1H\}$ NMR Spectrum of 1B (75 MHz, $CDCl_3$)

$^{13}C\{^1H\}$ NMR spectra of tactic polymers are characteristically well-resolved. Assessment of the multiplicity of the C_7 signal (δ_{C7} ≈40 ppm) was used to evaluate relative tacticity for polymers synthesized from symmetrical monomers (see Section 1.4.2). As discussed earlier, the C_7 carbon signal is sensitive to triads (two neighbouring repeat units) and will be divided into three signals ($\delta_{mm} > \delta_{mr/rm} > \delta_{rr}$) (Figure 3. 20). The integrated intensity of these signals is used to estimate the tacticity of a given polymer. Polymers **1A** and **2A** were estimated to be 71% isotactic, while **1B** was estimated to be 80% syndiotactic. Given that catalyst **A** has been associated with isotactic polymers and **B** with syndiotactic polymer, these results agree well with published reports.[13] All $^{13}C\{^1H\}$ spectra can be found in Appendix A.

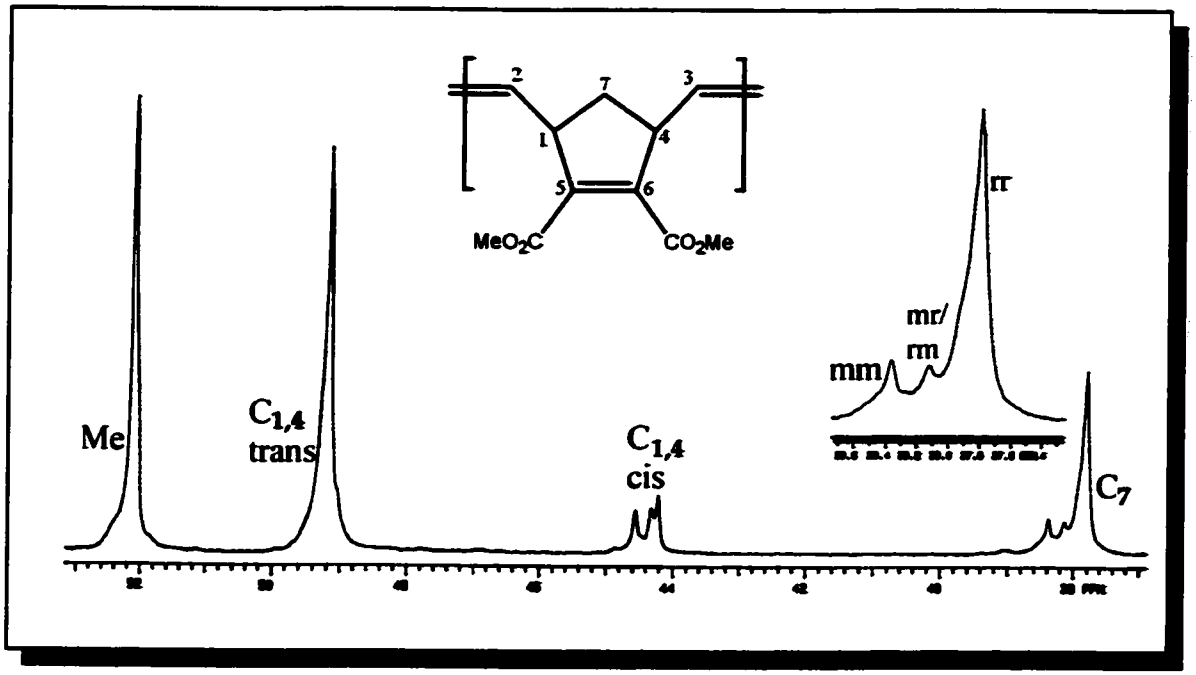

Figure 3. 20. Expansion of Aliphatic Region $^{13}C\{^1H\}$ NMR Spectrum of 1B (75 MHz, $CDCl_3$)

^1H-^1H COSY NMR analysis provides an explicit means of tacticity determination, as outlined in Section 1.4.2. Polymers **3A**, **3B**, **4A**, **4B** and **4C** were analyzed by this method as they were synthesized from unsymmetrical monomers. None of the polymers, with the exception of **3A**, exhibited cross-peaks, indicating that they contain racemic (syndiotactic) dyads. Observation of such a cross-peak for **3A** denotes that this polymer contains meso (isotactic) dyads. All three polymers (**4A**, **4B** and **4C**) made with monomer **4** were 100% syndiotactic, as indicated by the absence of cross-peaks. This result was unexpected, given that the catalysts were expected to yield isotactic (Mo-Biphen), syndiotactic ($Mo(O^tBu)_2$) and atactic ($Ru(^i Mes)$) polymers respectively. This may point toward chain-end control as the origin of enantioselectivity; that is, the growing polymer chain is directing monomer approach to the catalyst for poly(norbornenes). All ^1H-^1H NMR COSY spectra can be found in Appendix A.

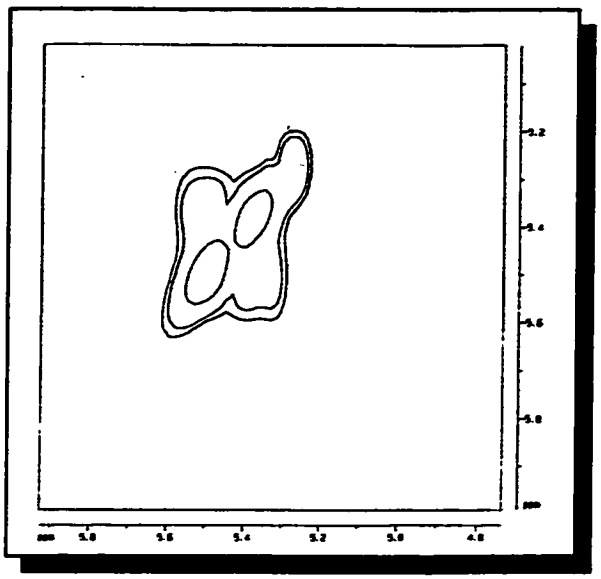

Figure 3. 21. Expansion of Olefinic Region of ^1H-^1H COSY of 3A (300 MHz, $CDCl_3$)

Table 3. 16. Results of NMR Tacticity Analyses

Polymer	*% cis*	*tacticity*
1A	81	iso (70%)
1B	20	syndio (80%)
2A	80	iso (72%)
3A	100	iso (100%)
3B	0	syndio (100%)
4A	50	syndio (100%)
4B	42	syndio (100%)
4C	49	syndio (100%)

3.4.2 Molecular Weight and Conformational Analysis

Polymer molecular weights were measured by GPC while the solution conformations were analyzed using light scattering. Results are summarized in Table 3. 17. Some of the molecular weights varied greatly from their theoretical values, but nonetheless showed narrow polydispersities (PDI). In some cases, the main elution peak is made up of two separate molecular weight fractions (**3A** & **4B** in Table 3. 17). It is possible that the second peak is due to slightly different rates of polymer chain growth from two different initiation sites on the catalyst. There are literature precedents where slightly

different rates of growth on two non-interconvertible enantiomers of a catalyst lead to bimodality in the GPC trace.[5, 15] This would explain the result for **3A**, but not for **4B**. The presence of an additional peak may thus, alternatively, be due contaminants which affected the polymerization reaction.

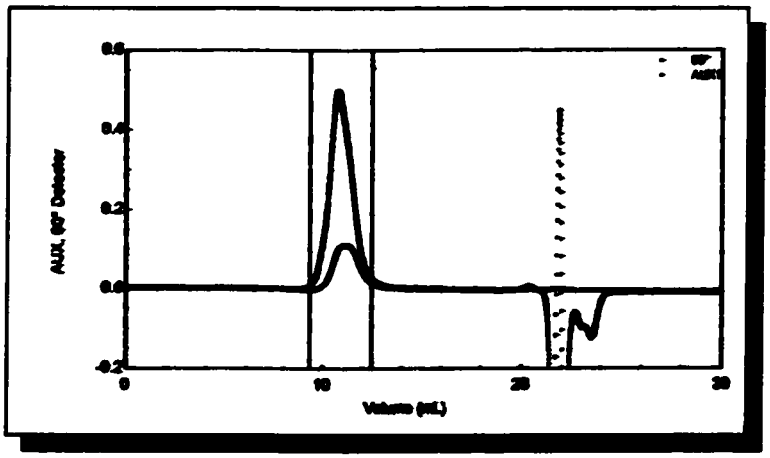

Figure 3. 22. GPC Trace for 3B

Conformation plots were generated from the light scattering data by plotting standard log-log plot of RMS radius vs. the molecular weight to assess the polymer conformation in solution (Section 2.5). All of the polymers have a spherical solution conformation, with slopes near the theoretical value of 0.33 for a sphere. (Stable helical polymers would behave as rods in solutions and would have a slope of 1, which is not the case for any of the polymers produced thus far.) However, the molecular weights and solution conformation were measured using Equations 10 to 19 with the assumption that the polymer was in its theta state and so A_2 is zero. Quite conceivably, the polymer may not have A_2=0 in dichloromethane and hence the conformation may be different.

Table 3. 17. Results of GPC/LS Analyses

Polymer	*[Mon.]/[Cat.]*	*Theoretical MW*	*Actual MW*	*PDI*	*Slope of Conf. Plot*
1A	500	104 125	156 300	1.139	0.28 (Sphere)
1B	200	41 650	156 700	1.064	
2A	500	146 190	165 200	1.087	0.38 (Sphere)
3A	500	228 335	1 054 000	1.054	0.33 (Sphere)
			1 353 000	1.087	0.38 (Sphere)
3B	500	228 335	462 200	1.087	0.42 (Sphere)
4A	500	229 350	238 100	1.090	0.44 (Sphere)
4B	500	229 350	866 500	1.042	0.33 (Sphere)
			1 013 000	1.242	0.38 (Sphere)
4C	500	229350	197 500	1.097	0.31 (Sphere)

3.4.3 Polarimetry and Circular Dichroism (CD) Spectroscopy

Optical activity was measured using both polarimetry and CD spectroscopy. Monomers **1** and **2** did not display any optical activity ($[\phi]_D = 0°$) or CD signal whereas **4** did ($[\phi]_D$ = +4.64°, c=1, CD spectrum in appendices). There was not enough material to complete optical activity measurements on monomer **3** or on polymer **1B**. Polymer **1A** did not display any optical activity. while **2A** did show a small amount of optical activity both by polarimetry and by CD spectroscopy. The presence of optical activity suggests that either the polymer exists as a slightly unequal mixture of enantiomers, or that the chain contains small helical segments separated by helical reversals. The band at ~230 nm is most likely due to an $n \rightarrow \pi^*$ transition of the carbonyl groups in some sort of chiral environment. It is difficult to determine if the band at 231 nm is part of a couplet since the solvent (CH_2Cl_2) masks any transitions lower than 229 nm. However, it is unlikely that this chain is purely helical as light scattering studies indicate a spherical solution conformation.

Polymers (**3A** – **4C**) made from chiral monomers exhibited large negative optical rotations and distorted CD couplets that resemble that of a P(-) helix (Figure 2. 18(c)). The polymers **4A**, **4B** and **4C** have opposite optical rotation from the monomer. Again, the optical activity may indicate an unequal mixture of enantiomers for the polymer chains, or helical segments separated by helical reversals.

The bands observed in the CD spectra of **3A** – **4C** are from an $n \rightarrow \pi^*$ transition for the carbonyl group. The presence of couplets in the CD spectra is significant because it indicates chiral arrangement of interacting chromophores. Distortion of couplets in CD spectra has been previously reported for helical poly(isocyanides) with chiral side groups.[16] Given this example, it is possible that the couplet is distorted by the chiral menthyl side groups. A typical spectra is shown in Figure 3. 23. All CD spectra are shown in the Appendix C.

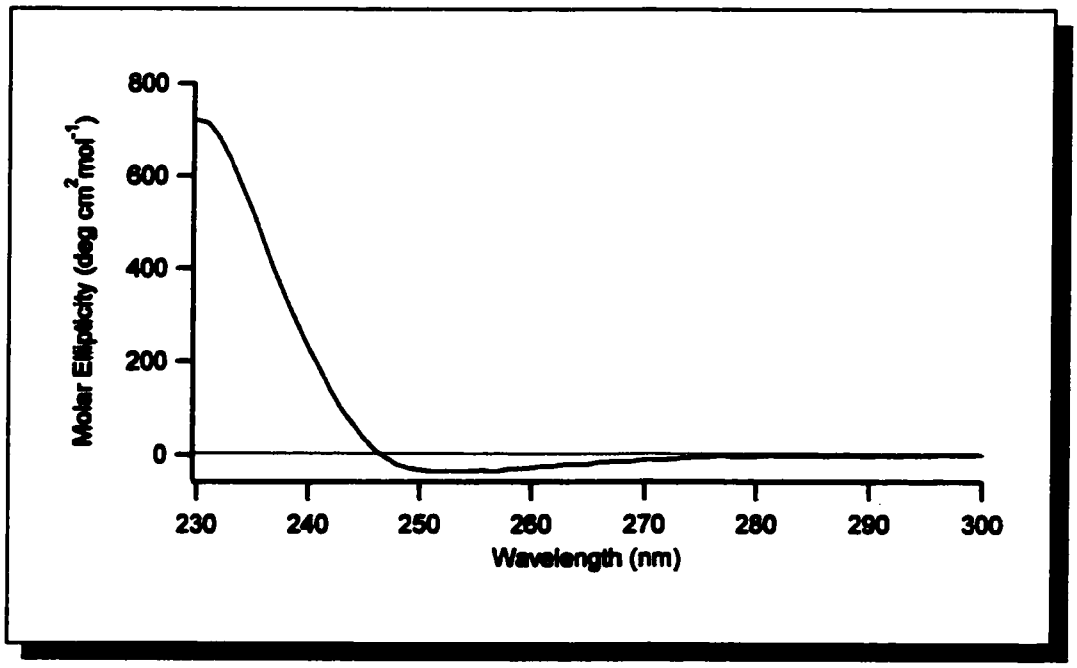

Figure 3. 23. CD Spectrum of 4C (CH_2Cl_2)

Table 3. 18. Results of Polarimetry and CD Analyses

Polymer	$[\phi]_D$ (c=1)	*Min. [θ] (°·cm²/mol)*	λ *(nm)*
1A	0	0	
1B			
2A	-1.0°	-637	231
3A	-93.45°	-34 234	247
3B	-83.23°	-12 472	240
4A	-91.92°	-27.09	257
4B	-83.27	-1066.92	230
4C	-77.16°	-36.18	253

3.4.4 Summary and Conclusions

Four monomers of the eight key targets (Figure 3. 17) were polymerized using catalysts **A, B** and **C** that typically yield cis/isotactic, trans/syndiotactic and atactic polymers respectively. Polymer microstructures were examined spectroscopically using ^{1}H, ^{1}H-^{1}H COSY, and $^{13}C\{^{1}H\}$ NMR. The expected microstructures were obtained for the norbornadiene polymers but all three polymers made of monomer **4** were 50% cis and completely syndiotactic. This would tend to suggest that stereospecific polymerizations of norbornadiene monomers proceed under enantiomorphic metal control whereas norbornene monomers carry on under chain end control.

Most molecular weights varied greatly from their theoretical values but nonetheless had narrow polydispersities. The conformation plots from light scattering data showed that the polymer chains exist as spheres in solution.

Polymers made from optically active monomers were also optically active, but with inverse optical rotation and CD spectra from the monomers. A small amount of optical

activity was detected for polymer **2A** which was made from an optically inactive monomer suggesting some amount of chiral induction.

3.5 References

1. Nolte, R.J.M. *Chem. Soc. Rev.*, **1994**, 11

2. Okamoto, Y.,Nakano, T. *Chem. Rev.*, **1994**, *94*, 349

3. Percec, V., Schlueter, D., Ronda, J.C., Johansson, G., Ungar, G.,Zhou, J.P. *Macromolecules*, **1996**, *29*, 1464

4. Mikami, M.,Shinkai, S. *Chemistry Letters*, **1995**, 603

5. O'Dell, R., McConville, D.H., Hofmeister, G.E.,Schrock, R.R. *J. Am. Chem. Soc.*, **1994**, *116*, 3414

6. Feast, W.J., Gibson, V.C., Ivin, K.J., Kenwright, A.M.,Khosravi, E. *J. Mol. Catal.*, **1994**, *90*, 87

7. Hunter, C.A.,Sanders, J.K.M. *J. Am. Chem. Soc.*, **1990**, *112*, 5525

8. Hasenknopf, B., Lehn, J.-M., Boumediene, N., Leize, E.,Van Dorsselaer, A. *Angew. Chem. Int. Ed.*, **1998**, *37*, 3625

9. Cuccia, L.A., Lehn, J.-M., Homo, J.-C.,Schmutz, M. *Angew. Chem. Int. Ed.*, **2000**, *39*, 233

10. Jeffrey, G.A.,Saenger, W. *Hydrogen Bonding in Biological Structures*, Springer, Verlag, **1991**, p.29

11. Tabor, D.C., White, F.H., Collier, L.W.,Evans, S.A. *J. Org. Chem.*, **1983**, *48*, 1638

12. Delaude, L., Demonceau, A.,Noels, A.F. *Macromolecules*, **1999**, *32*, 2091

13. Bazan, G.C., Khosravi, E., Schrock, R.R., Feast, W.J., Gibson, V.C., O'Regan, M.B., Thomas, J.K.,Davis, W.M. *J. Am. Chem. Soc.*, **1990**, *112*, 8378

14. Schrock, R.R., Lee, J.-K., O'Dell, R.,Oksam, J.H. *Macromolecules*, **1995**, *28*, 5933

15. Totland, K.M., Boyd, T.J., Lavoie, G.G., Davis, W.M.,Schrock, R.R. *Macromolecules*, **1996**, *29*, 6114

16. Kamer, P.C.J., Cleij, M.C., Nolte, R.J.M., Harada, T., Hezemans, A.M.F.,Drenth, W. *J. Am. Chem. Soc.*, **1988**, *110*, 1581

CHAPTER 4

CONCLUSIONS AND FUTURE DIRECTIONS

The work summarized in this thesis described the molecular modelling study of norbornene and norbornadiene polymers and the spectroscopic characterization of their microstructures and macrostructures. Modelling was accomplished using two methods of study. The first and less accurate method only examined single repeat units, and produced high energy helical oligomers. The second method that considered torsion angles of dyads, resulted in oligomer models that should be closer to their minimum energy conformation. Model polymers produced by the second method are more compressed, displayed regular helical parameters throughout the model and less flexibility in the chain ends than those made by the first method. Cis/isotactic and trans/syndiotactic models of poly(norbornenes) and poly(norbornadienes) had the most tube-like conformations respectively. Generally, isotactic dyads had one negative and one positive torsion angle, whereas syndiotactic dyads had two negative torsion angles. Cis dyads, one torsion angle was generally less than 90° and one greater than 90°. Trans dyads had torsion angles that were both greater than 90°. Increasing the bulk of aliphatic substituents (tert-butyl and adamantly groups) caused elongation of the helix whereas groups capable of π-stacking and hydrogen-bonding (phenyl, guanine) gave helices judged by the alignment of substituents on neighbouring repeat units. Little change was observed on changing the tether from an ester to an ether, or on changing the C_7 atom from a carbon to an oxygen. Of the 73 models studied, eight key targets emerged.

Previously reported polymers were chosen as baseline references. Large three-dimensional aliphatic bulk as for an adamantyl group, may stabilize the helix by prevention rotation about main-chain carbon bonds. Hydrogen-bonding and π-stacking as for guanine, may enforce helical rigidity through substituent interactions with neighbouring repeat units and even neighbouring helical turns. This offers the highest probability of producing helical polymers of norbornenes and norbornadienes with stable solution conformations.

Polymer microstructures and macrostructures were analyzed for four monomers and their resulting polymers by NMR, GPC/LS, polarimetry and CD spectroscopy. ^{1}H, ^{1}H-^{1}H COSY and $^{13}C\{^{1}H\}$ NMR analysis indicated that poly(norbornadienes) had tacticities consistent with literature reports (cis/isotactic for Mo-Biphen and trans/syndiotactic for $Mo(O^{t}Bu)_2$). However, polymers of menthyl ester norbornene (**4**) all had the same microstructure (50% cis, 100% syndiotactic) regardless of the catalyst used (Mo-Biphen, $Mo(O^{t}Bu)_2$ and $Ru(^{i}Mes)$). This suggests that the polymerizations of norbornadienes are directed by the catalyst (enantiomorphic site control) whereas polymerizations of norbornenes are directed by the growing polymer chain (chain end control). GPC analysis of two polymers (**3A** and **4B**), revealed the existence of two overlapping molecular weight peaks. This may be due to slightly different rates of growth at the two catalyst enantiomers or contaminants in solution. Conformation plots from LS data show that all the polymers have a spherical conformation in solution. Optically active monomers resulted in optically active polymers and non-optically monomers yielded non-optically active polymers. However, poly(2,3-dicarbo-^{t}butoxynorbornadiene) (**2A**)

displayed a small amount of optical activity both by polarimetry and CD spectroscopy despite the lack of optical activity in the monomer. Since light-scattering indicated a spherical solution conformation for all polymers, the optical activity cannot be due to helicity (which would give rise to a rod-like morphology). The spherical conformation may be due to small helical segments in the polymer chain separated by helical reversals, or from an unequal mixture of enantiomers. Bends in the chain caused by the helical reversals would cause the chain to collapse and hence appear more spherical. If there is an excess of segments of one sense, then optical activity may result.

There is a higher chance of helicity for polymers with substituents capable of π-stacking and hydrogen bonding. Dynamics studies should be performed on these more rigid systems and a model of DNA to determine if the chain collapse still occurs before determining the stability of the helices. The energies of both left and right-handed models should be examined in order to determine if helix-sense selective polymerization is likely to occur. Monomer and polymer synthesis should be directed towards adamantyl and guanine derivatives of norbornenes and norbornadienes. Chromophores from the guanine and other substituents capable of π-stacking and hydrogen bonding should also be considered as they cause a red shift of CD bands. Dye inclusion may prove a useful adjunct method for estimation of solution topology.

APPENDICES

Appendix A: NMR Experiments

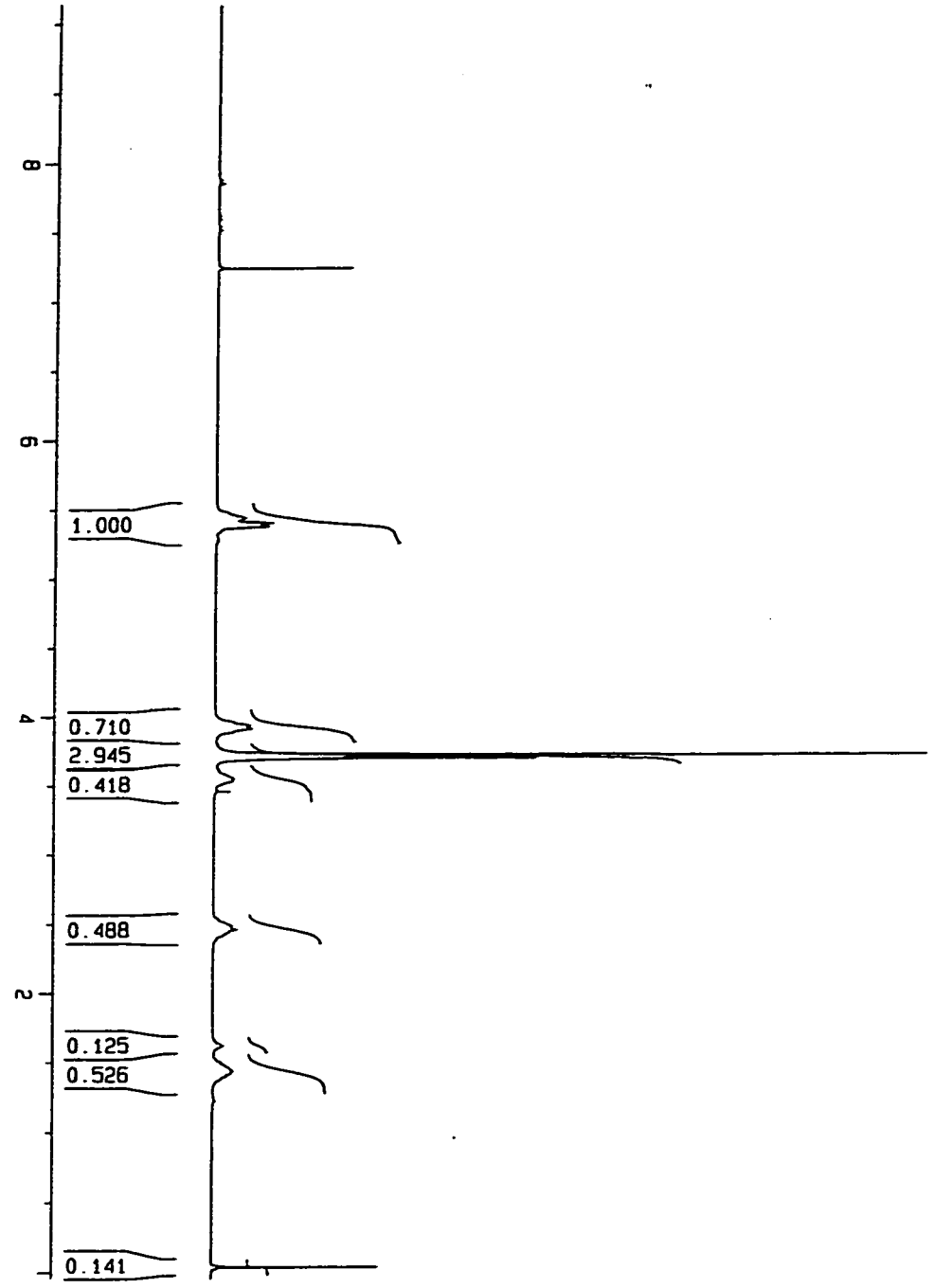

Figure A. 1. ^{1}H NMR Spectrum (300 MHz, $CDCl_3$) of 1A

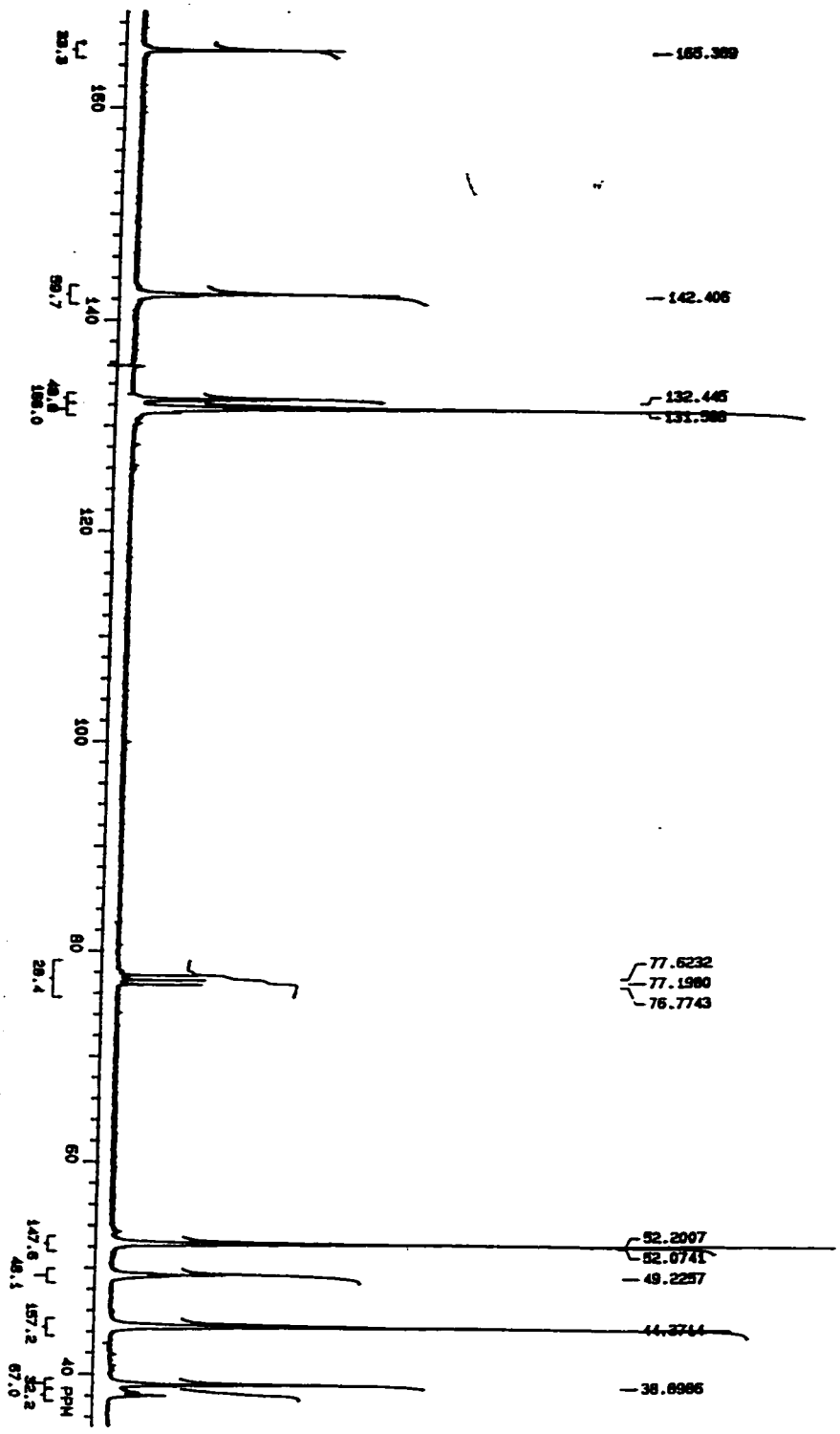

Figure A. 2. $^{13}C\{^{1}H\}$ NMR Spectrum (75 MHz, $CDCl_3$) of 1A

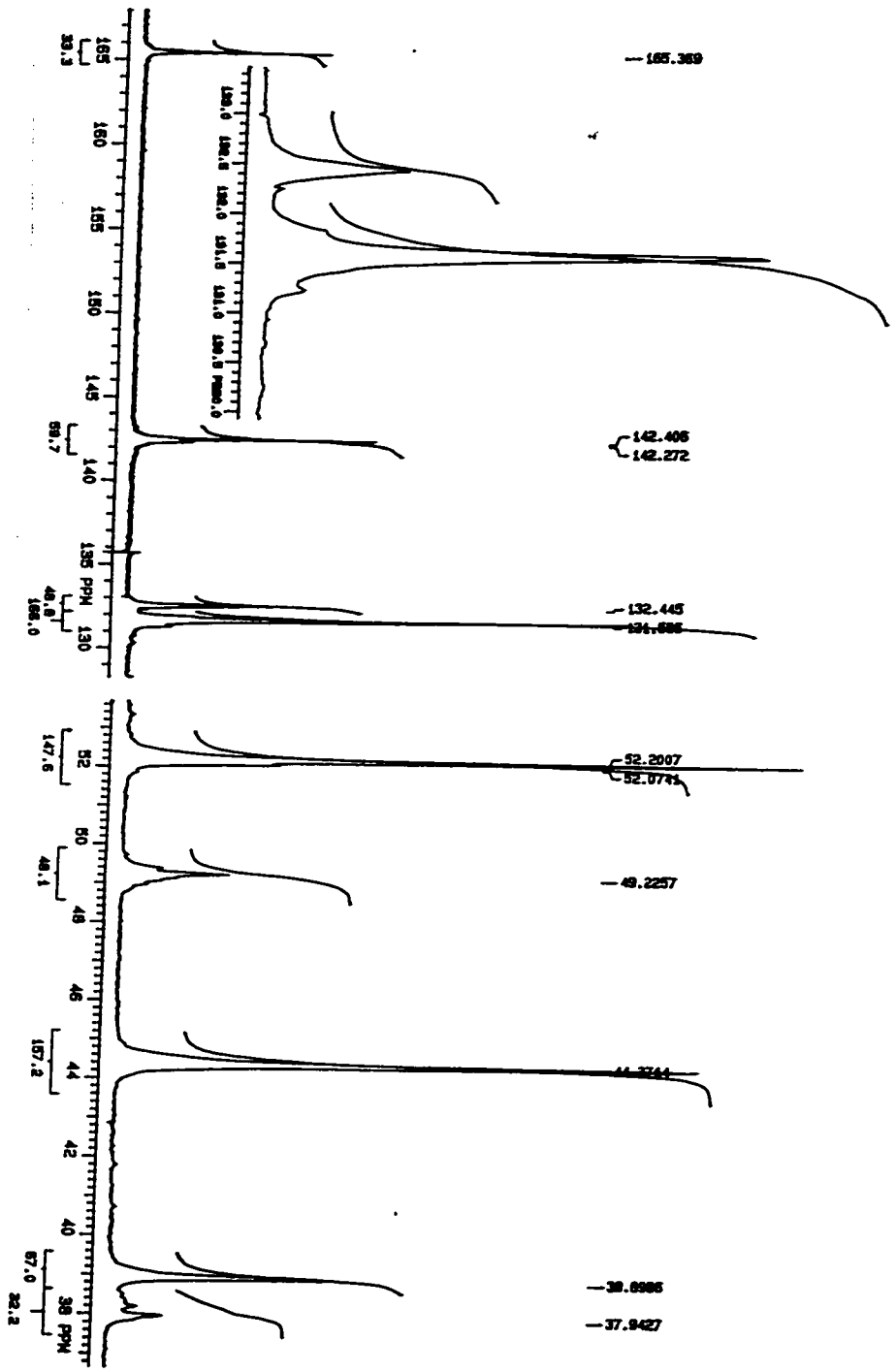

Figure A. 3. Expansion of Olefinic and Aliphatic Regions of $^{13}C\{^{1}H\}$ NMR Spectrum of 1A

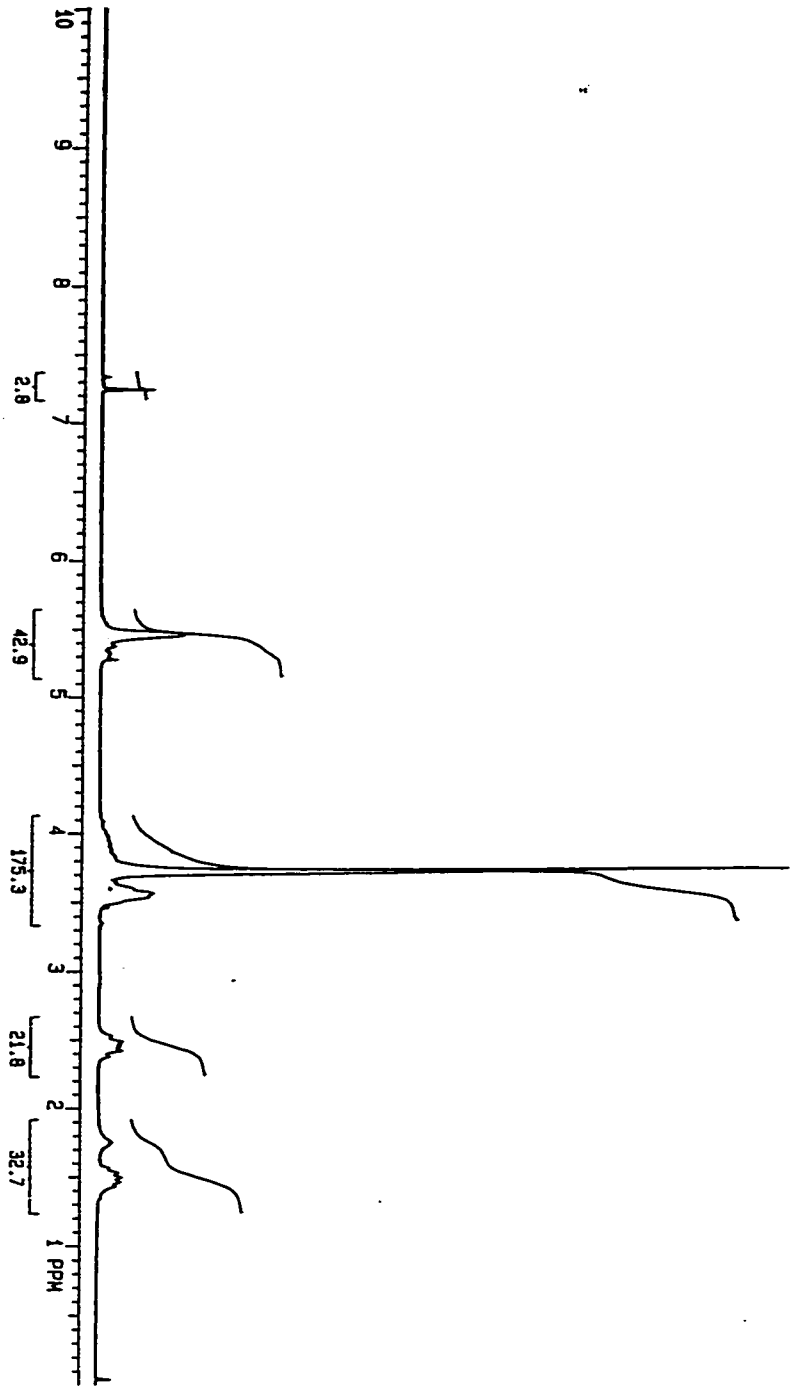

Figure A. 4. ^{1}H NMR Spectrum (300 MHz, $CDCl_3$) of 1B

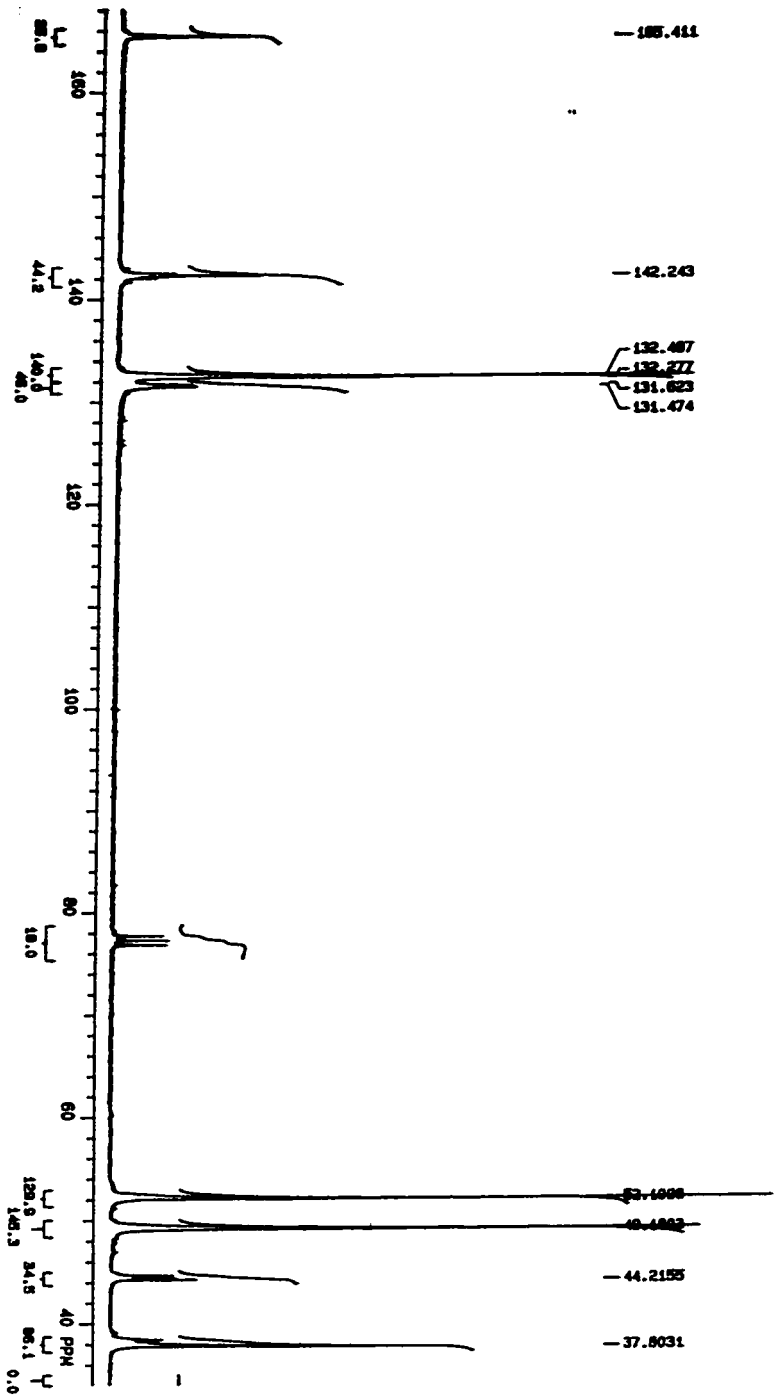

Figure A. 5. $^{13}C\{^{1}H\}$ NMR Spectrum (75 MHz, $CDCl_3$) of 1B

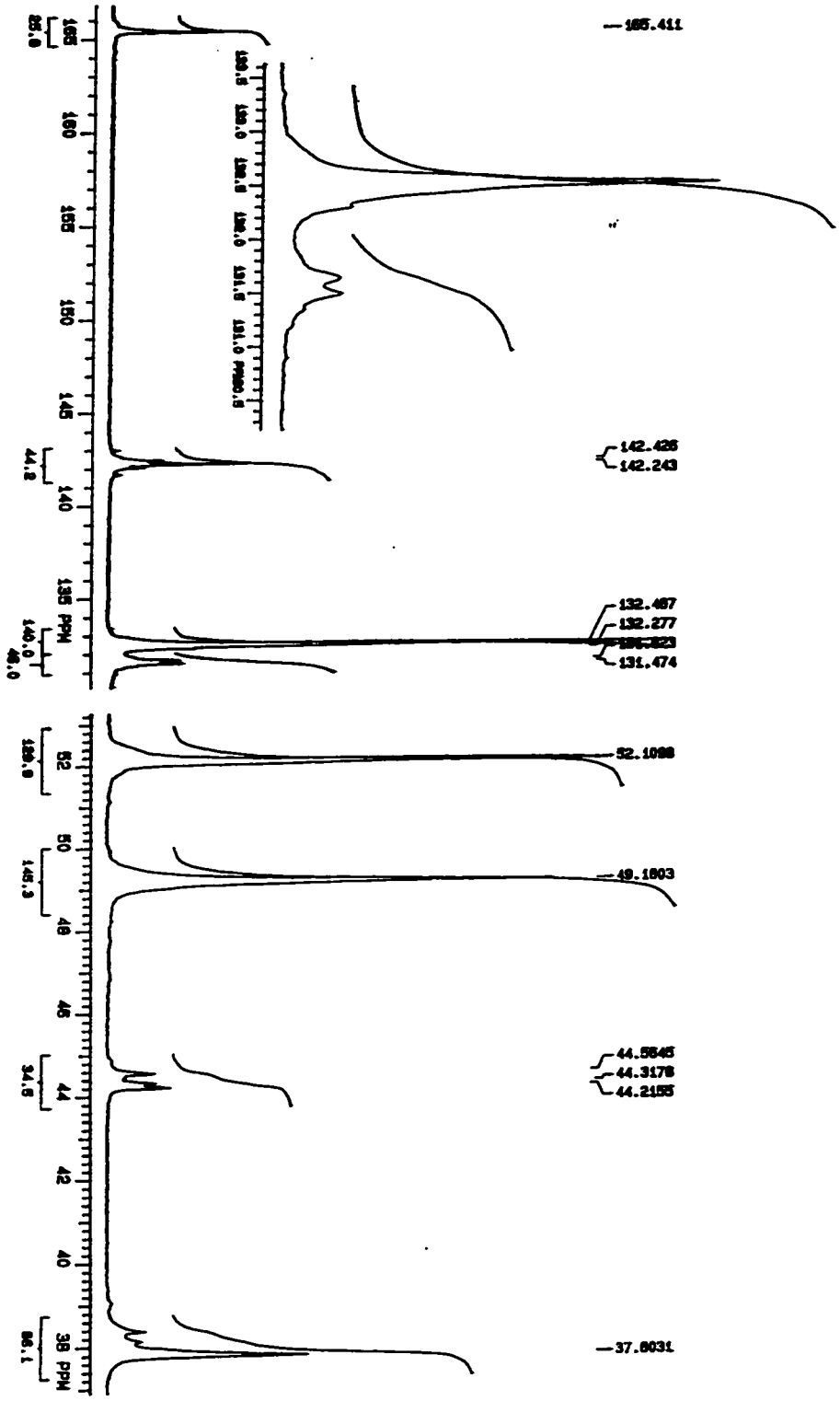

Figure A. 6. Expansion of Olefinic and Aliphatic Regions of $^{13}C\{^{1}H\}$ NMR Spectrum of 1B

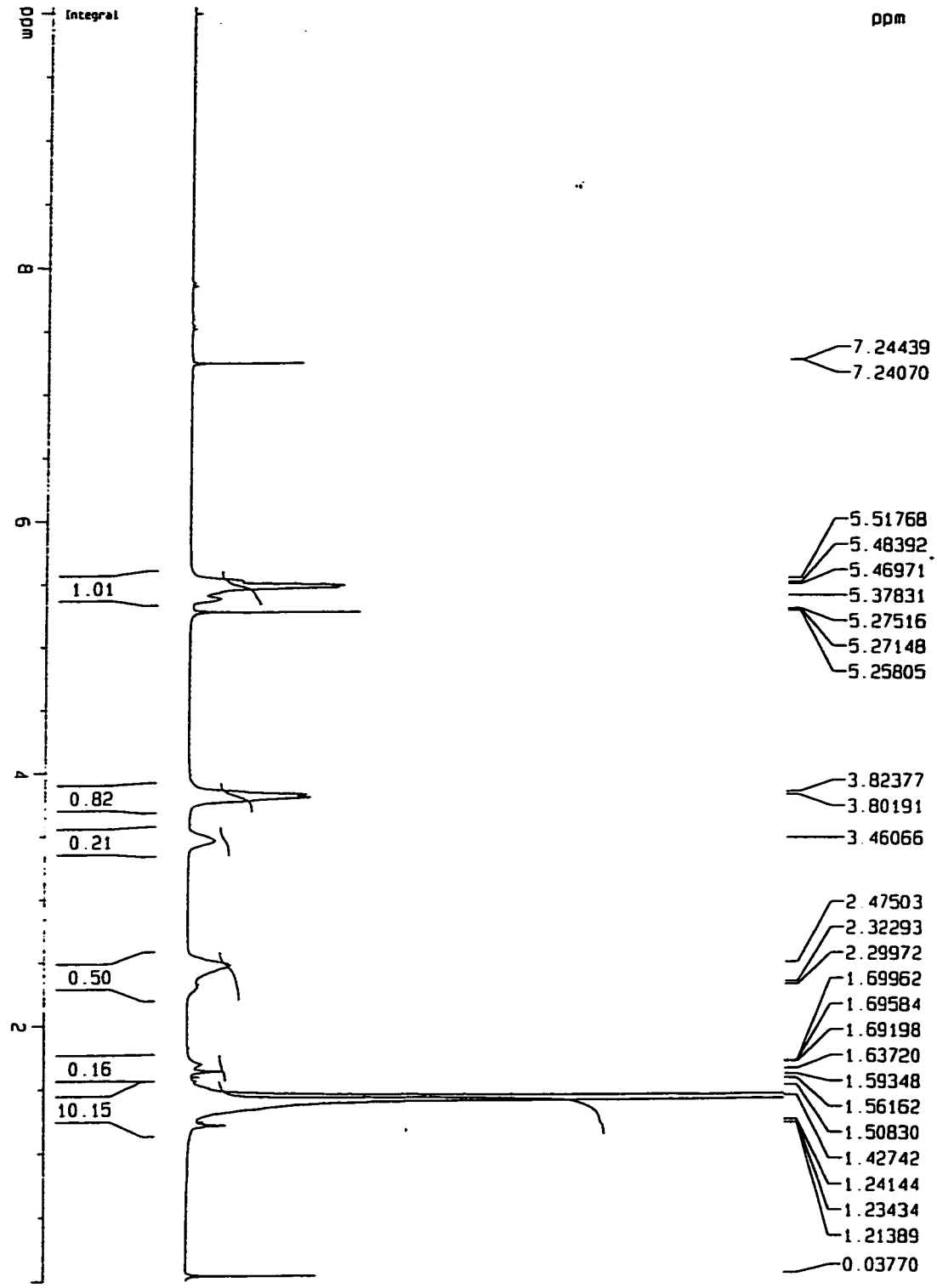

Figure A. 7. ^{1}H NMR Spectrum (300 MHz, $CDCl_3$) of 2A

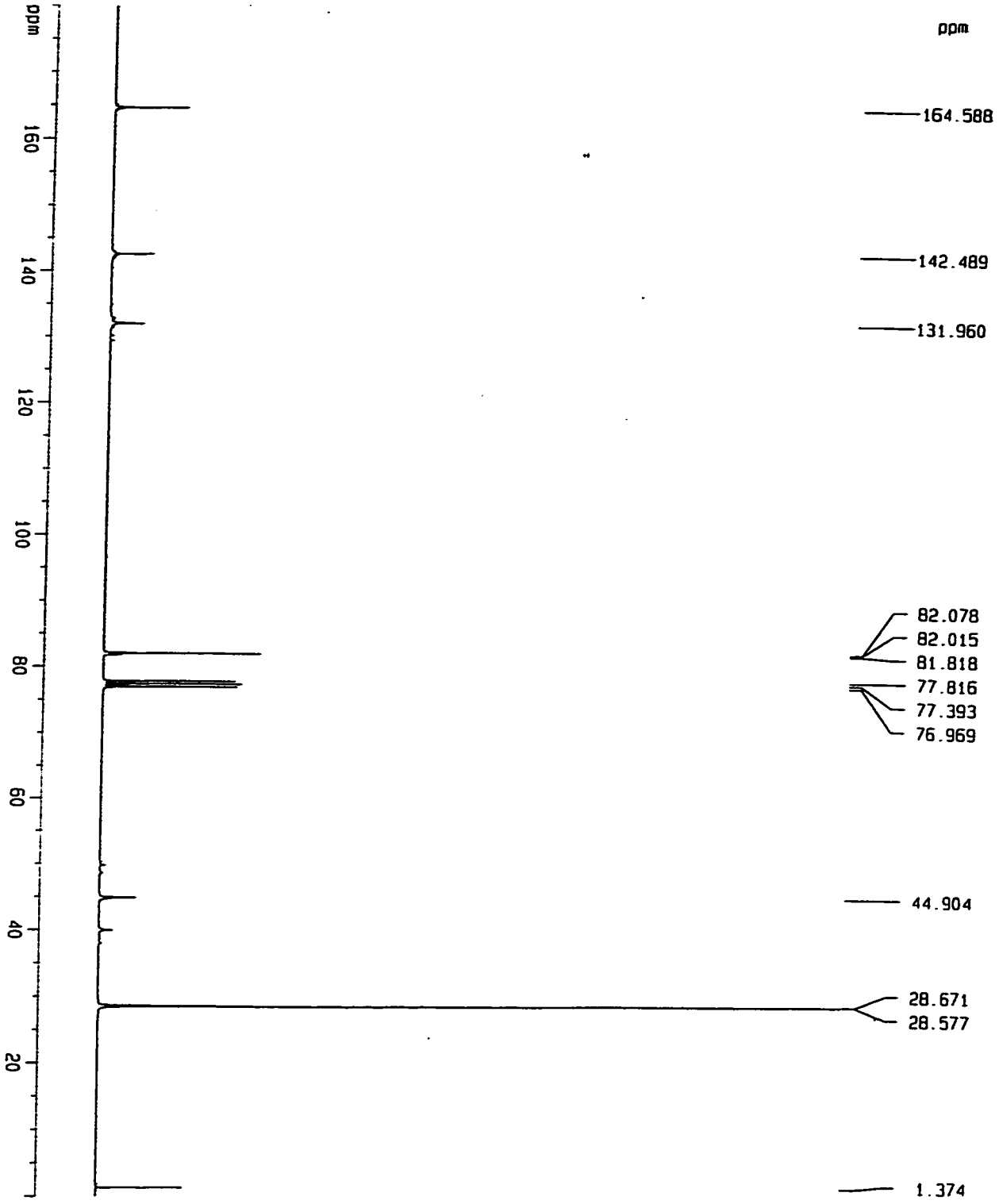

Figure A. 8. $^{13}C\{^{1}H\}$ NMR Spectrum (75 MHz, $CDCl_3$) of 2A

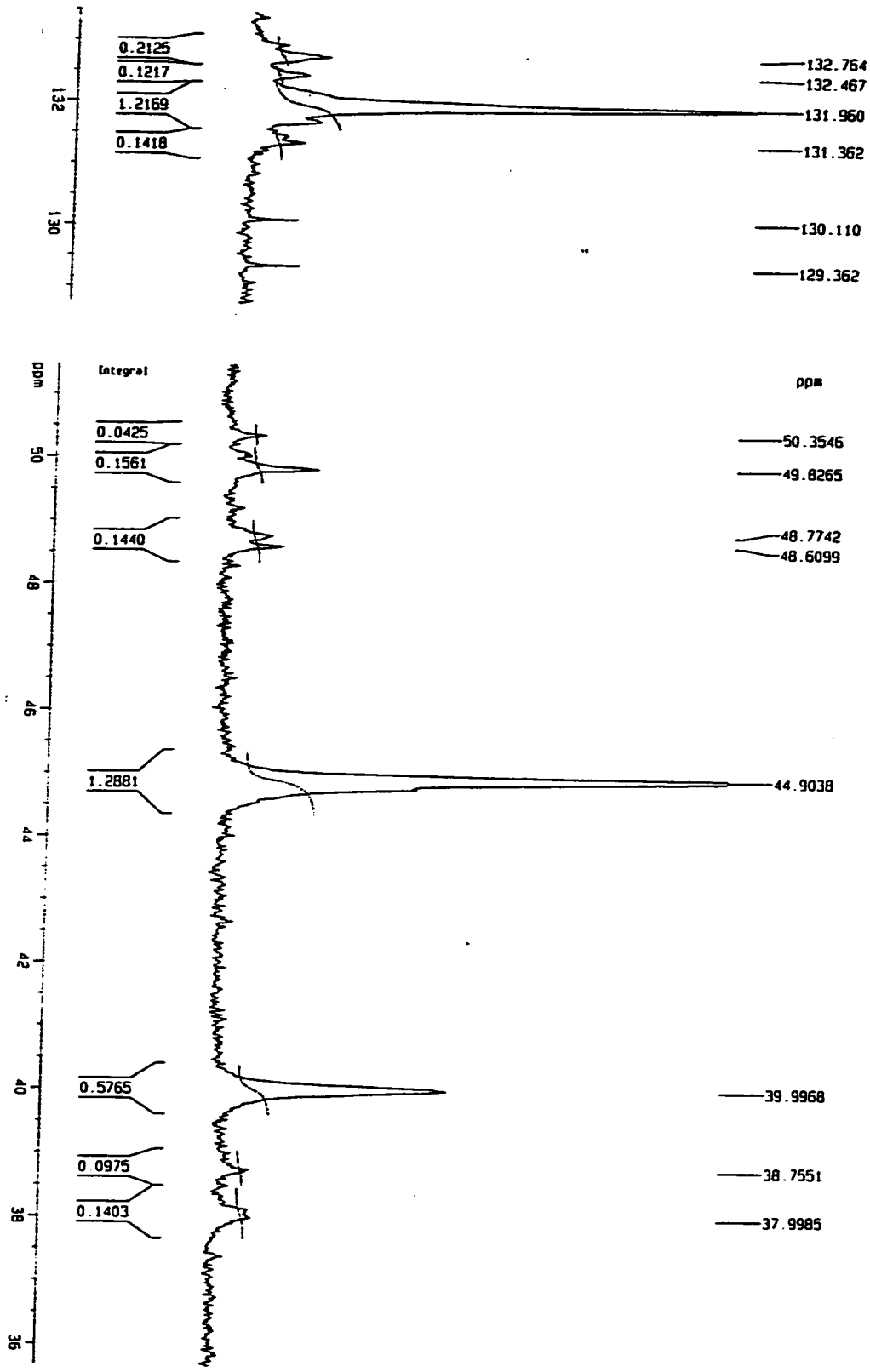

Figure A. 9. Expansion of Olefinic and Aliphatic Region of $^{13}C\{^{1}H\}$ NMR Spectrum of 2A

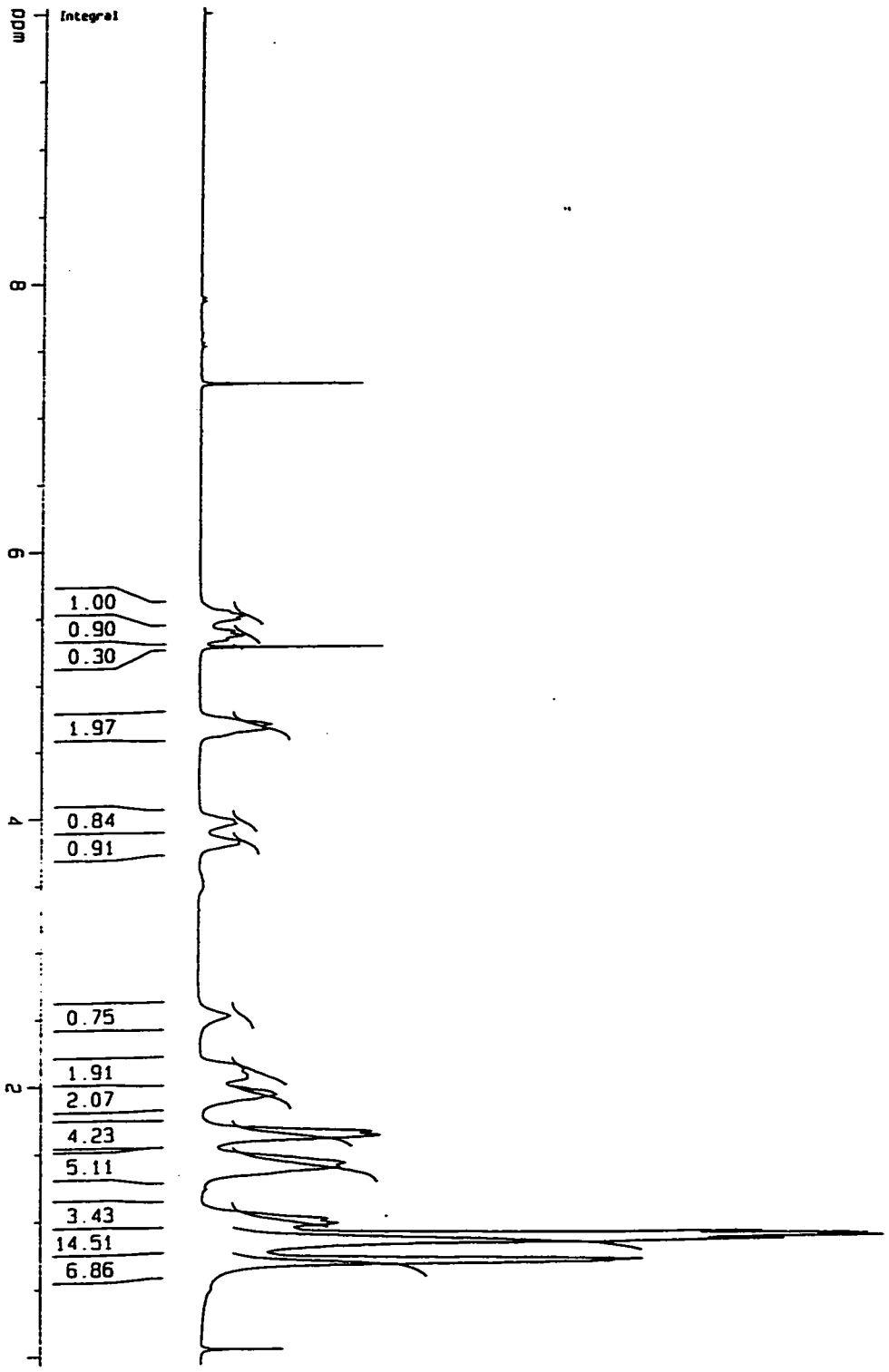

Figure A. 10. ^{1}H Spectrum (300 MHz, $CDCl_3$) of 3A

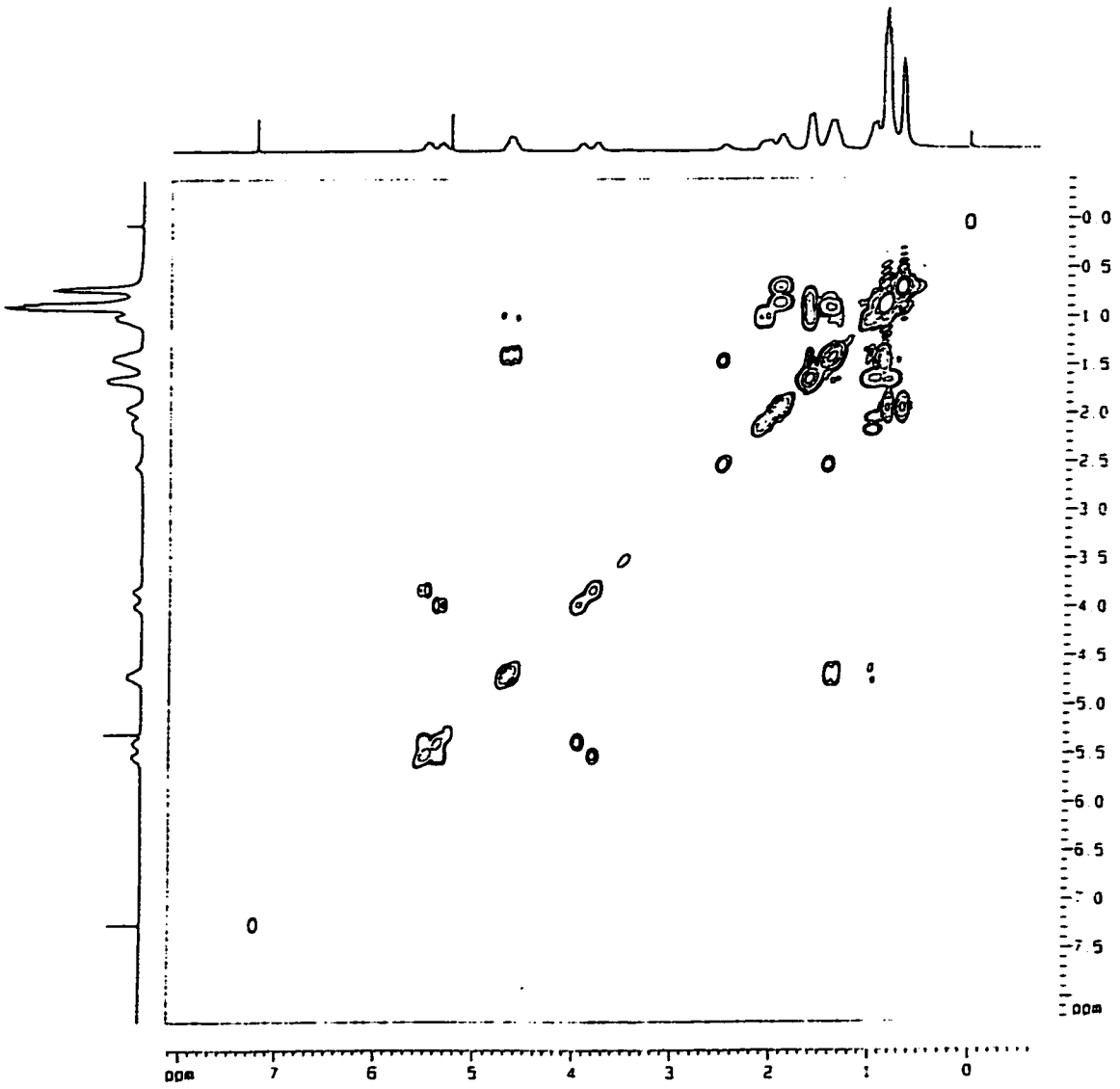

Figure A. 11. ^{1}H-^{1}H COSY NMR Spectrum (300 MHz, $CDCl_3$) of 3A

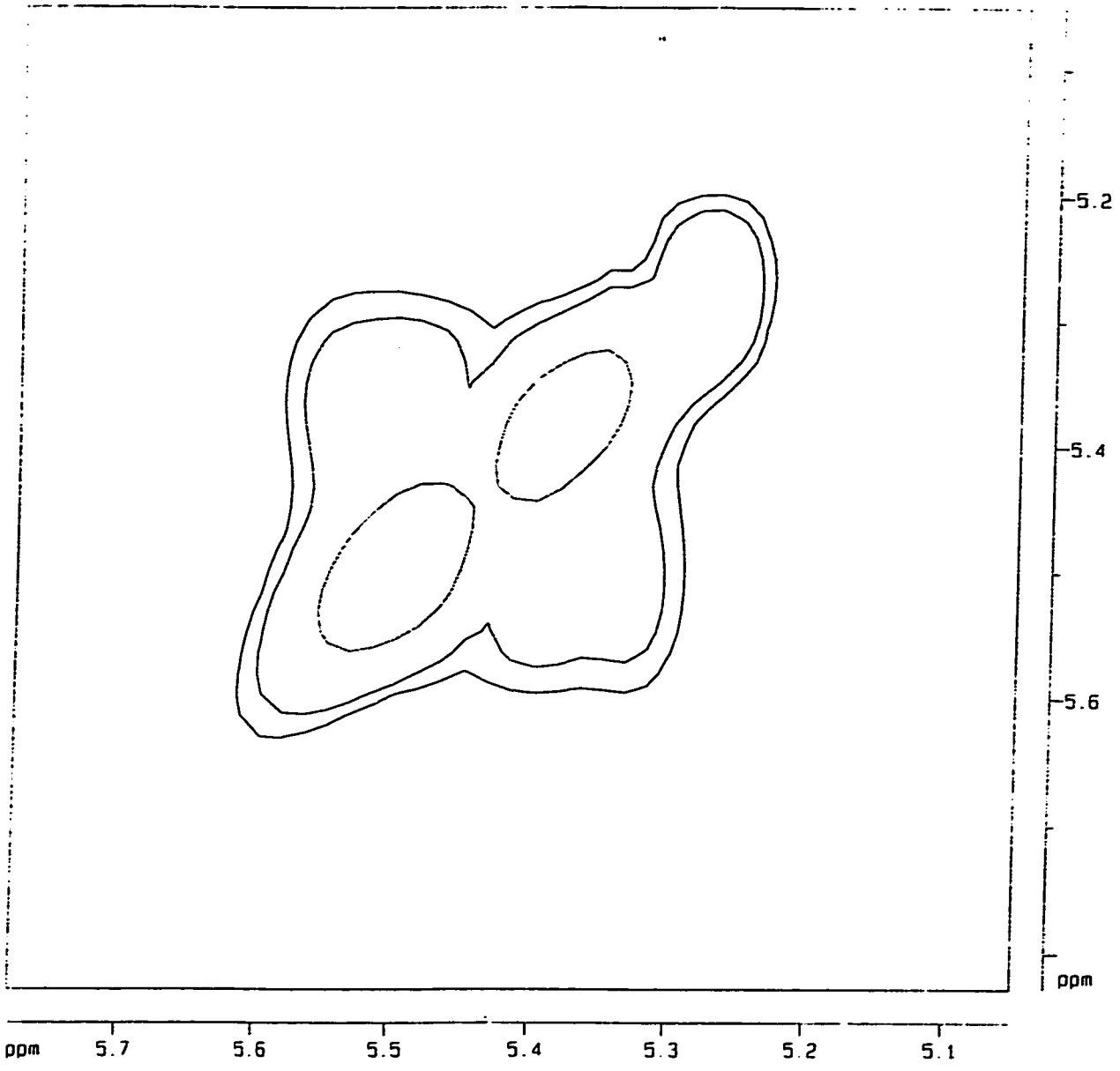

Figure A. 12. Expansion of Olefinic Region of ^{1}H-^{1}H COSY NMR Spectrum of 3A

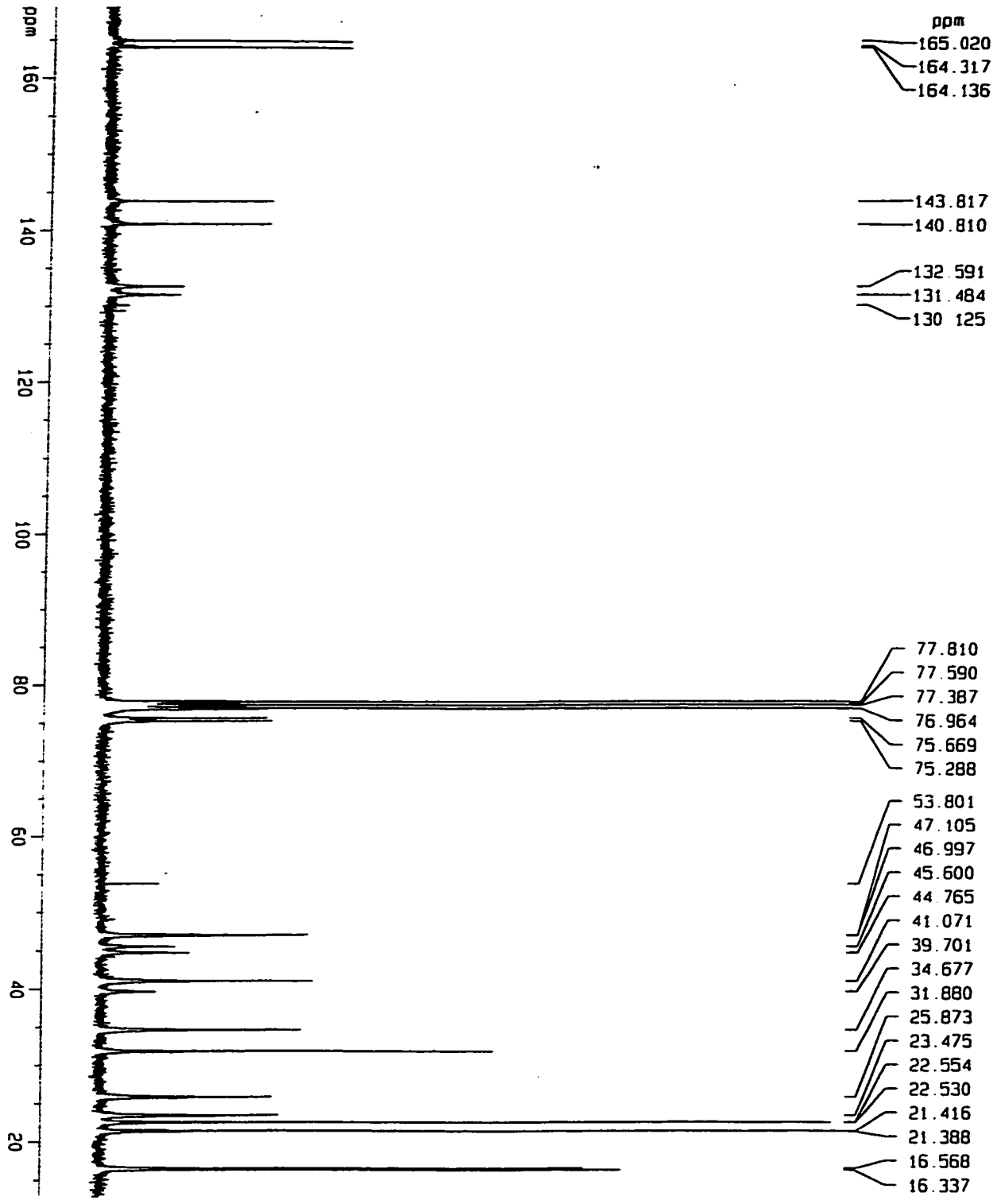

Figure A. 13. $^{13}C\{^{1}H\}$ NMR Spectrum (75 MHz, $CDCl_3$) of 3A

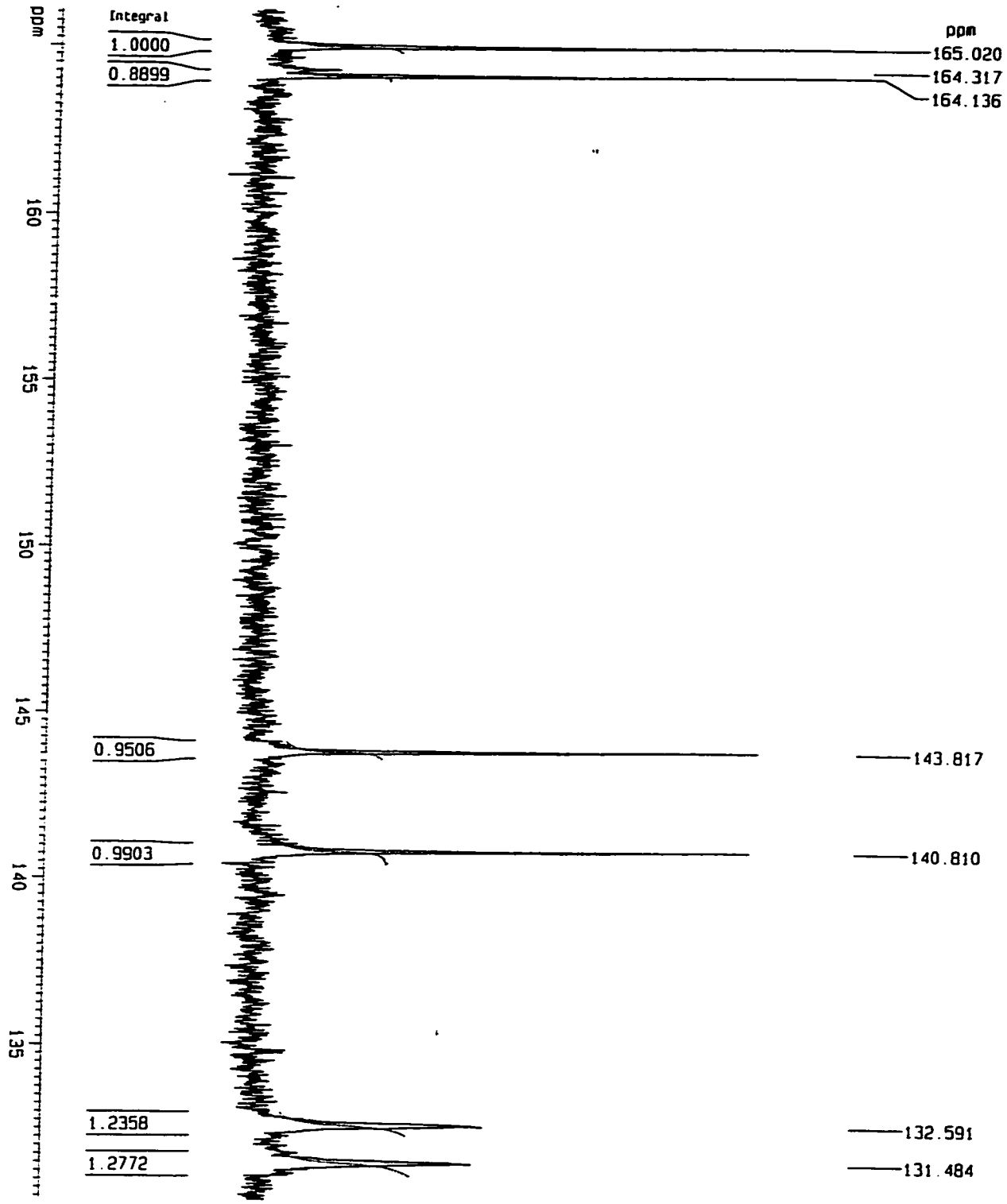

Figure A. 14. Expansion of Olefinic Region of $^{13}C\{^{1}H\}$ NMR Spectrum of 3A

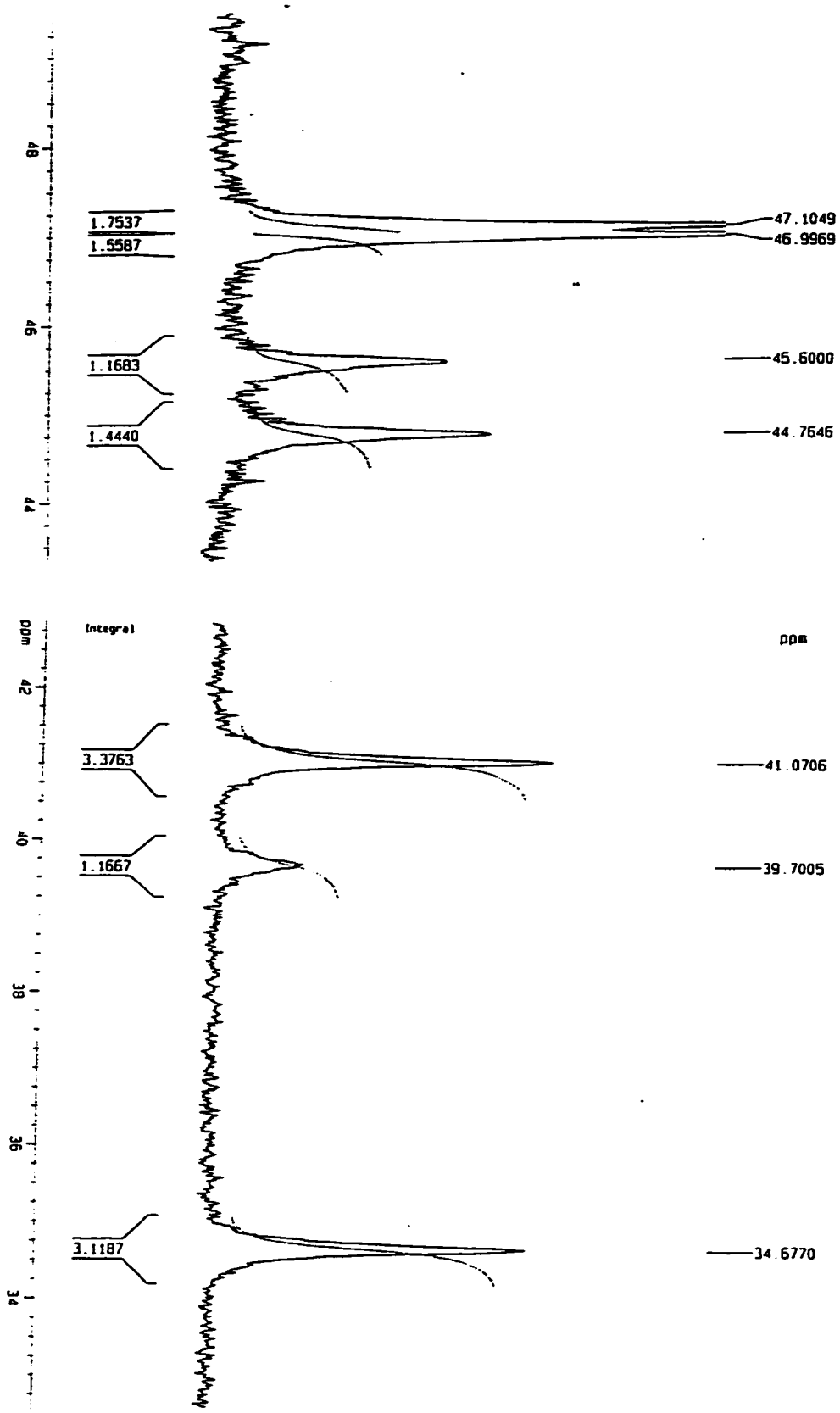

Figure A. 15. Expansion of Aliphatic Region of $^{13}C\{^{1}H\}$ NMR Spectrum of 3A

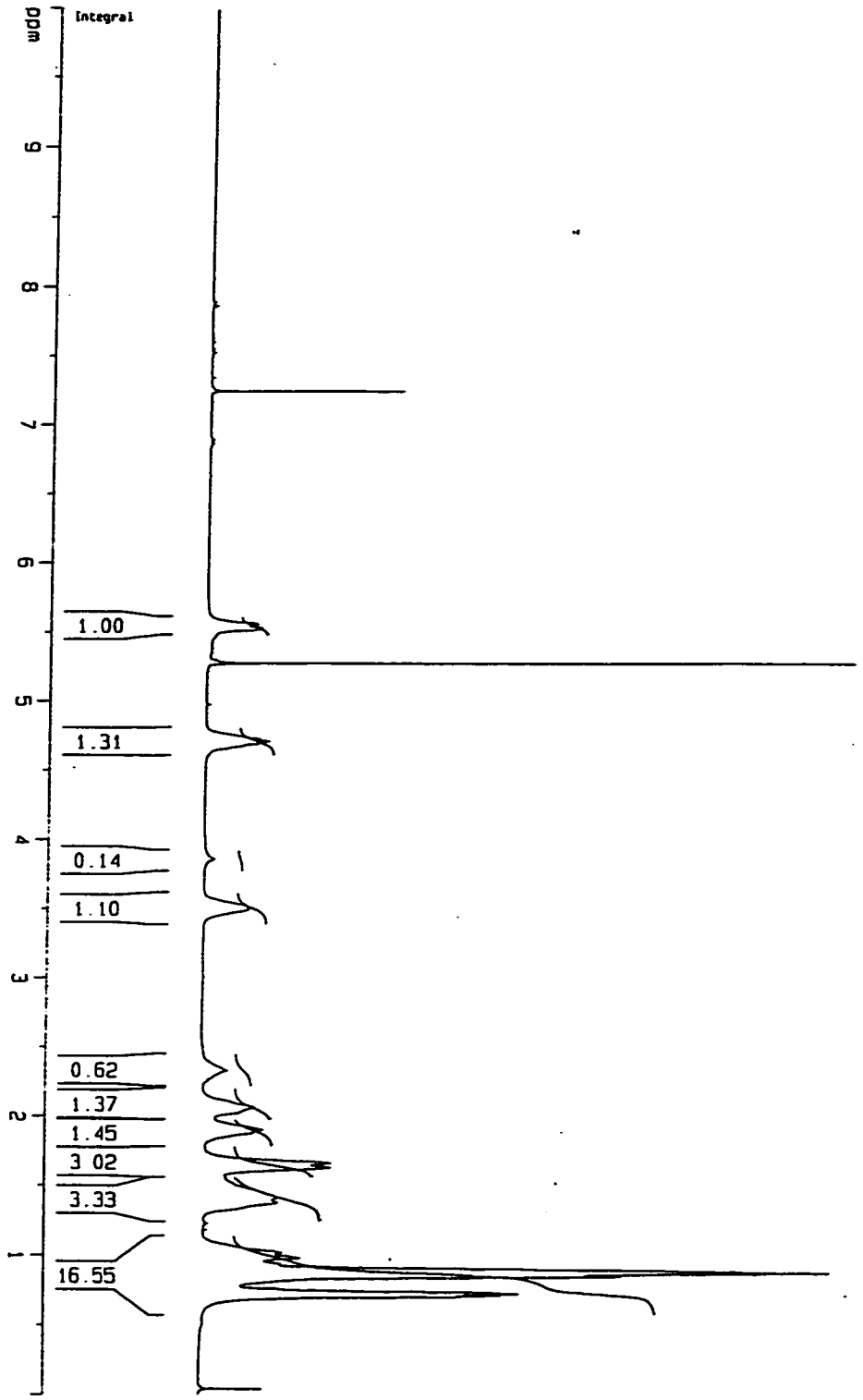

Figure A. 16. ^{1}H NMR Spectrum (300 MHz, $CDCl_3$) of 3B

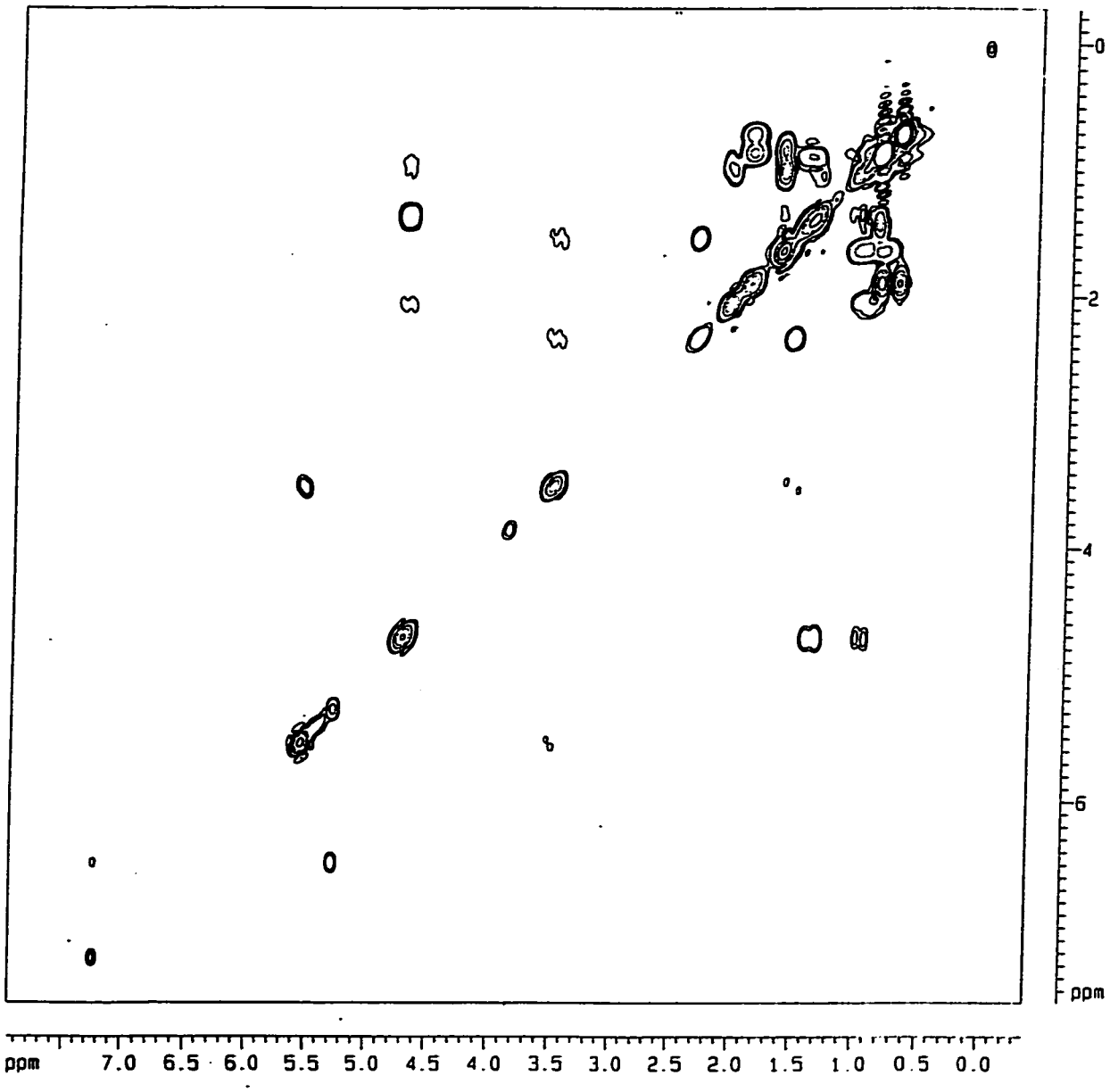

Figure A. 17. ^{1}H-^{1}H COSY NMR Spectrum (300 MHz, $CDCl_3$) of 3B

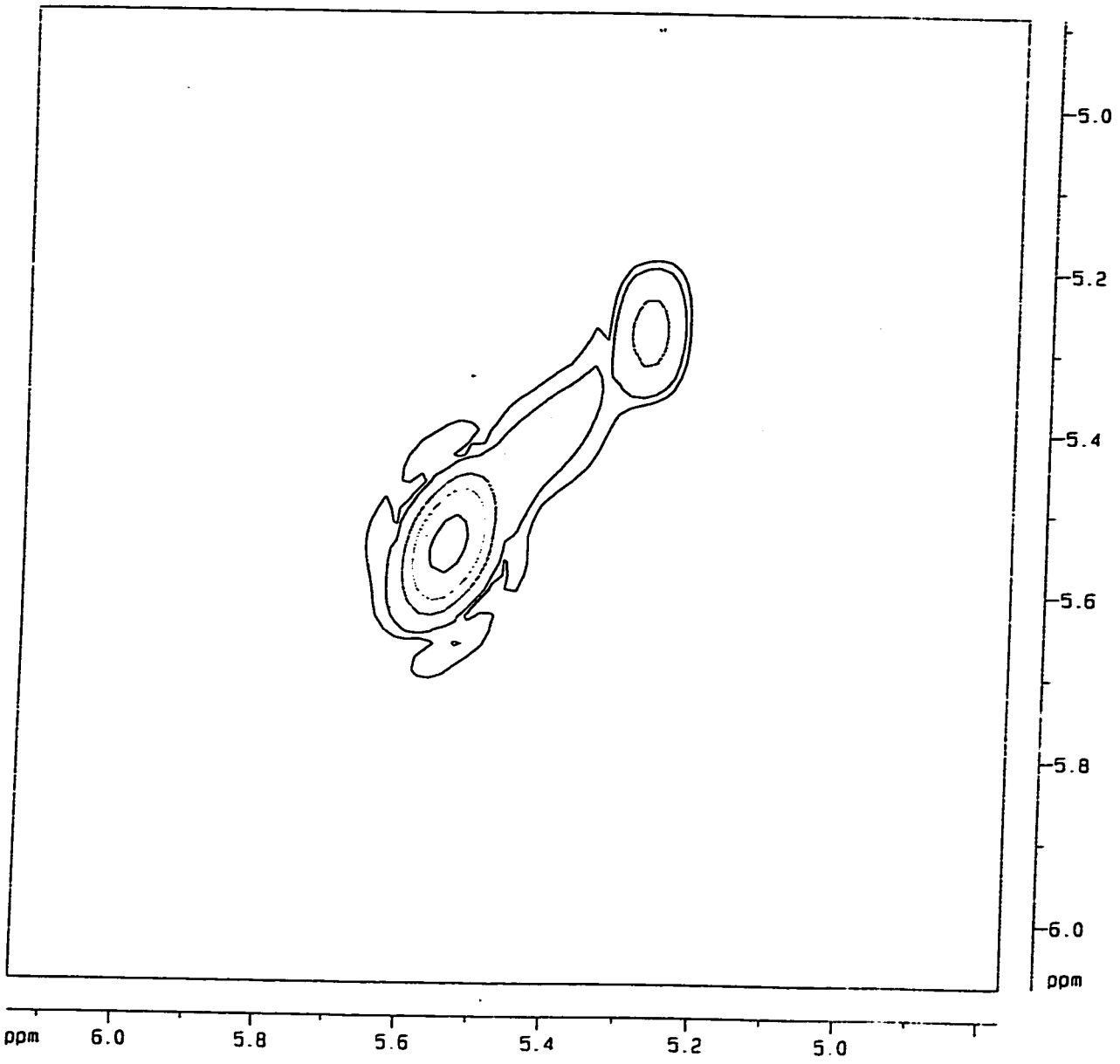

Figure A. 18. Expansion of olefinic region of ^{1}H-^{1}H COSY NMR Spectrum of 3B

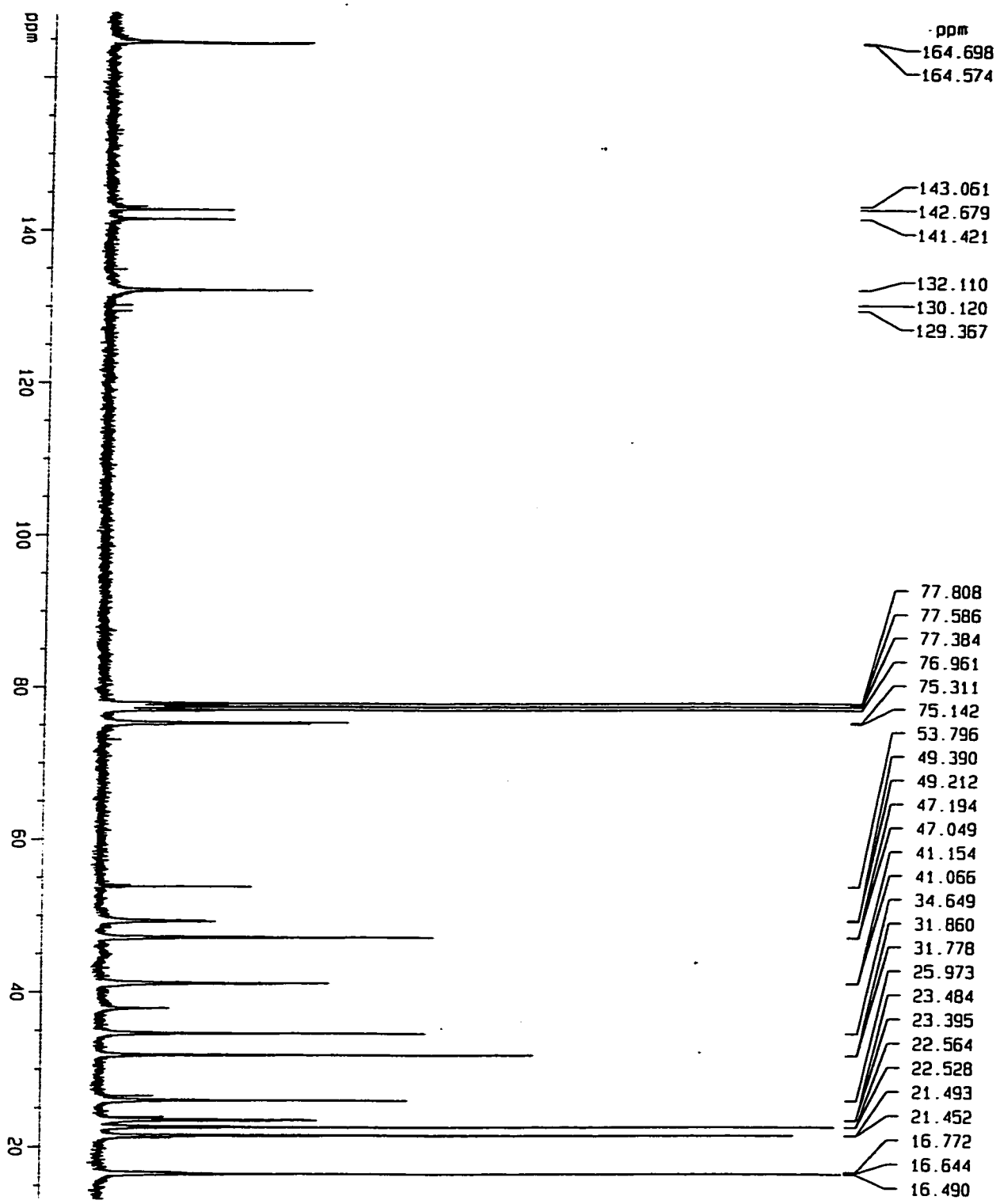

Figure A. 19. $^{13}C\{^{1}H\}$ NMR Spectrum (75 MHz, $CDCl_3$) of 3B

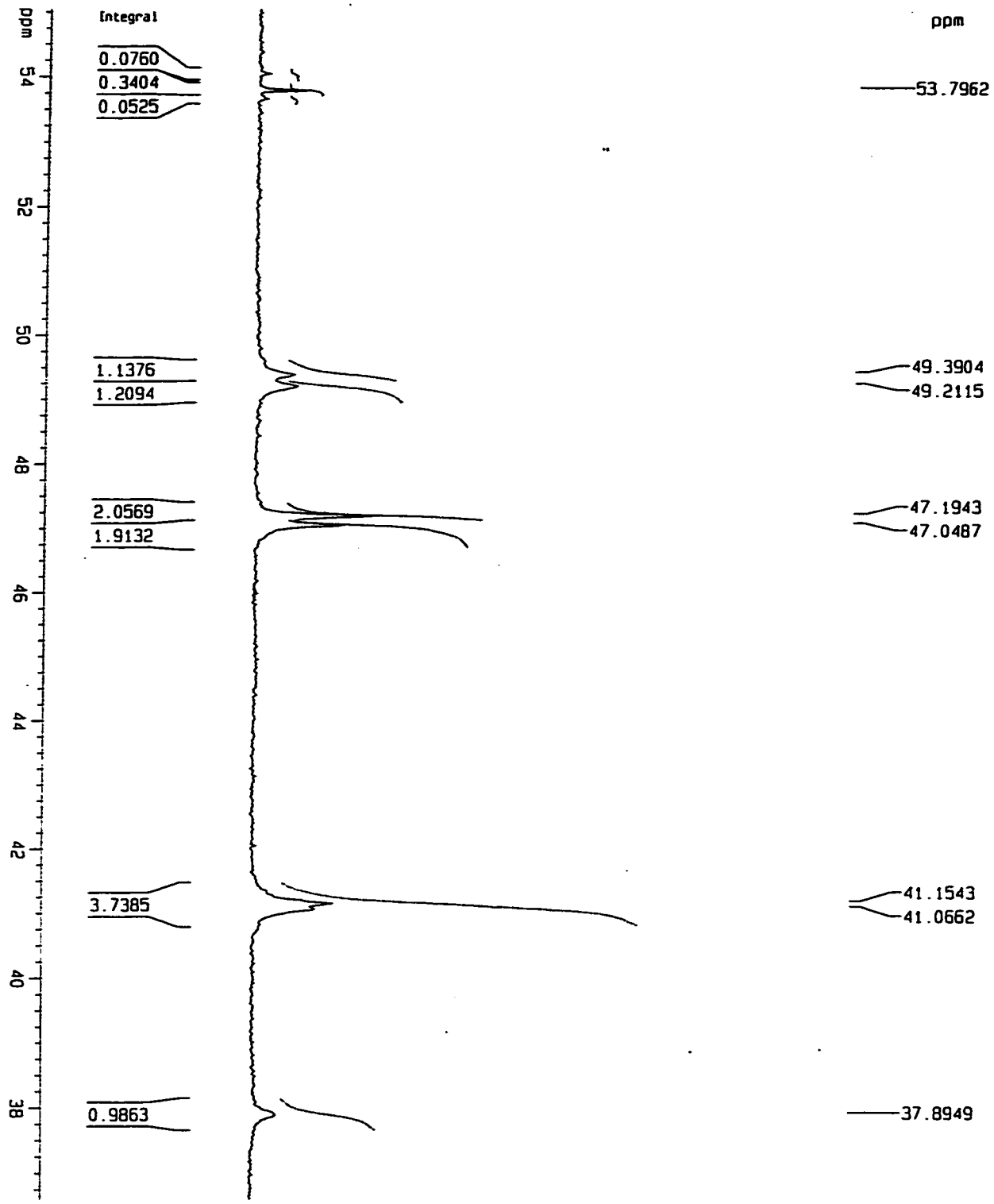

Figure A. 20. Expansion of Aliphatic Region of $^{13}C\{^{1}H\}$ NMR Spectrum of 3B

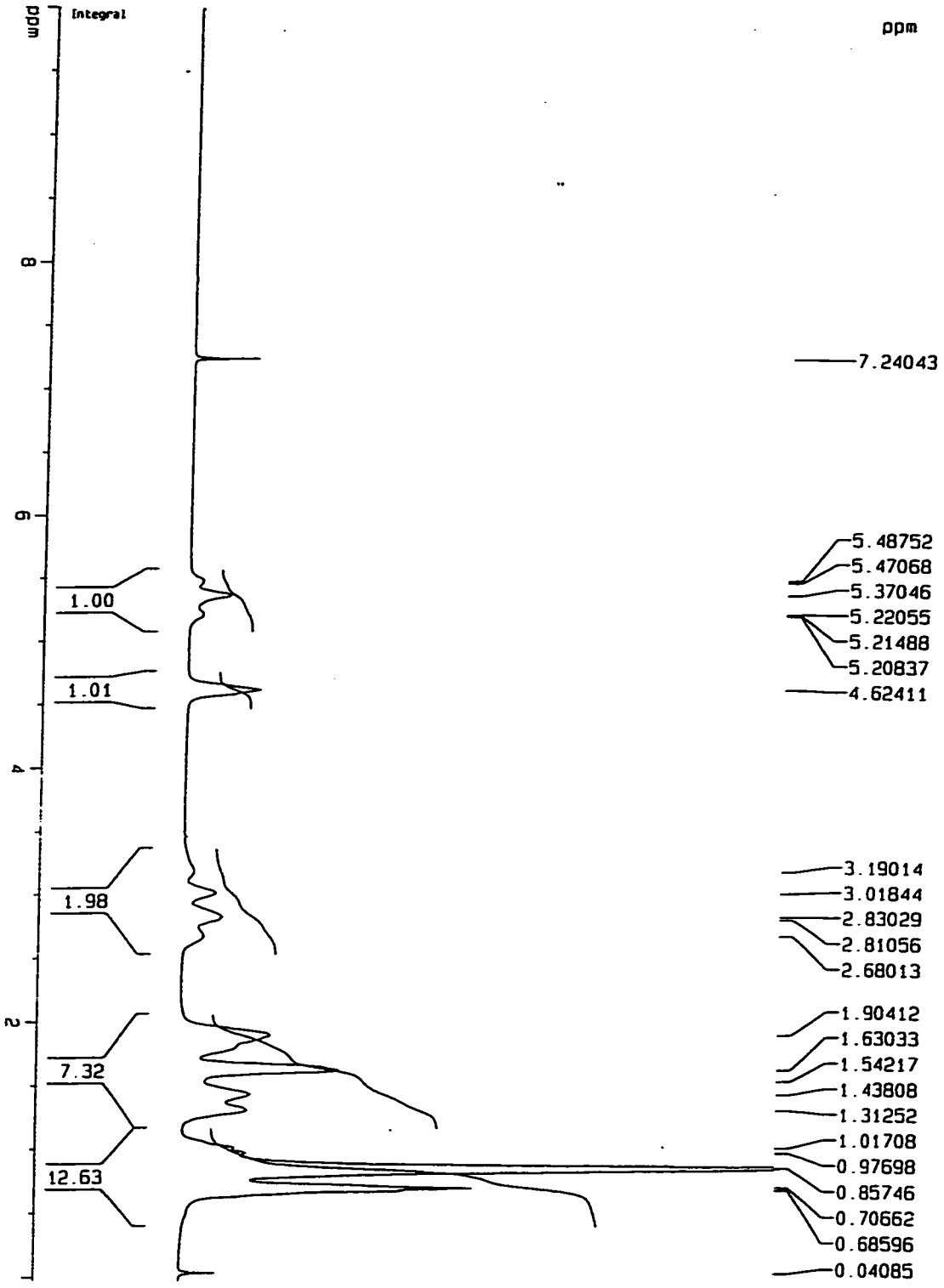

Figure A. 21. ^{1}H NMR Spectrum (300 MHz, $CDCl_3$) of 4B (same for 4Aand 4C)

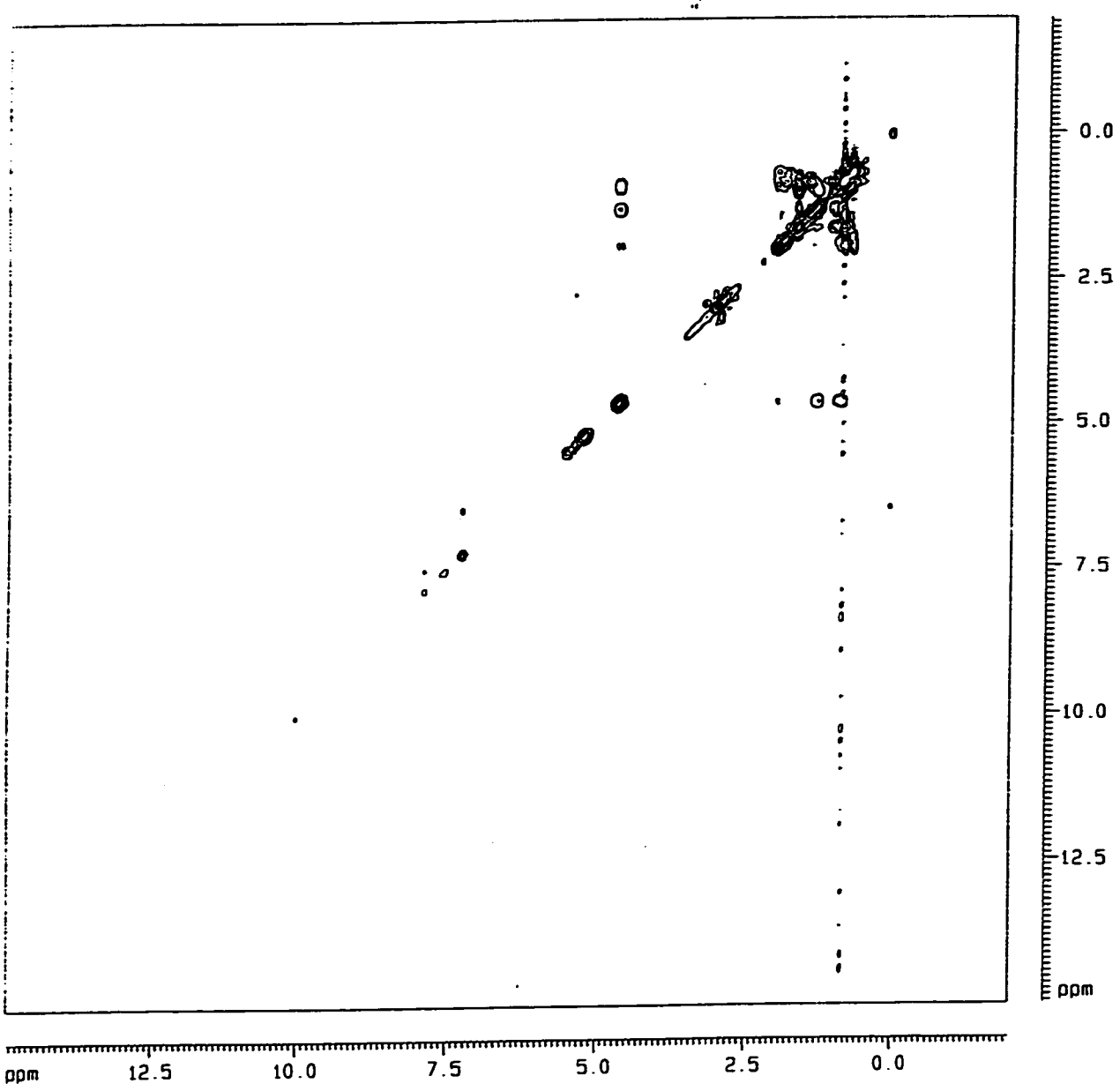

Figure A. 22. ^{1}H-^{1}H COSY NMR Spectrum (300 MHz, $CDCl_3$) of 4A (same for 4B and 4C)

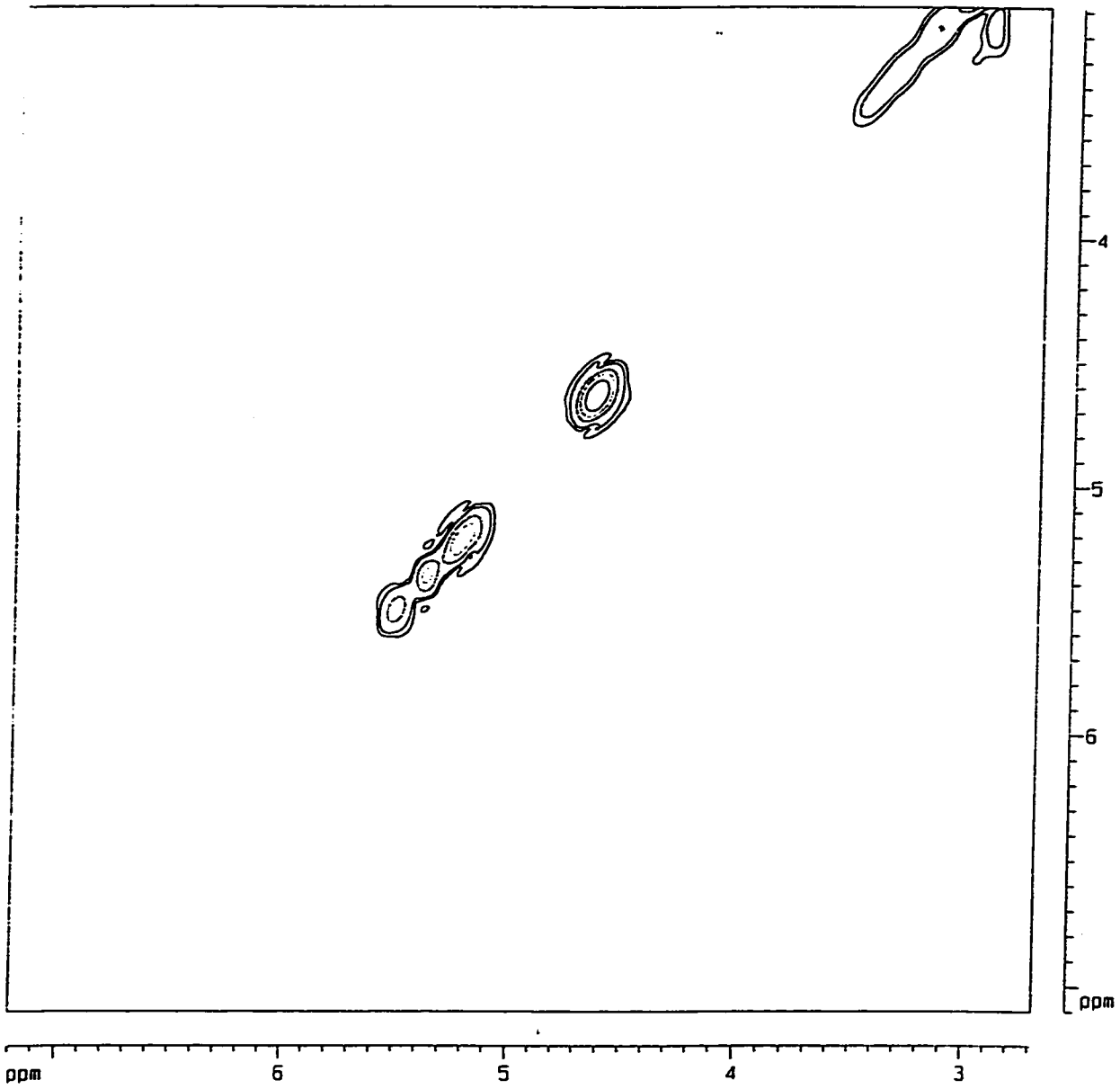

Figure A. 23. Expansion of Olefinic Region of ^{1}H-^{1}H COSY NMR Spectrum of 4A (same for 4B and 4C)

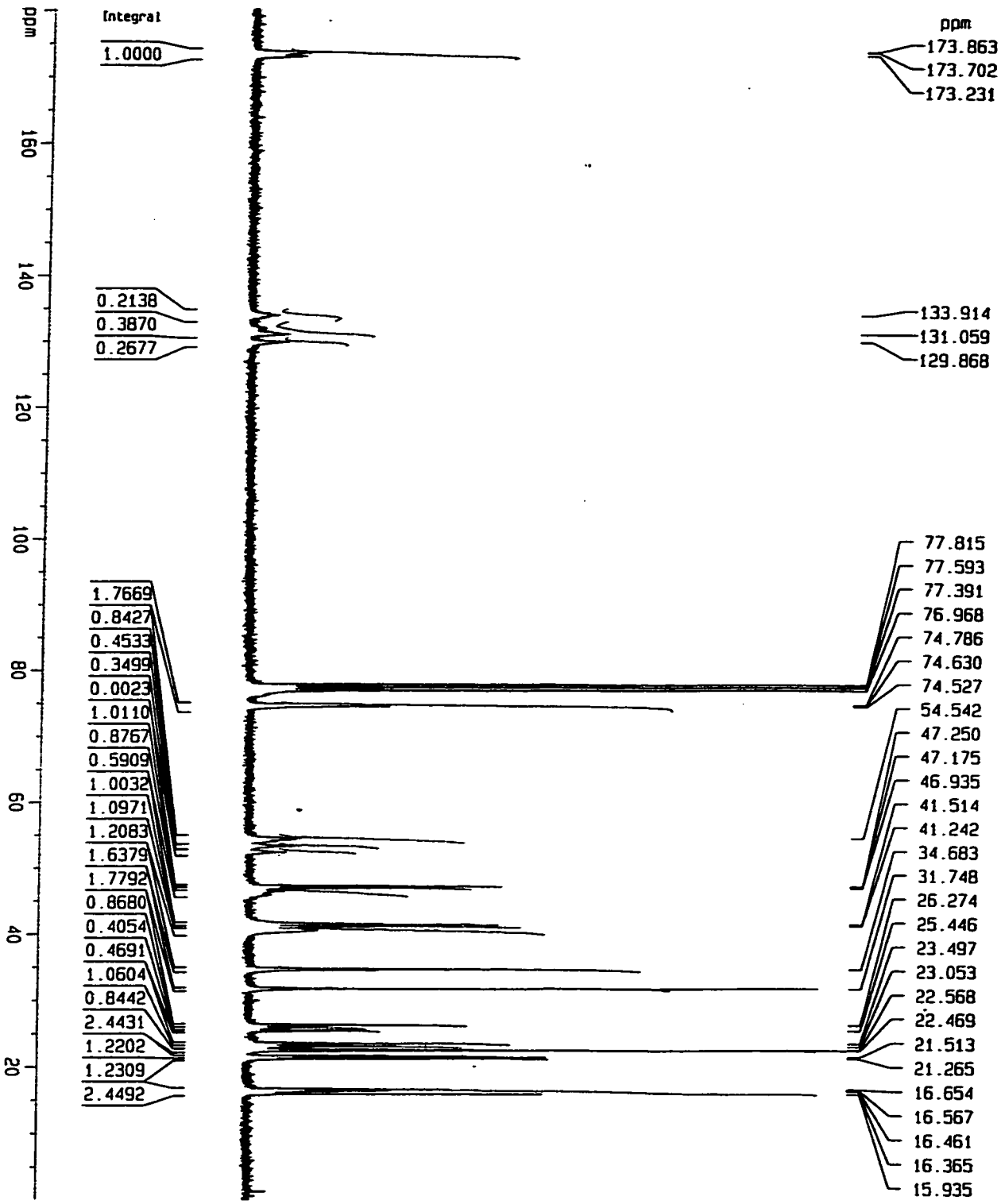

Figure A. 24. $^{13}C\{^1H\}$ NMR Spectrum (75 MHz, $CDCl_3$) of 4C (same for 4A and 4B)

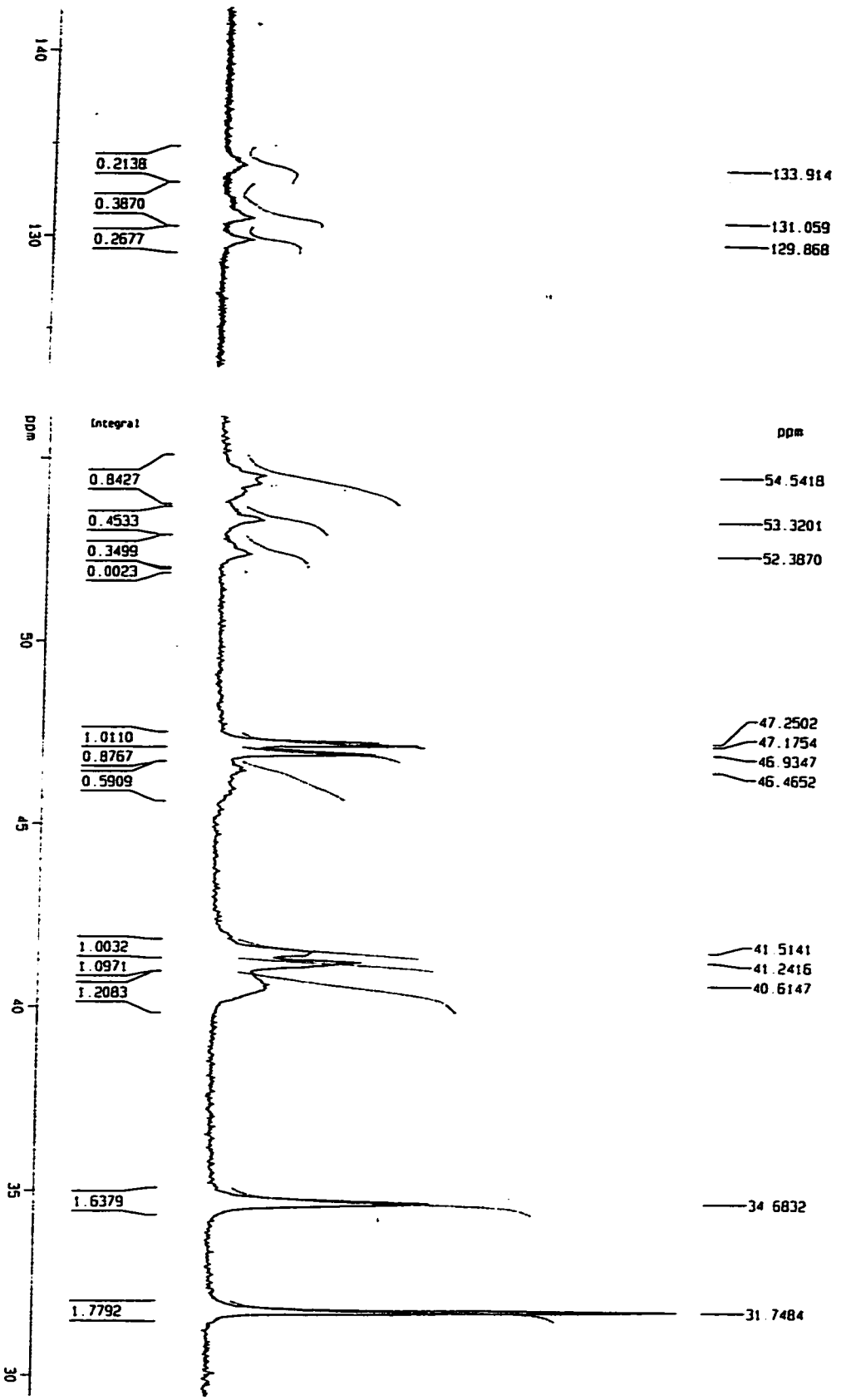

Figure A. 25. Expansion of Olefinic and Aliphatic Region of $^{13}C\{^{1}H\}$ NMR Spectrum of 4C (same for 4A and 4B)

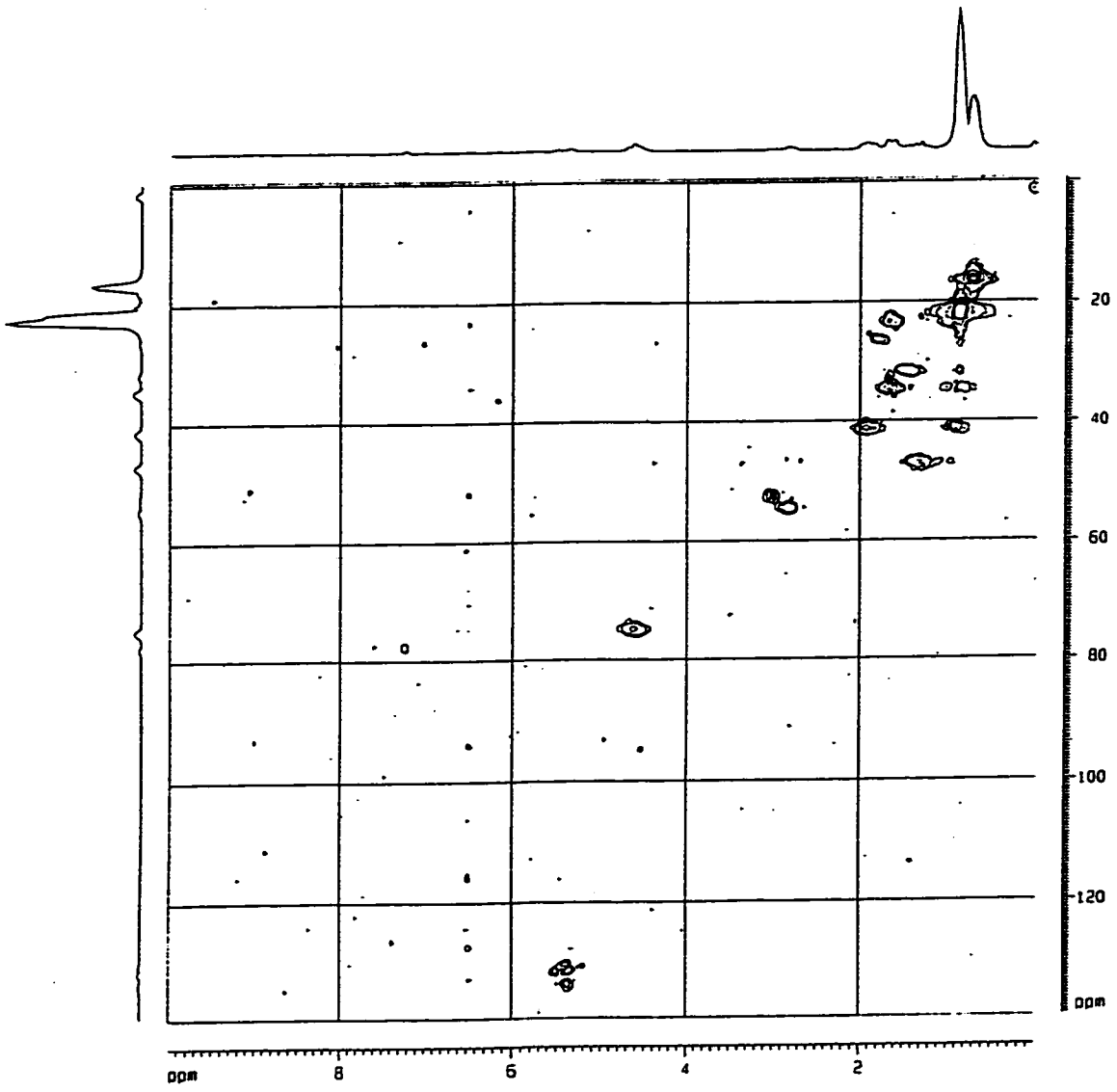

Figure A. 26. ^{1}H-^{13}C HMQC NMR Spectrum (300 MHz, $CDCl_3$) of 4B (same for 4A and 4C)

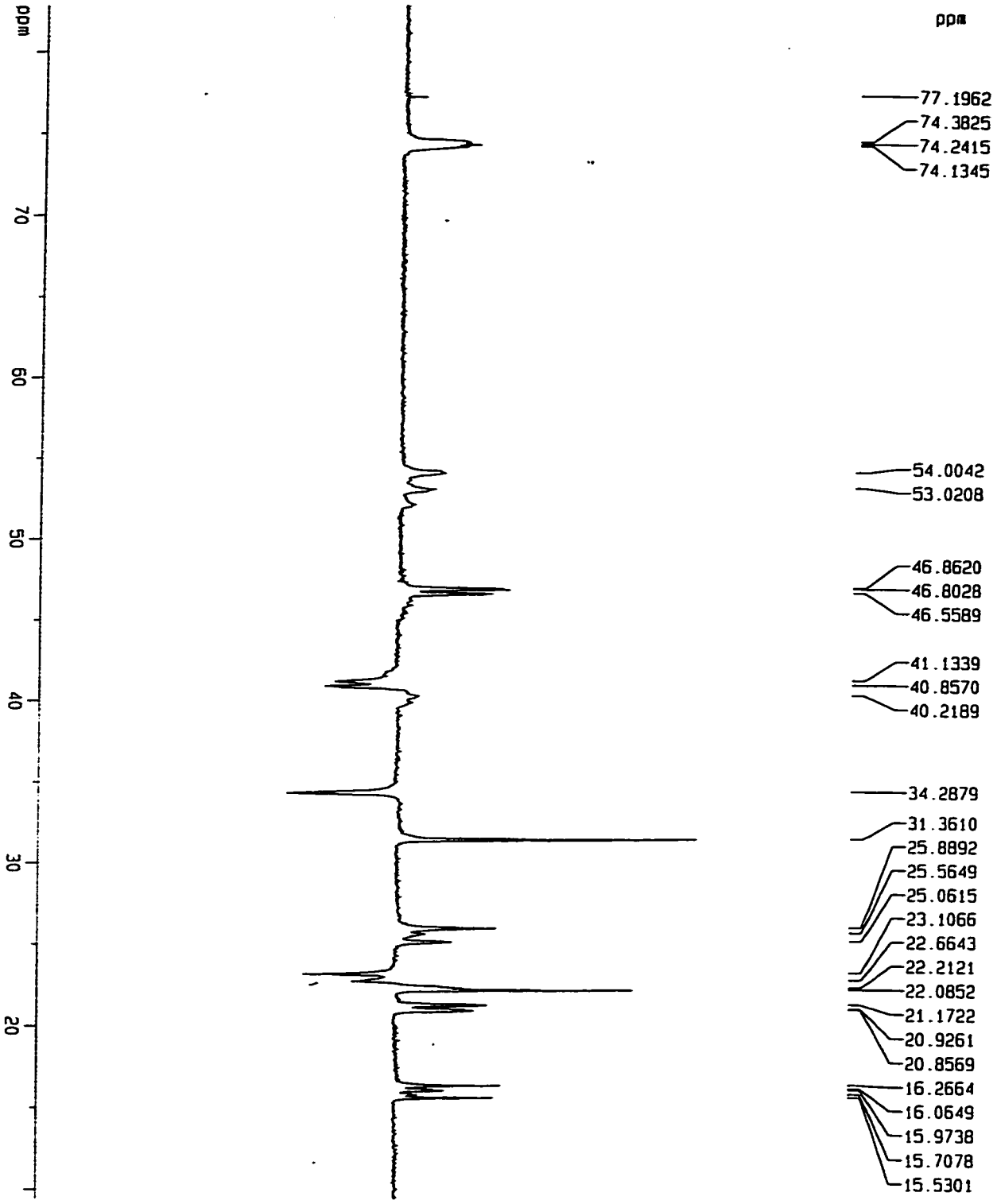

Figure A. 27. DEPT-135 NMR Spectrum (75 MHz, $CDCl_3$) of 4A (same for 4B and 4C)

Appendix B: Conformation Plots

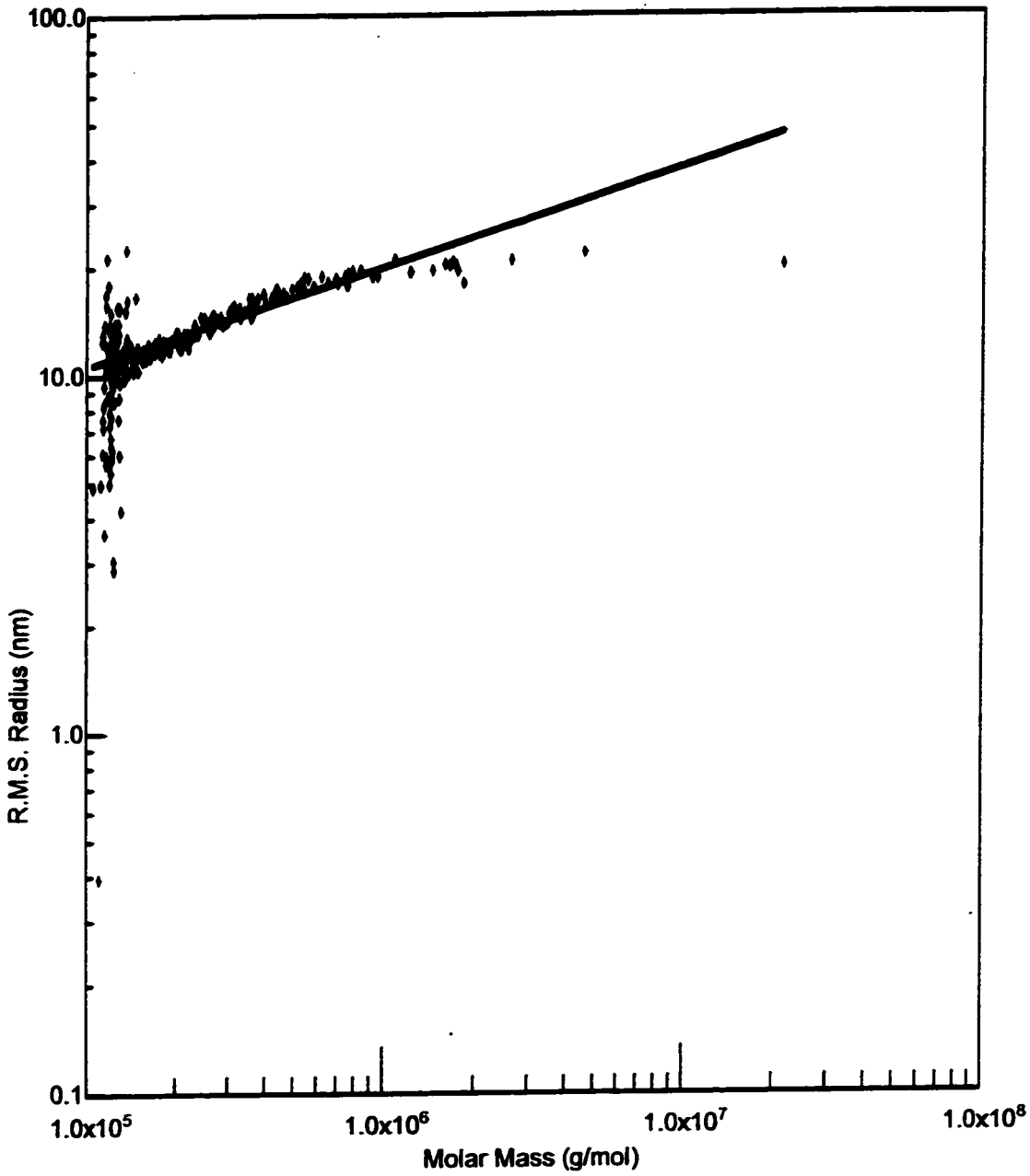

Figure B. 1. Conformation Plot for 1A

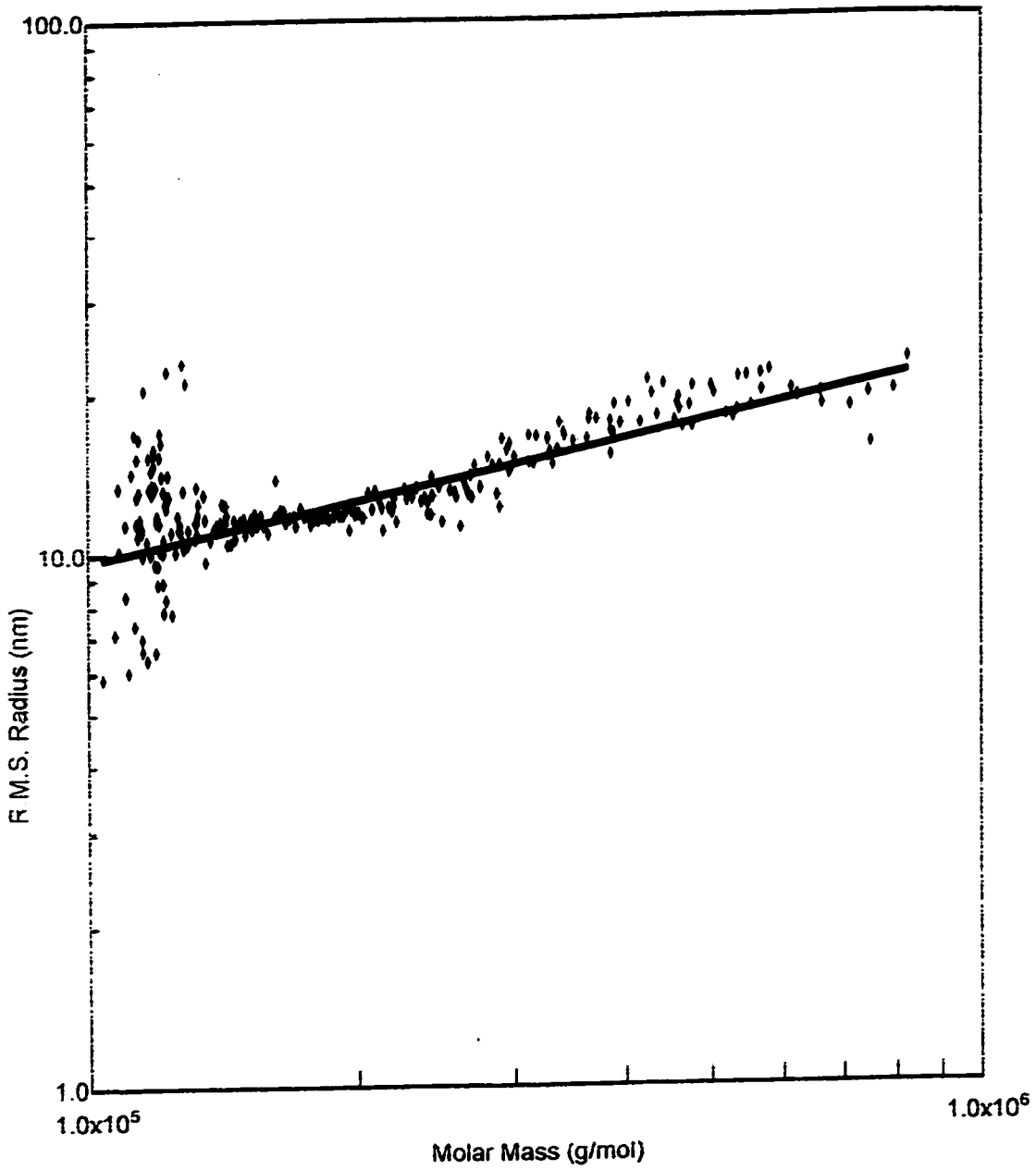

Figure B. 2. Conformation Plot for 2A

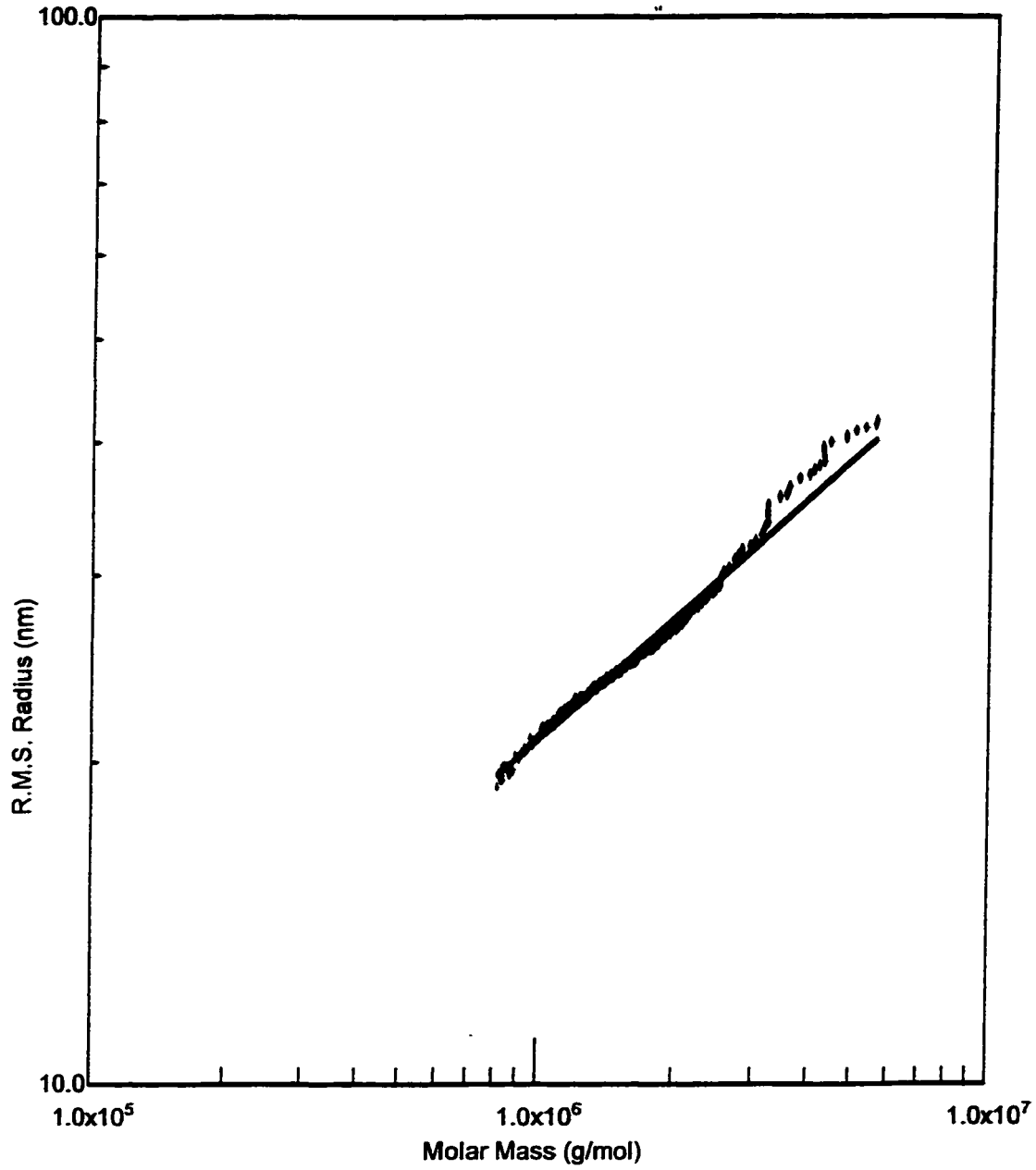

Figure B. 3. Conformation Plot for 3A (Peak#2)

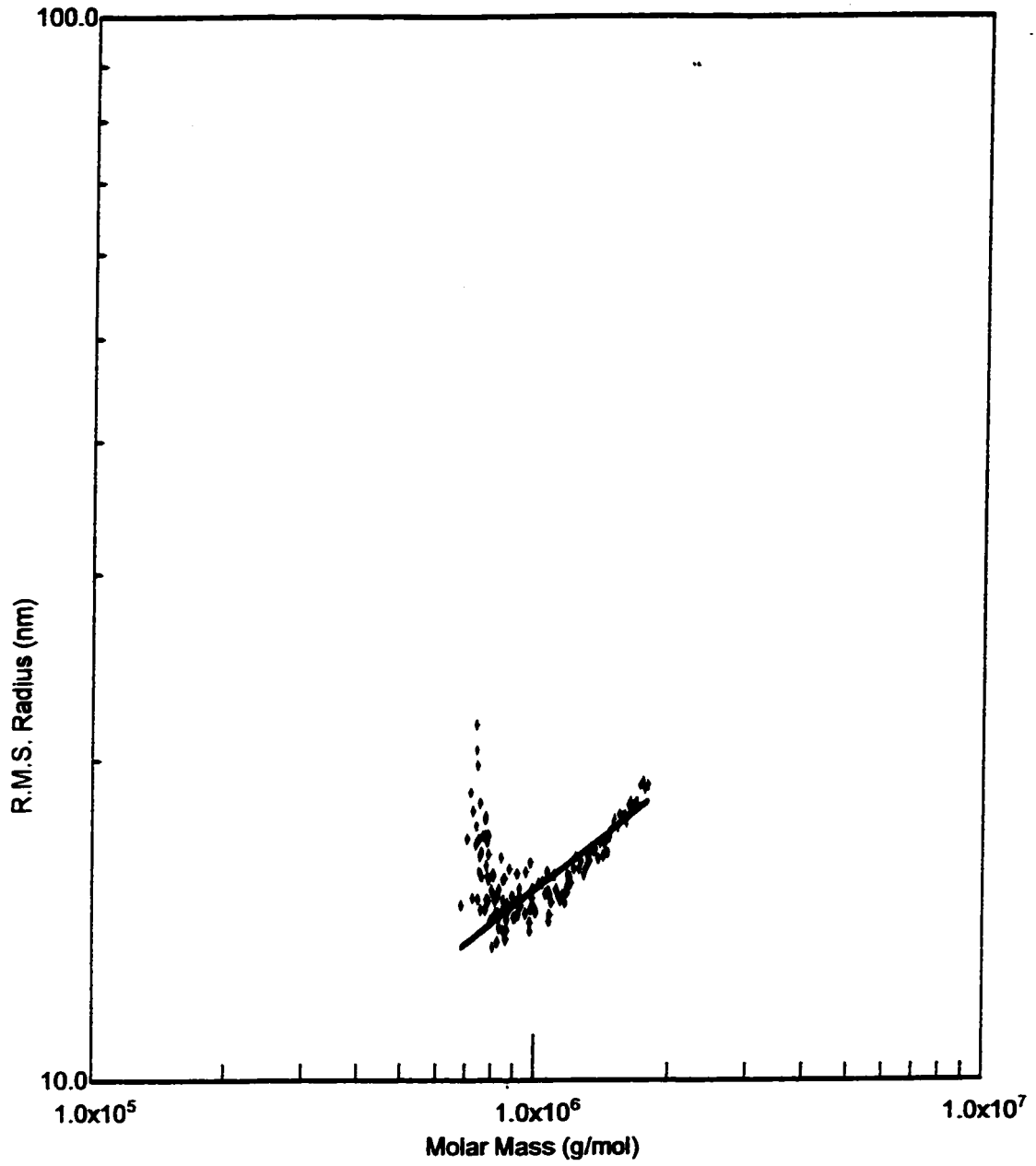

Figure B. 4. Conformation Plot for 3A (Peak#3)

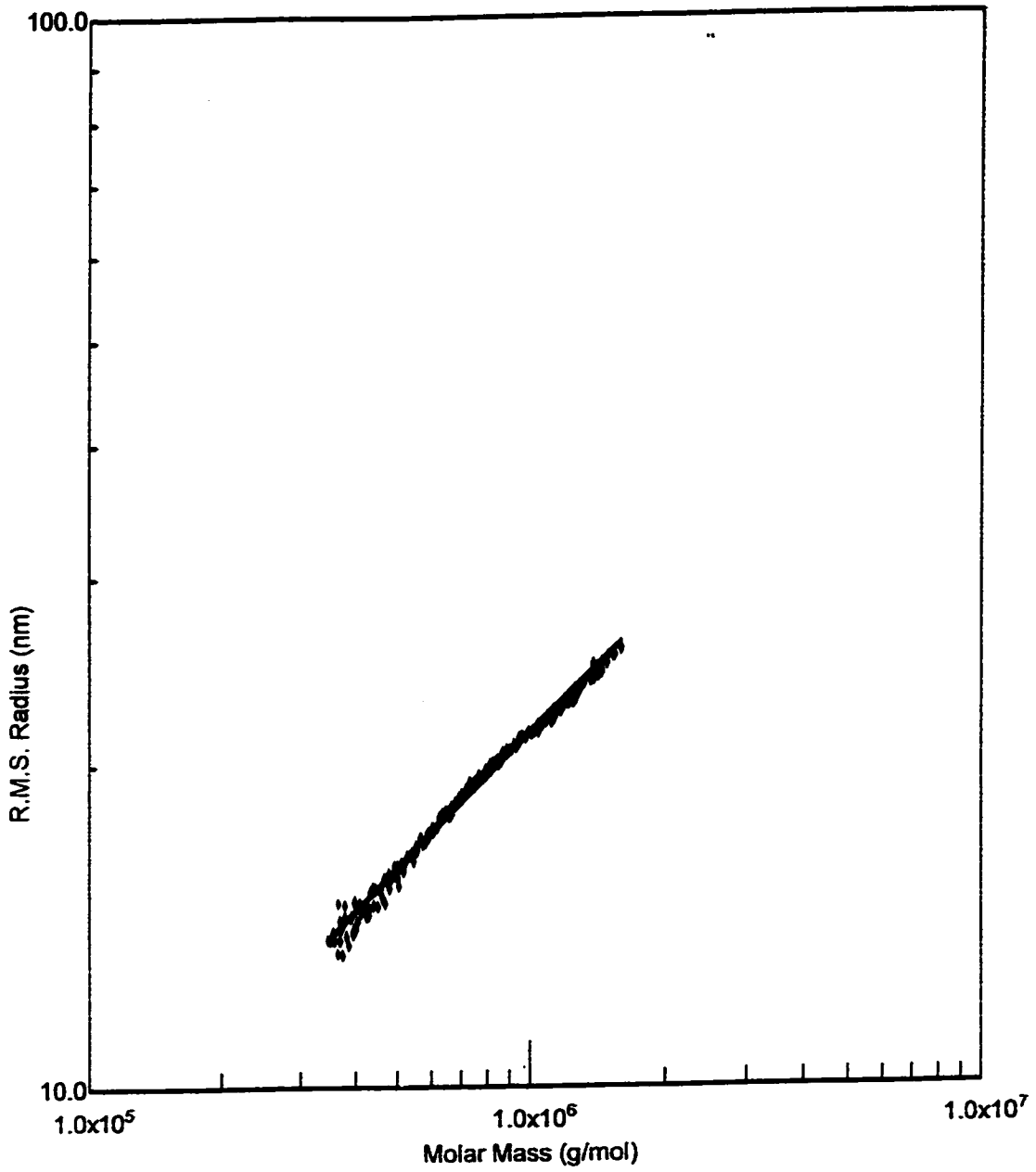

Figure B. 5. Conformation Plot for 3B

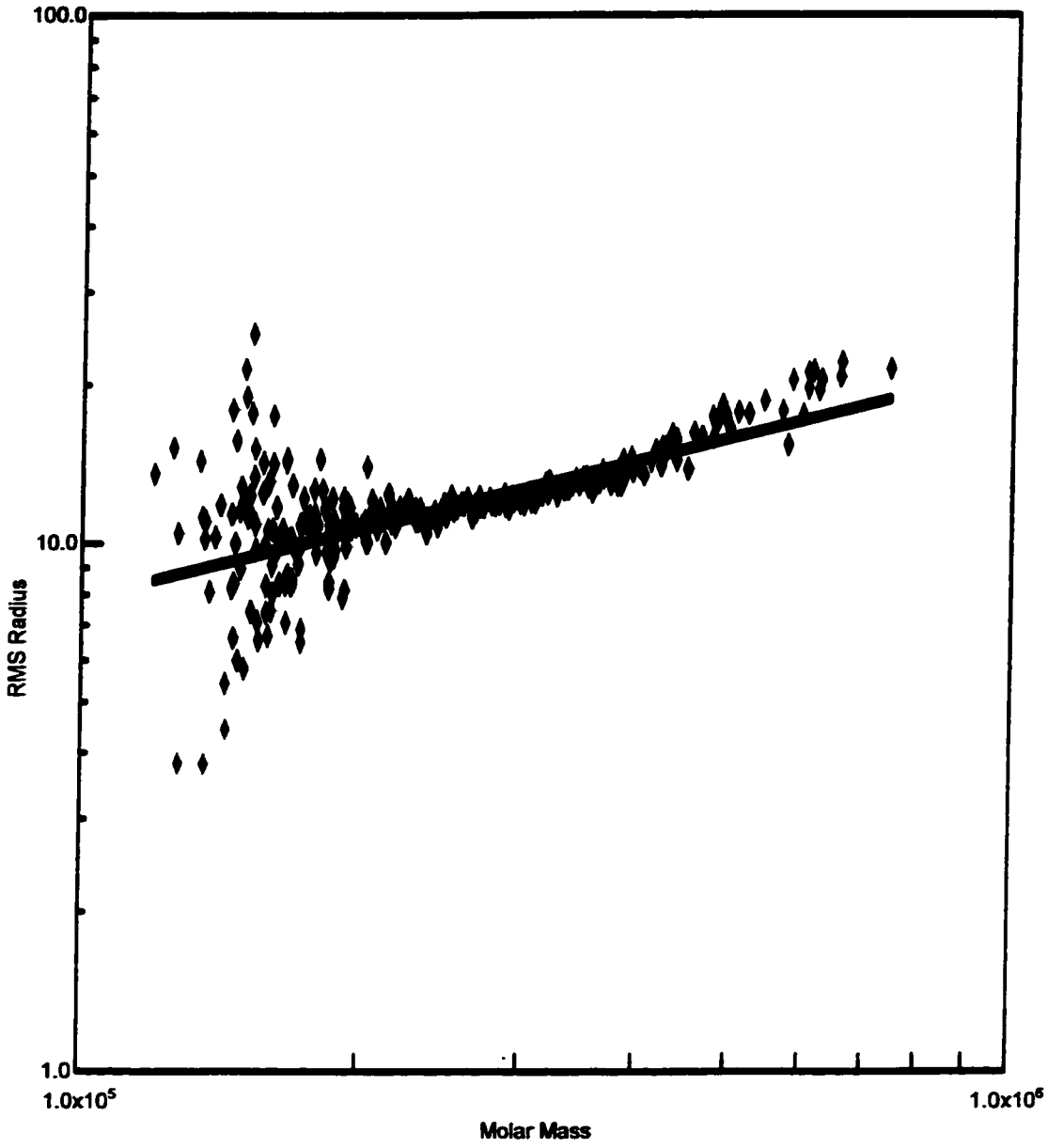

Figure B. 6. Conformation Plot for 4A

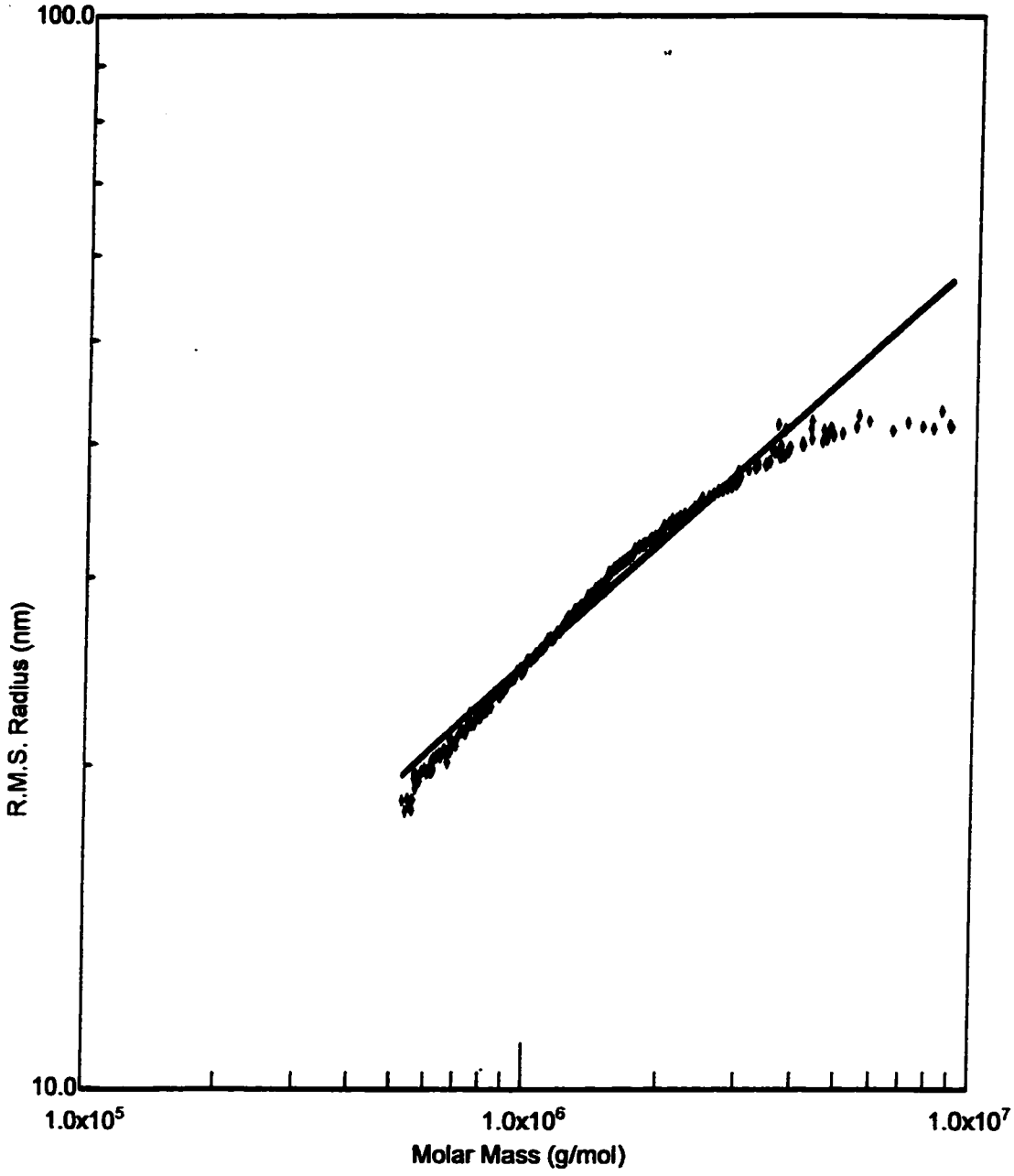

Figure B. 7. Conformation Plot for 4B (Peak#2)

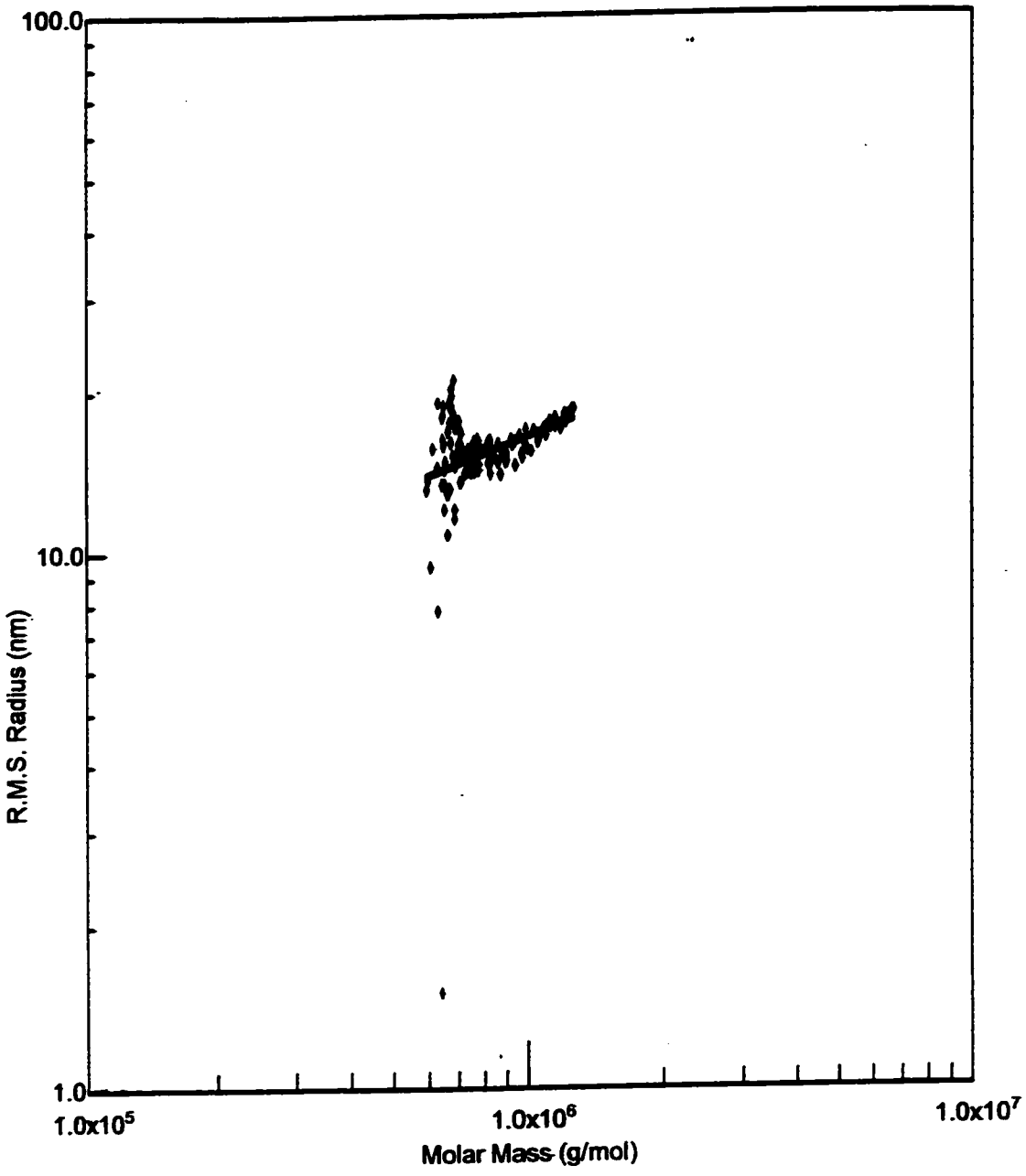

Figure B. 8. Conformation Plot for 4B (Peak#3)

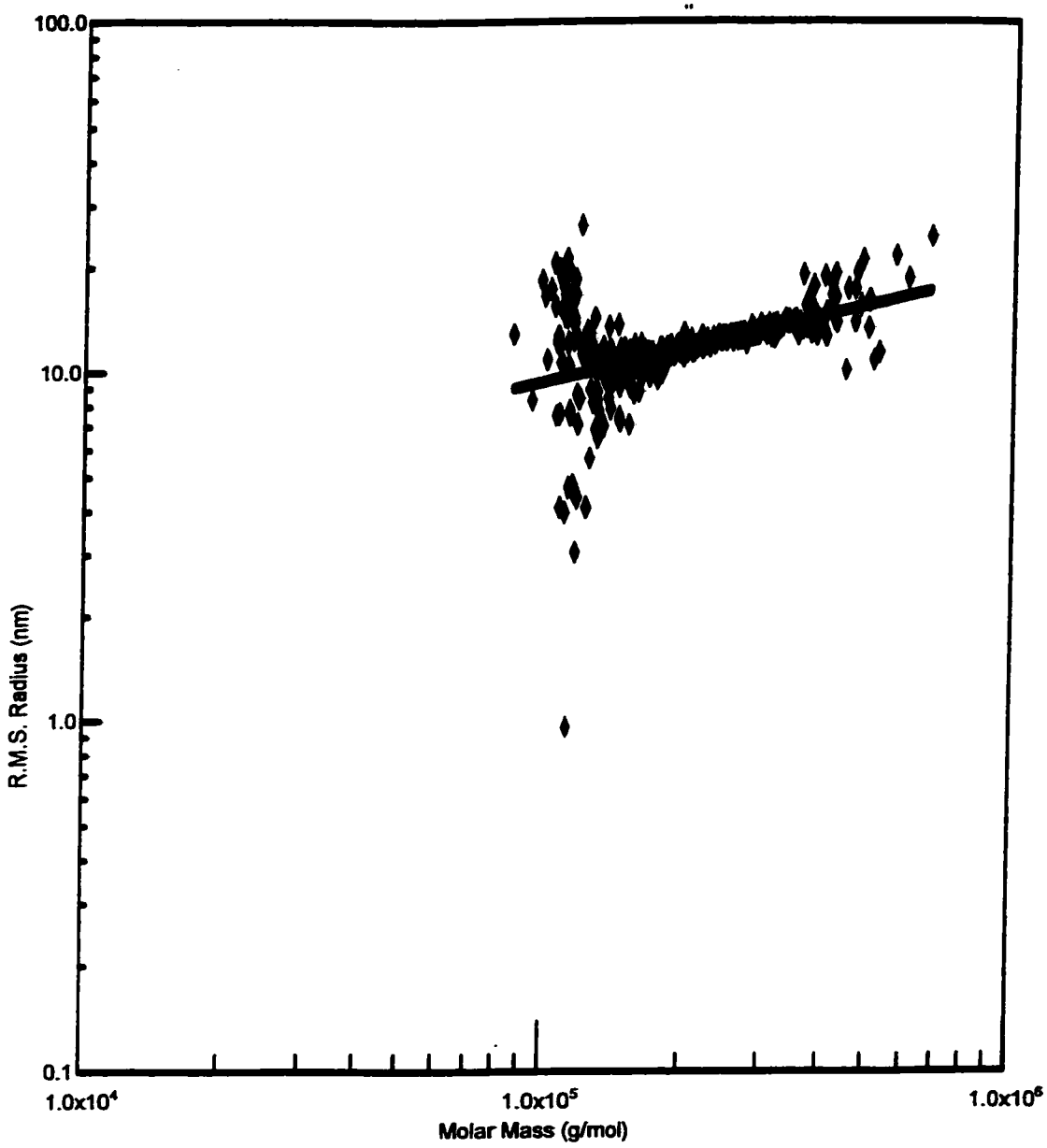

Figure B. 9. Conformation Plot for 4C

Appendix C: CD Spectra

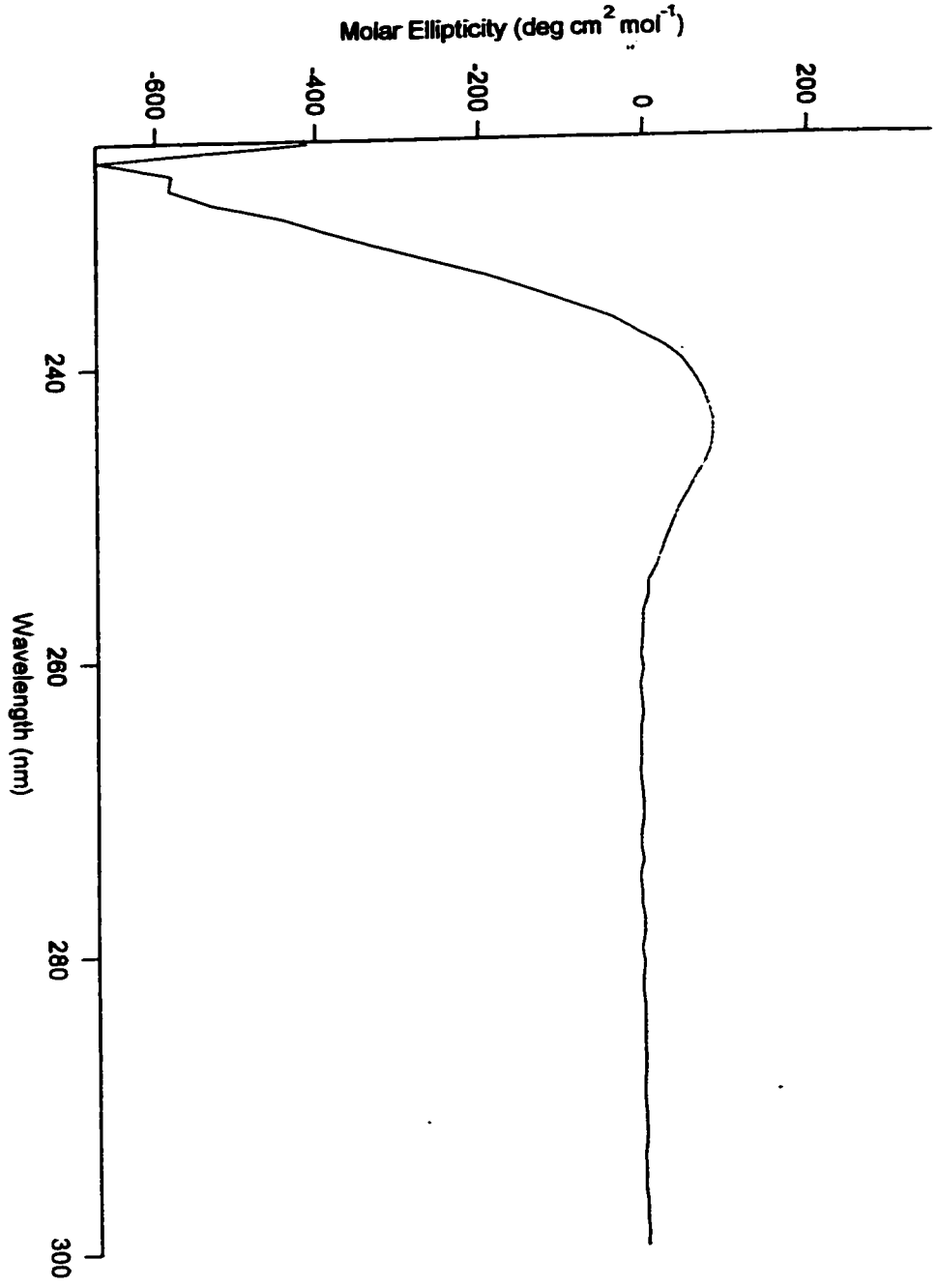

Figure C. 1. CD Spectrum (CH_2Cl_2) of 4

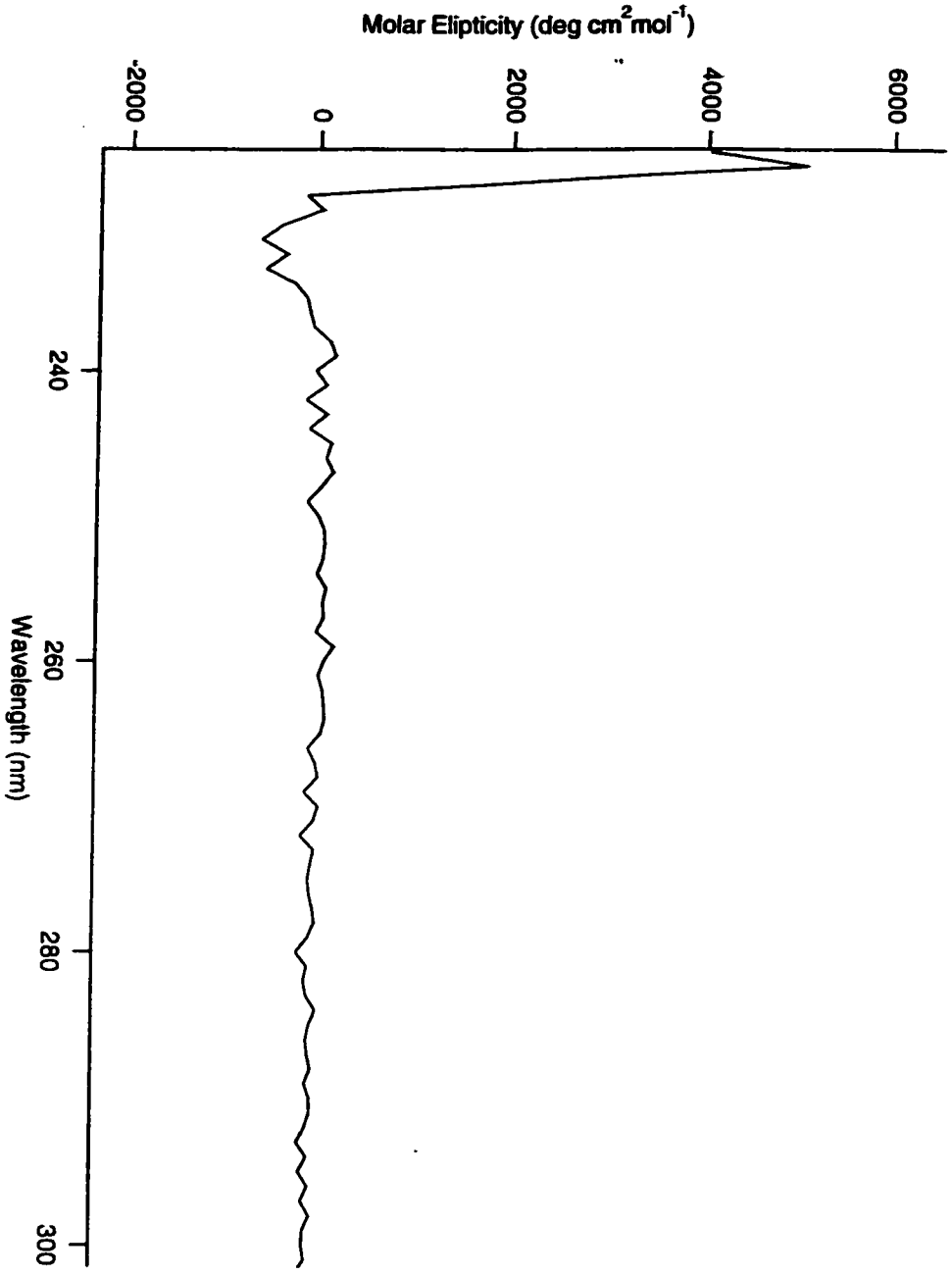

Figure C. 2. CD Spectrum (CH_2Cl_2) of 2A

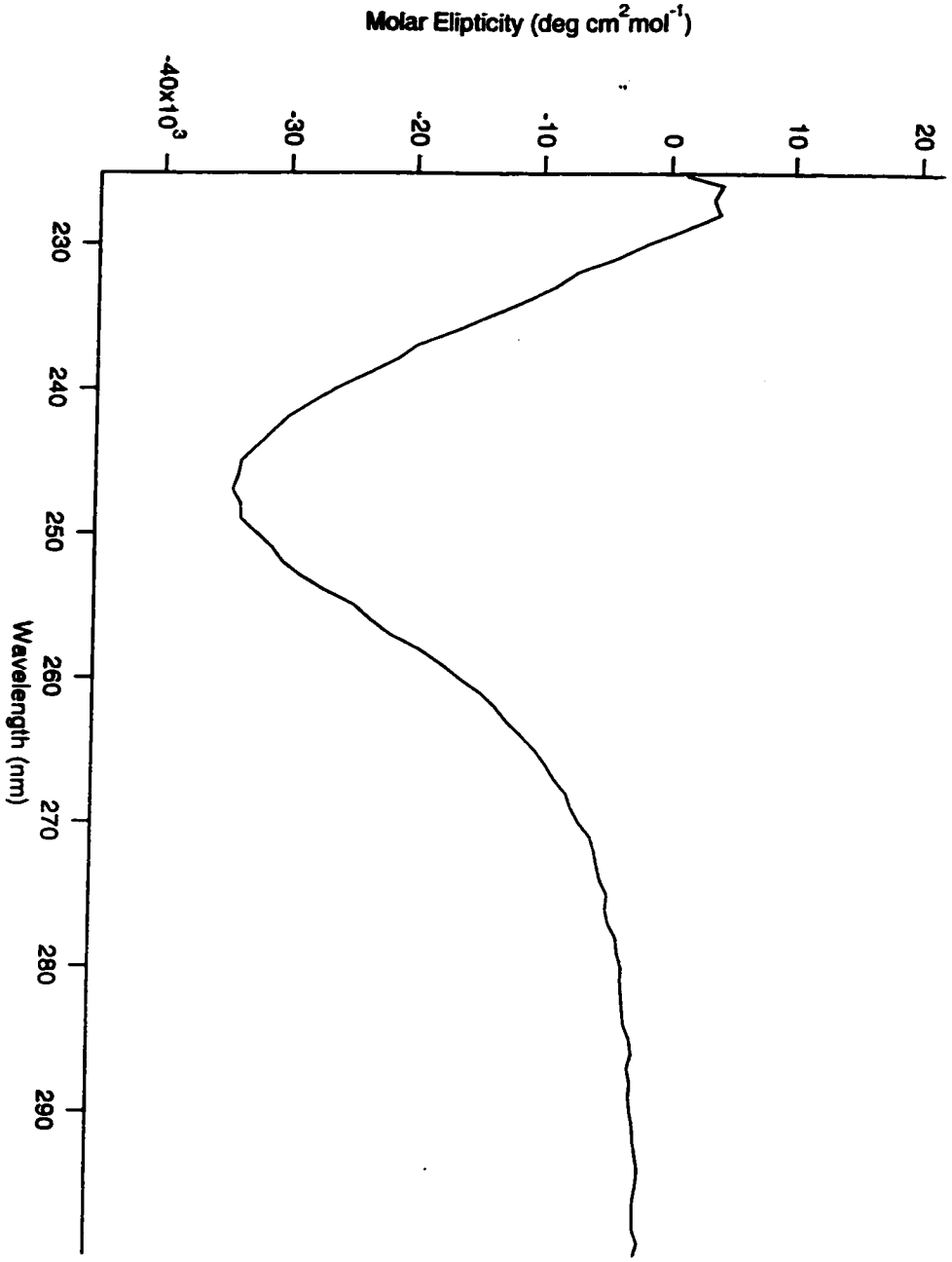

Figure C. 3. CD Spectrum (CH_2Cl_2) of 3A

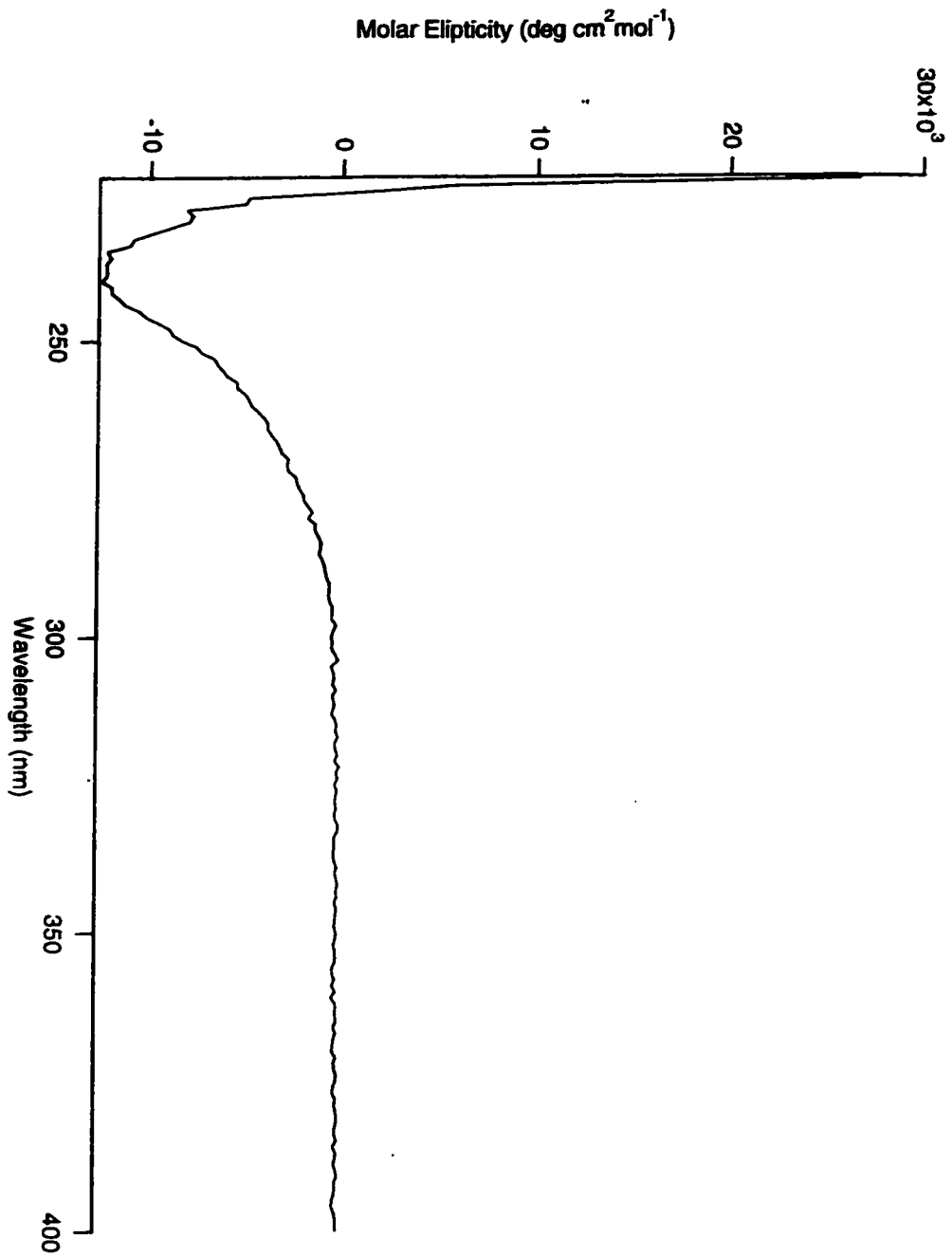

Figure C. 4. CD Spectrum (CH_2Cl_2) of 3B

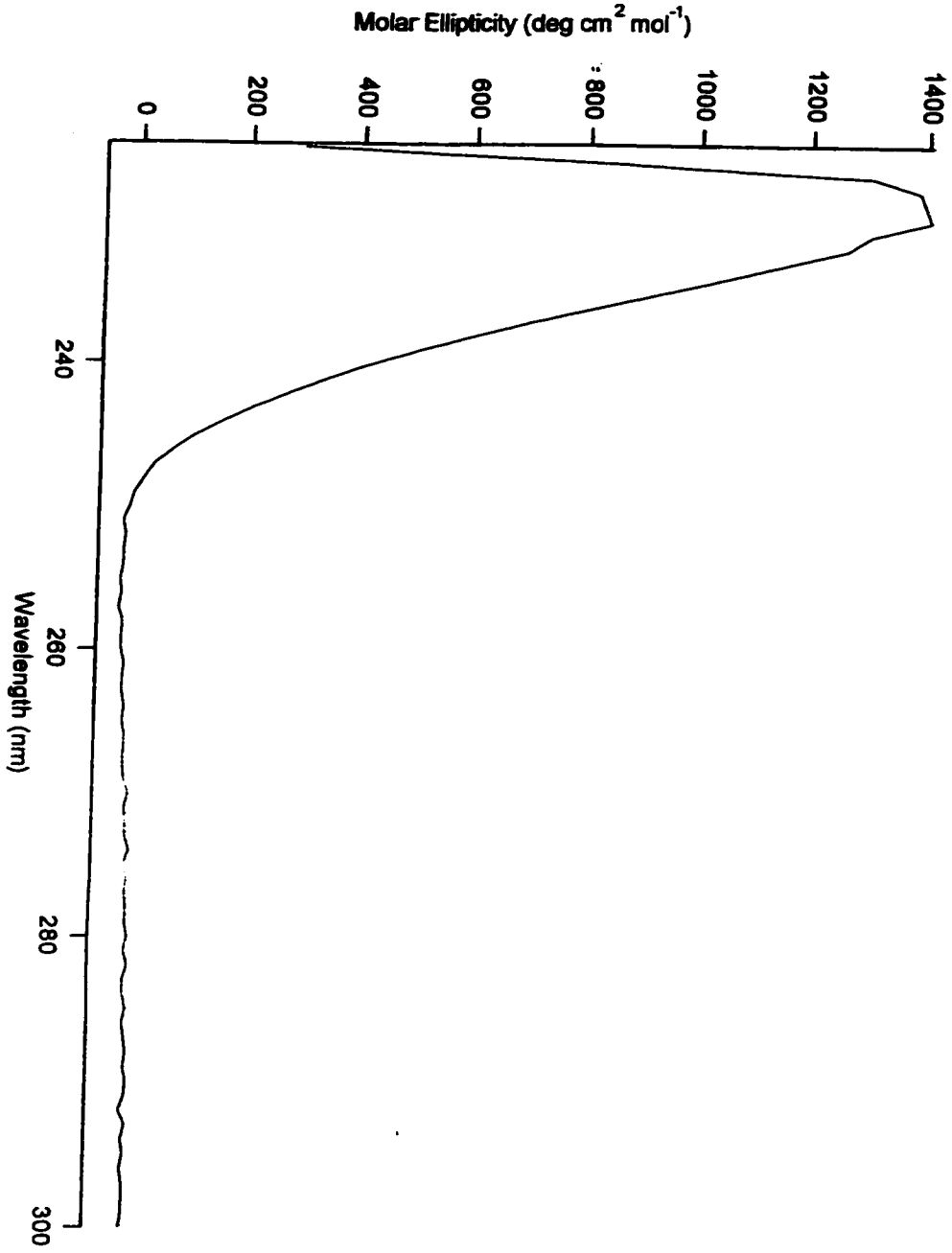

Figure C. 5. CD Spectrum (CH_2Cl_2) of 4A

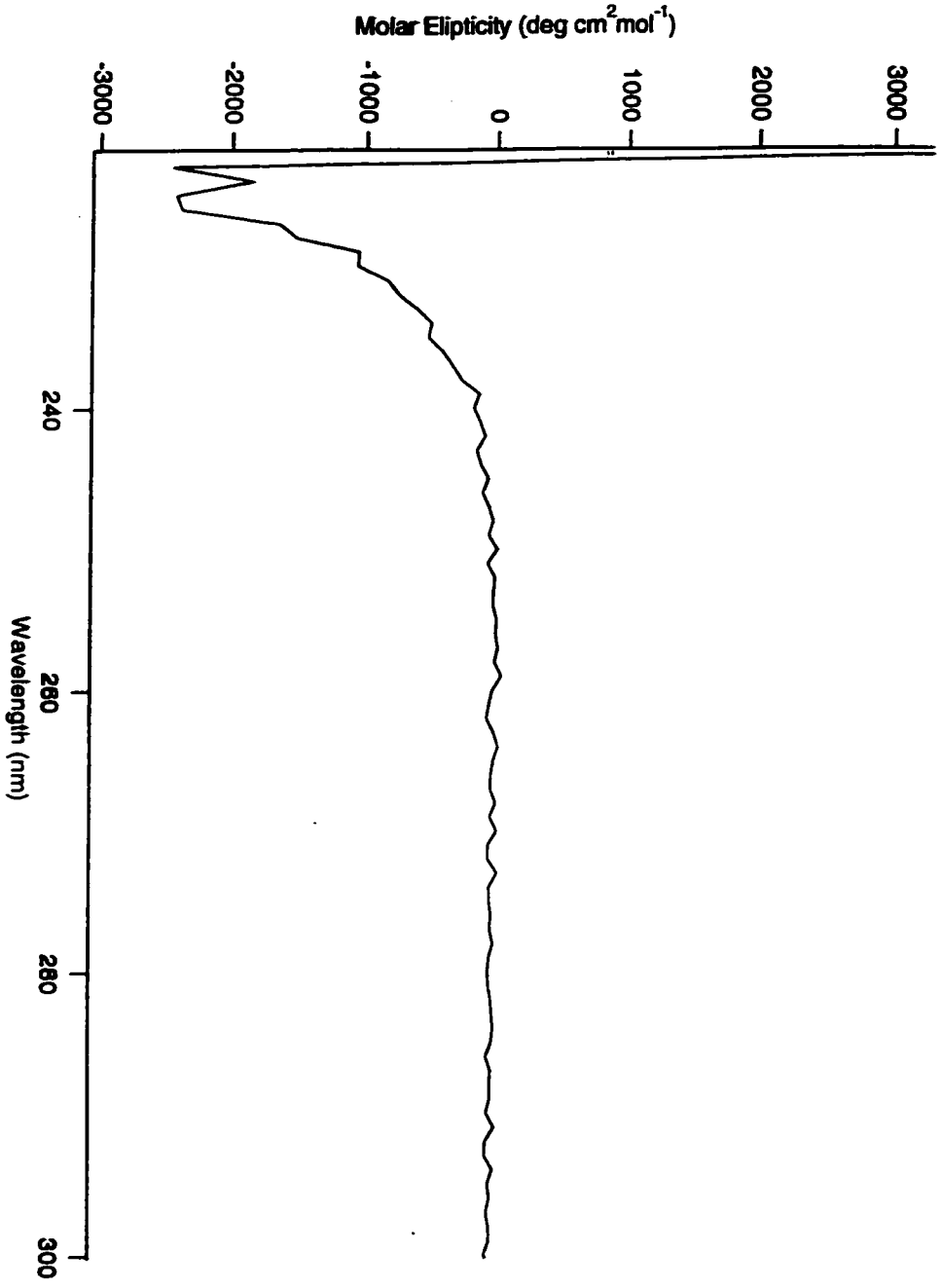

Figure C. 6. CD Spectrum (CH_2Cl_2) of 4B

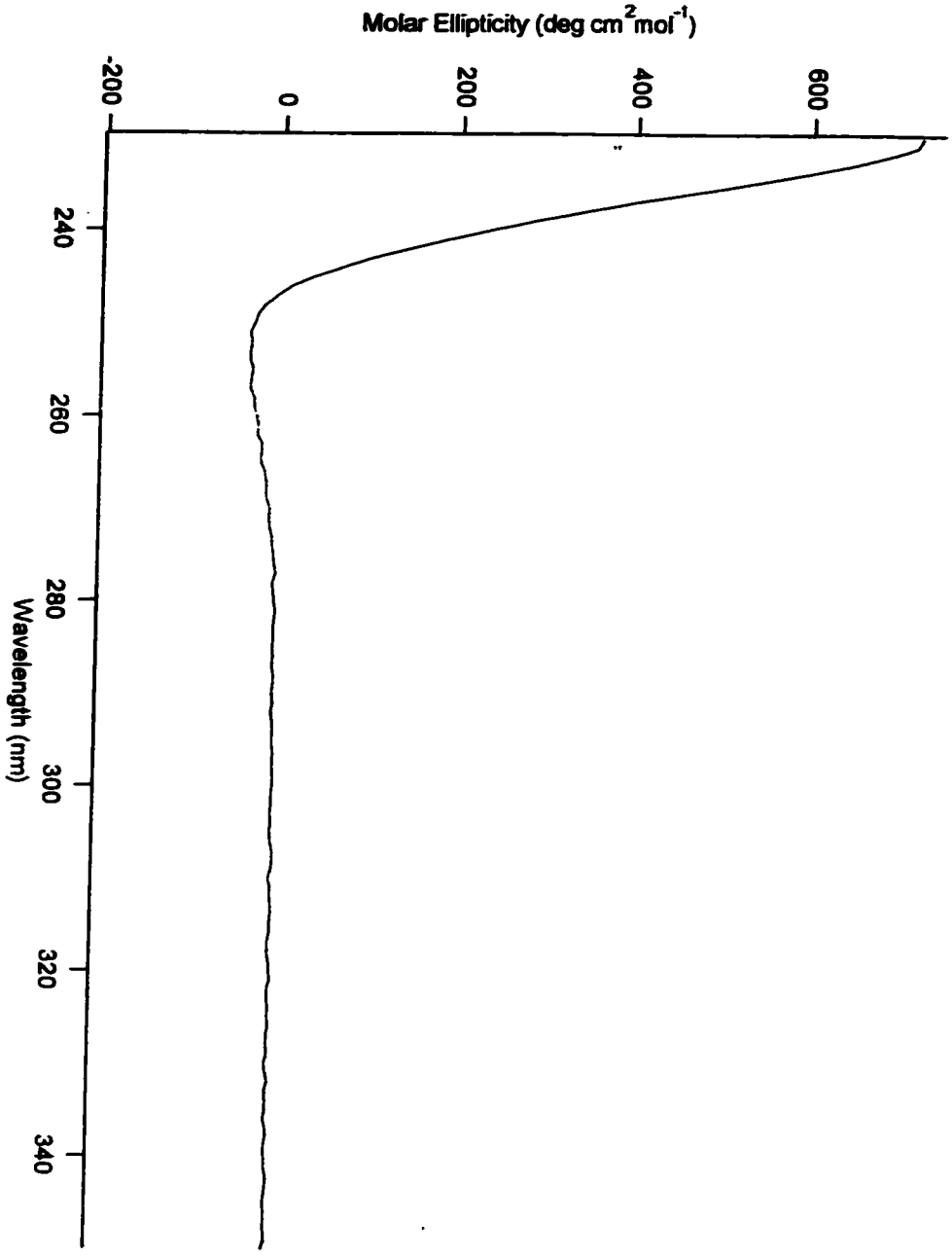

Figure C. 7. CD Spectrum (CH_2Cl_2) of 4C

Appendix D: Results for Computer Modelling

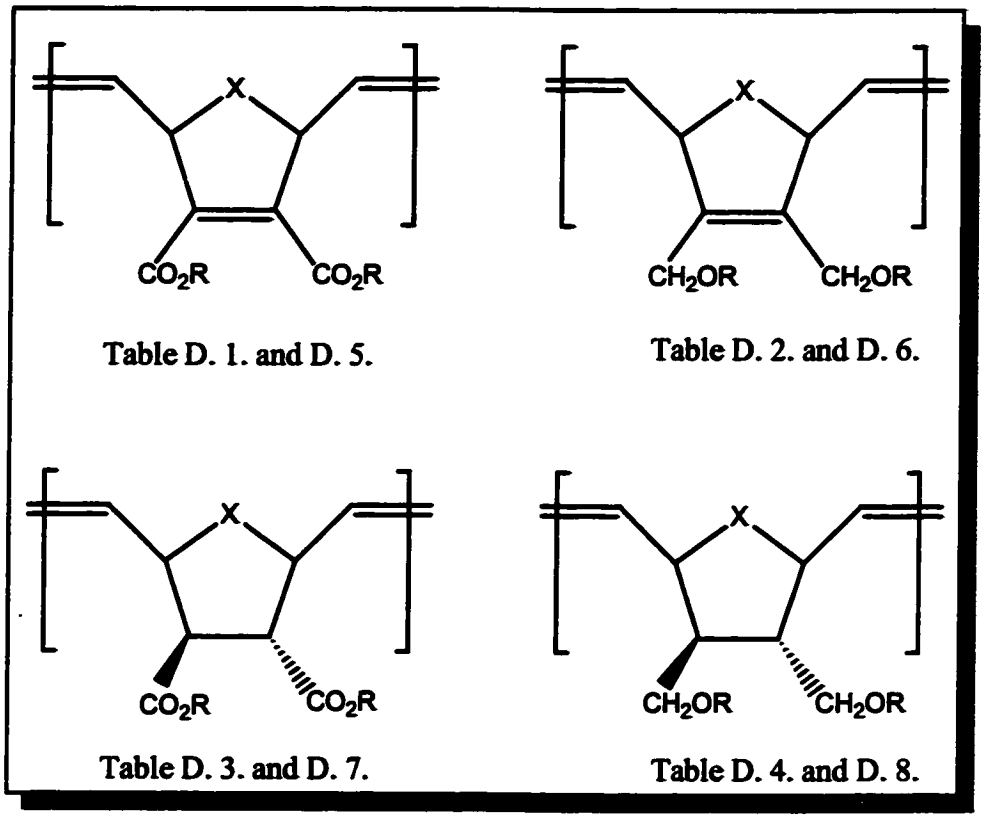

Figure D. 1. Polymer Type Descriptions

Table D. 1. First Survey Models of Poly(norbornadiene) With Ester (CO_2)Tether

R	*X*		*Helical Turn*	*Inner Diameter (Å)*	*Pitch (Å)*	*Length for 50 units*	*Model ID*
None		C/I	10/1	7	45	205	Rm268b
Me	CH_2	C/I	10/1	5	37	200	Rm235b
	O	C/I	10/1	5	50	240	Rm258h
^{t}Bu	CH_2	C/I	10/1	5	45	220	Rm236e
		T/I	7/1	0.2	75	240	Rm306a
		C/S	8/1	0	35	170	Rm306c
		T/S	17/1	14	50	195	Rm306e
Ad	CH_2	C/I	10/1	4	40	220	Rm272f
Ph	CH_2	C/I	10/1	8	40	215	Rm273d
Ph(2,6-^{t}Bu)	CH_2	C/I	10/1	6	48	235	Rm274h

Table D. 2. First Survey Models of Poly(norbornadiene) With Ether (CH_2O)Tether

R	*X*		*Helical Turn*	*Inner Diameter (Å)*	*Pitch (Å)*	*Length for 50 units*	*Model ID*
None		C/I	10/1	7	45	205	Rm268b
Me	CH_2	C/I	10/1	6	40	190	Rm249f
	O	C/I	8/1	5	45	240	Rm259b
^{t}Bu	CH_2	C/I	10/1	0	50	220	Rm249h
Ad	CH_2	C/I	10/1	5	40	220	Rm272d
Ph	CH_2	C/I	10/1	5	40	210	Rm273b
Ph(2,6-^{t}Bu)	CH_2	C/I	10/1	6	45	220	Rm274f

Table D. 3. First Survey Models of Poly(norbornene) With Ester (CO_2)Tether

R	*X*		*Helical Turn*	*Inner Diameter (Å)*	*Pitch (Å)*	*Length for 50 units*	*Model ID*
None		C/I	6/1	5	25	185	Rm268d
Me	CH_2	C/I	16/1	18	40	130	Rm247c
	O	C/I	16/1	18	50	160	Rm258b
^{t}Bu	CH_2	C/I	16/1	16	35	135	Rm247e
		T/I	17/1	0	90	260	Rm307a
		C/S	10/1	0	35	210	Rm307c
		T/S	20/1	18	20	70	Rm307e
CH_2^{t}Bu	CH_2	C/I	14/1	8	35	120	Rm264b
$(CH_2)_2$^{t}Bu	CH_2	C/I	16/1	5	40	140	Rm266d
Ad	CH_2	C/I	14/1	8	40	145	Rm271f
Ph	CH_2	C/I	16/1	11	40	150	Rm274b
Ph(2,6-^{t}Bu)	CH_2	C/I	15/1	16	42	150	Rm278b

Table D. 4. First Survey Models of Poly(norbornene) With Ether (CH_2O)Tether

R	*X*		*Helical Turn*	*Inner Diameter (Å)*	*Pitch (Å)*	*Length for 50 units*	*Model ID*
None		C/I	6/1	5	25	185	Rm268d
Me	CH_2	C/I	14/1	17	35	130	Rm248b
	O	C/I	16/1	16	60	180	Rm258d
^{t}Bu	CH_2	C/I	12/1	16	32	135	Rm248d
$CH_2{}^t$Bu	CH_2	C/I	11/1	12	35	135	Rm264f
$(CH_2)_2{}^t$Bu	CH_2	C/I	10/1	11	30	145	Rm265b
$(CH_2)_2{}^t$Bu	CH_2	C/I	12/1	9	35	150	Rm266b
Ad	CH_2	C/I	14/1	8	40	150	Rm271d
Ph	CH_2	C/I	14/1	16	30	110	Rm273h
Ph(2,6-^{t}Bu)	CH_2	C/I	13/1	14	30	130	Rm278d

Table D. 5. Second Survey Models of Poly(norbornadiene) With Ester (CO_2)Tether

R	*X*		ψ	ϕ	*Helical Turn*	*Inner Diameter (Å)*	*Pitch (Å)*	*Length for 50 units*	*Model ID*
None		C/I	-72.6°	125°	19/4	2.3	12	105	Rm361b
Me	CH_2	C/I	-74°	111°	4/1	2	5	65	Rm352b
	O	C/I	-67.5°	110°	4/1	2.5	6	70	Rm353f
^{t}Bu	CH_2	C/I	-73.5°	123°	4/1	2	10	90	Rm343a
		T/I	-125°	165°	22/1	0	120	250	Rm343d
		C/S	-85°	-110°	115/1	58	500	230	Rm344a
		T/S	-135°	-150°	50/3	13	35	105	Rm344d
Ad	CH_2	C/I	-72.5°	130°	5/1	3	10	110	Rm356d
Ph	CH_2	C/I	-76°	113°	4/1	2	8	65	Rm355b
Mn	CH_2	C/I	-67.5°	120°	13/3	1	9	100	Rm358b
Gu	CH_2	C/I	-82.5	140°	6/1	4	18	140	Rm359d

Table D. 6. Second Survey Models of Poly(norbornadiene) With Ether (CH_2O)Tether

R	*X*		ψ	ϕ	*Helical Turn*	*Inner Diameter (Å)*	*Pitch (Å)*	*Length for 50 units*	*Model ID*
None		C/I	-72.6°	125°	19/4	2.3	12	105	Rm361b
Me	CH_2	C/I	-77.5°	130°	21/4	3	13	110	Rm353b
	O	C/I	-70°	130°	14/3	3	12	115	Rm354d
^{t}Bu	CH_2	C/I	-73°	122°	19/4	2	10	95	Rm345b
Ad	CH_2	C/I	-70°	125°	14/3	2	10	105	Rm357b
Ph	CH_2	C/I	-90°	140°	7/1	6	20	150	Rm355f
Mn	CH_2	C/I	-70°	130°	19/4	2.5	12	130	Rm358d
Gu	CH_2	C/I	-77.5°	130°	21/4	3	14	115	Rm360b

Table D. 7. Second Survey Models of Poly(norbornene) With Ester (CO_2)Tether

R	*X*		ψ	ϕ	*Helical Turn*	*Inner Diameter (Å)*	*Pitch (Å)*	*Length for 50 units*	*Model ID*
None		C/I	-72.5°	113°	15/4	1	6	75	Rm362d
Me	CH_2	C/I	-79°	125°	21/4	3	12	110	Rm352f
	O	C/I	-70°	120°	4/1	1	10	115	Rm354b
^{t}Bu	CH_2	C/I	-88.5°	140°	19/4	0	14	150	Rm346d
		T/I	-121°	163°	41/3	8	40	150	Rm346f
		C/S	-120°	-170°	10/1	2.5	18	95	Rm347b
		T/S	-125°	-133°	25/2	15	10	50	Rm347d
Ad	CH_2	C/I	-90°	135°	11/2	2.5	20	165	Rm356f
Ph	CH_2	C/I	-92.5°	145°	9/1	9	20	115	Rm355d
Mn	CH_2	C/I	-72°	137°	6/1	3.5	14	115	Rm358f
		C/S	-85°	-131°	40/3	5	40	140	Rm364b
Gu	CH_2	C/I	-95°	148°	20/3	4.5	25	150	Rm360d

Table D. 8. Second Survey Models of Poly(norbornene) With Ether (CH_2O)Tether

R	*X*		ψ	ϕ	*Helical Turn*	*Inner Diameter (Å)*	*Pitch (Å)*	*Length for 50 units*	*Model ID*
None		C/I	-72.5°	113°	15/4	1	6	75	Rm362d
Me	CH_2	C/I	-82°	127°	5/1	2.5	12	110	Rm353d
	O	C/I	-75°	128°	13/3	2.5	12	135	Rm354f
'Bu	CH_2	C/I	-90°	135°	11/2	3.5	16	140	Rm348b
Ad	CH_2	C/I	-73.5°	136°	5/1	3	12	115	Rm357d
Ph	CH_2	C/I	-110°	160°	11/2	0	23	185	Rm356b
Mn	CH_2	C/I	-92.5°	138°	6/1	4	18	150	Rm359b
Gu	CH_2	C/I	-104°	158°	25/4	3	20	190	Rm360f